Biomass waste-derived catalysts for biodiesel production: Recent advances and key challenges

Supongsenla Ao [a], *Bishwajit Changmai* [a,b], *Chhangte Vanlalveni* [c], *Michael Van Lal Chhandama* [d,e], *Andrew E. H. Wheatley* [f,**], *Samuel Lalthazuala Rokhum* [a,*]

[a] Department of Chemistry, National Institute of Technology Silchar, Silchar, 788010

[b] Department of Chemistry, Bhattadev University, Bajali, Pathsala- 781325, India

[c] Department of Botany, Mizoram University, Tanhril, Aizawl, Mizoram, 796001, India

[d] Department of Biotechnology, JAIN (deemed-to-be University), Bangalore, Karnataka, 560027, India

[e] Department of Biotechnology, School of Life Sciences, Mizoram University, Tanhril, Mizoram 796001, India

[f] Yusuf Hamied Department of Chemistry, University of Cambridge, Lensfield Road, Cambridge, CB2 1EW, UK

Corresponding authors email: rokhum@che.nits.ac.in (SLR); aehw2@cam.ac.uk (AEHW)

Contents

Abstract

Biomass-derived catalysts are being intensively studied as potential replacements for traditional chemical catalysts in the sustainable generation of biodiesel because of their unique combination of characteristics; catalytic activity, low-cost, plentiful supply and ecologically friendly and efficient manufacturing procedures. This critical review discusses the recently reported approaches that have been used (mostly since 2016) towards cost-effective and environmentally benign solid base/acid/acid-base catalysts from a range of biomass. Sources include shells, animal bones, and plants. Outlined alongside the push for optimized conversion and yield is the increasing trend for enhanced catalyst reusability and recyclability. Outstanding technical problems associated with catalyst preparation or stability, or waste generation are considered individually. The outlook for solving each of these is discussed, as is the potential of biomass-derived catalysts and the biodiesel they produce to develop the fields of fuel synthesis and energy use. Overall, this review aims to assess the viability of biomass-derived catalysts in the commercial sector and the most promising routes for transferring new technologies from the academic environment to industry.

Keywords: Biodiesel, biomass, transesterification, esterification, renewable energy, heterogeneous catalyst

Graphical Abstract

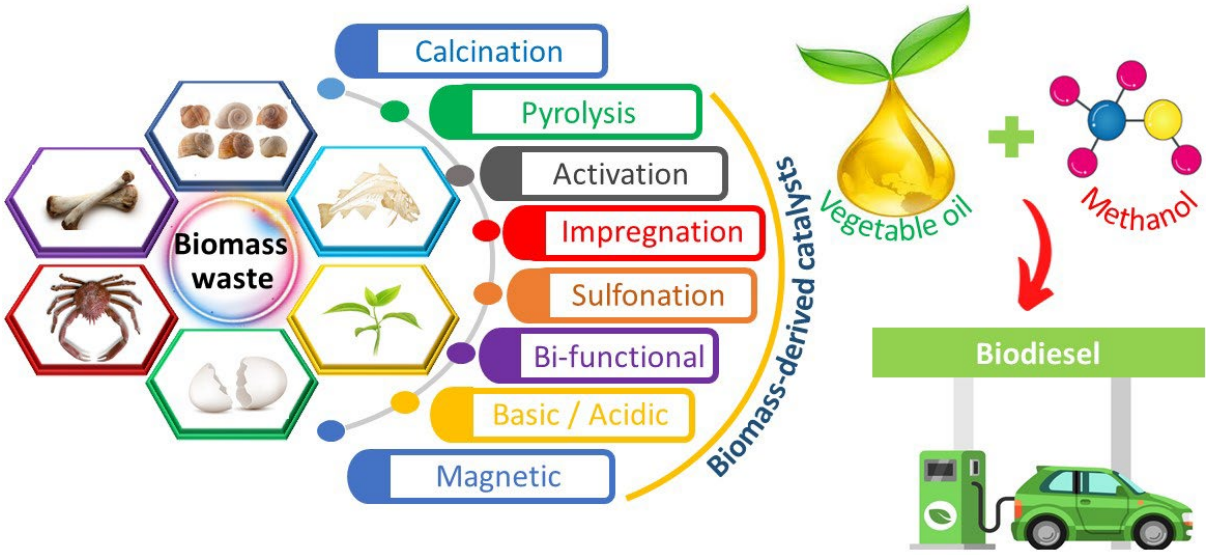

1 General introduction

In recent years, increased global energy demand has combined with the depletion of fossil fuel reserves and skyrocketing CO_2 emissions to drive the search for more sustainable and environmentally benign ways to power modern economies [1]. Complementary to it, biofuels have come to represent a compelling research vector because they can be created from renewable, sustainable resources (biomass) [2]. They are non-toxic and their combustion emits less carbon monoxide (CO), sulfur dioxide (SO_2) and unburned hydrocarbons (HCs) than traditional fossil fuels [3][4]. Biomass-derived catalysts are now attracting significant interest because of their biodegradability, eco-friendly nature, and the abundance of raw materials for their preparation that can be sourced from food waste like fruit peel, waste groceries, and other food remnants [5][6]. Additionally, materials from plant and crop biomass waste as well as discarded animal and egg shells represent convenient, inexpensive raw materials, whose repurposing can in fact obviate the need for costly and energy-intensive waste management and disposal [1][3]. Consequently, catalyst systems derived from waste biomass have emerged as a focus of intensive study for more sustainably producing biodiesel. This focus is driven by the combination of specific notable attributes: high activity, widespread availability of catalyst precursors, cost-effectiveness, and the ability to yield high-quality products. Additionally, this approach is of great interest in developing countries, because these catalysts can be used with only minimally modified existing infrastructure [7]. The starting point for biofuels has historically taken one of two forms; edible or inedible biomass. Edible biomass is typically rich

in triglycerides (TRIGs). These are simply converted by monofunctional bases through transesterification. However, particularly in developing economies, the use of inedible biomass is easier to justify because of its widespread availability, often lower cost, and because it doesn't compete with the demand for food. That said, it often contains more free fatty acids (FFAs), which must be esterified, and this complicates the process and adds cost [8]. In general, if the acid value of any biodiesel feedstock is more than 4.0 mg KOH g^{-1}, a pre-treatment (esterification step) has to be carried out before the alkaline transesterification reaction [9].

1.1 Biodiesel production

Biodiesel, aka fatty acid methyl ester (FAME), is obtained by the transesterification of TRIGs (esters of FFAs and glycerol) and/or esterification of FFAs in vegetable oils and animals fats. A representative mechanism for the transesterification and esterification of TRIGs and FFA is shown in **Fig. 1**. The composition of these TRIGs greatly influences the physicochemical properties of the oils and fats and largely dictates the quality of biodiesel produced from them. FFAs are broadly classified into two types depending on their carbon backbones: i) saturated, and ii) unsaturated. In vegetable oils and animal fats, the most commonly found FFAs are oleic acid, linolenic acid, palmitic acid, palmitoleic acid, linoleic acid, myristic acid, arachidic acid, and stearic acid [4][10][11].

a

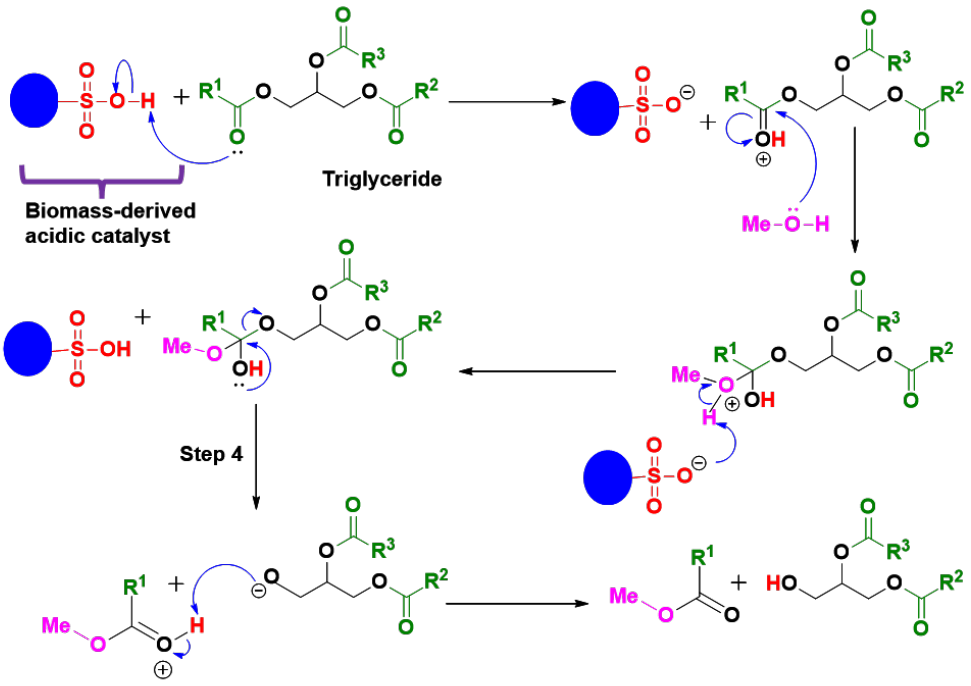

Final product of overall transesterification

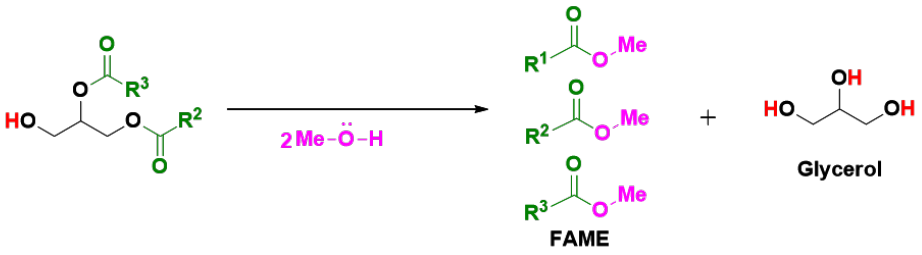

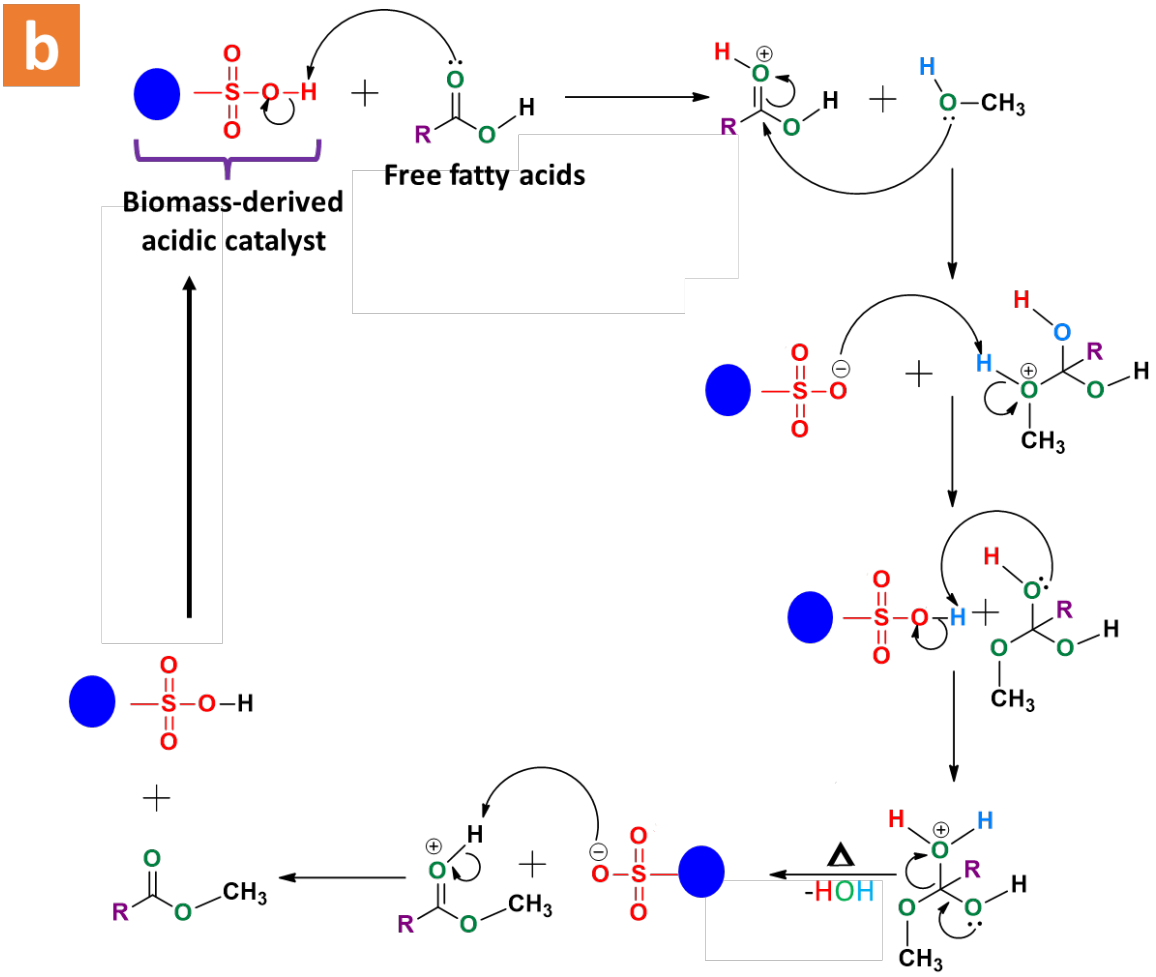

Fig. 1. Plausible mechanisms of transesterification (a) and esterification (b) using a typical biomass-derived acidic catalyst.

An enormous range of feedstocks have been, and continue to be, explored for the production of biodiesel. These include edible plant oils, non-edible oils, waste cooking oils, animal fats, and algal oil [8][12]. However, using the first of these creates a *food vs fuel* nexus as potential food for human consumption is converted to fuel. In recent years, inedible oils such as *Jatropha curcus* oil, *Pongamia glabra* (karanja) oil, *Pongamia pinnatta* (Honge) oil, palm fatty acid distillate (PFAD), and rubber seed oil (RSO) have therefore received more attention [4][12]. This has had consequences, because in the past base catalysts have usually been preferred over acid catalysts in the transesterification of vegetable oils to biodiesel owing to them being more reactive and costing less. However, with the reorientation of research to inedible oils it has become apparent that base catalysts tend to react with the FFA component being introduced, resulting in soap formation. This may consume the catalyst and reduce its reactivity [6][13]. The presence of high FFA levels in inedible oils has therefore necessitated the development of acid catalysts. These have made possible the simultaneous transesterification of TRIGs and esterification of FFAs but tend to suffer from relatively poor activity.

Apart from the dichotomy between base and acid catalysis, there is also one of homogeneous and heterogeneous approaches to address. Homogenous acid or base catalysts have certainly achieved satisfactory yields in biodiesel manufacture [14]. However, while homogeneous catalysts can provide benefits that include high catalytic activity under modest conditions, they cause a number of issues. These include soap generation, reactor corrosion, catalyst recovery difficulties, and the production of huge amounts of waste. These complexities are inevitably reflected in overall biodiesel production costs [9][10]. The potential of heterogeneous catalysts to address many of these issues has therefore assumed importance. If prepared straightforwardly from relatively easily sourced materials, these can offer to reduce environmental impact whilst bringing greater cost-effectiveness, largely through their simple isolation and recovery [12]. In principle, heterogeneous catalysts can be recycled and reused multiple times, maintaining morphology, active site density and activity and making biodiesel manufacture significantly more cost-effective [13][14][15]. As a result, in spite of many studies [16][17], the use of heterogeneous catalysts for large-scale biodiesel production remains problematic from both economic and long-term sustainability standpoints.

1.2 Aims and scope of the review

Attempts to address the issues highlighted above, essentially maximizing environmental sensitivity while reducing production costs, have underpinned the use of (particularly waste) biomass as both biofuel precursor and catalyst source [18][19][20][21]. Indeed, the latter approach has been highlighted as aligning with the principles of carbon neutral and zero-waste economics [19]. It is recent efforts in the use of biomass as a source of heterogeneous catalysts that will be critically reviewed here. Coverage will focus on the last 5 years (2016-) and take in a broad range of approaches to catalyst formation. For the most part, animal- and plant-based biomass will be considered. Other sources, such as municipal solid waste (MSW) or lignocellulosic biomass are, of course, established, have been lately reviewed [22][23][24] and, for recent lignin-rich biomass work, incorporated here. However, the need for complex separation and preparation of MSW or to structurally modify lignin-rich material complicates the use of these biomass sources. Meanwhile, though algal biomass has recently emerged as a candidate for biodiesel synthesis in combination with carbon sequestering, this technology is currently somewhat far from the marketplace [25]. A range of more tractable and established catalyst sources are considered in the current article and this introduces the possibility of producing biodiesel of variable quality. Unless stated, biodiesel reported in this work can be assumed by the reader to meet ASTM standards. This work seeks to incorporate some of the most recent developments in the area and so add to previous reviews [26]. The current work clarifies the breadth of potential for generating catalysts from both animal- *and* plant-based biomass. As such, it contrasts with more specialized surveys of the recent literature on chemical engineering aspects of biodiesel production [27] and the use of specific catalyst feedstocks, e.g. animal-based biomass [28], industrial waste [29], or lignocellulosic material [30]. Turning to methods for enhancing catalyst activity (e.g., calcination, doping), we particularly outline recent advances by ourselves and others in the development of sulfonated catalysts in the context of limiting active site leaching and/or regenerating spent catalysts. This leads to a discussion of truly bifunctional catalysts, with a focus on the promise these more designed catalysts offer for the use of inedible biomass in biodiesel production. This attempt to look at how to address the basic technical challenges that remain with biomass-derived catalysts (e.g. deactivation, mass transfer limitations, the need for downstream treatment) is drawn together in Section 4, where the issues are explicitly discussed. Section 5 covers the reasons for switching to biofuels from more conventional fuels generally, and the relevance of biodiesel generated using sustainably sourced catalysts specifically. This is done from a purely scientific perspective (comparing emissions of bio- and petrodiesel) and also in broader societal and political terms (looking at the cost implications of moving to biomass for catalysts, the energy

169 security gained by avoiding fossil fuels, the effects of repurposing industry waste). Sections 4
170 and 5 finally combine to allow us to finally point to the specific strategies the catalysis
171 community is now developing to address outstanding problems in Table 6. In general terms,
172 however, current catalysts for biodiesel production with their associated merits and demerits
173 are summarized in **Table 1**.

Table 1. Current catalysts for biodiesel production (adapted from ref. [4]).

Catalyst type	Examples	Advantages	Disadvantages
Homogeneous			
Alkali	KOH, NaOH	• High activity • Cheap • Fast reaction rate • Mild operational conditions	• Requires low FFA content (< 1 wt. %) • High sensitivity to FFA and water • Saponification • Wastewater generation • Equipment corrosion • Non-recyclable
Acid	HCl, H_2SO_4, HF	▪ Insensitive to FFA and water content ▪ Simultaneously catalyzes (trans)esterification ▪ No soap formation.	▪ Low activity ▪ Long reaction time ▪ High reaction temperature ▪ Equipment corrosion ▪ Non-recyclable
Heterogeneous			
Alkali	(Mixed) metal oxides eg. CaO, MgO, SrO, zeolites, CaO-MgO, La_2O-ZrO_2, CaO-La_2O_3	• Stable • Non-corrosive • Recyclable • Fewer disposal problems • Easy to separate	• Slow reaction rate due to diffusion limitations • Requires low FFA content (< 1 wt. %) • High sensitivity to FFA and water • Saponification • Active site leaching • Wastewater generation

			• Complex synthesis • Expensive
Acid (*Amphoteric)	TiO, ZnO,* ZrO,* ion-exchange resin, sulfated and sulfonated metal oxides and carbon materials.	▪ Insensitive to FFA and water content ▪ Simultaneously catalyzes (trans)esterification ▪ Recyclable ▪ Non-corrosive	▪ Slow reaction rate due to diffusion limitations ▪ Low activity ▪ High reaction temperature ▪ Low acid density ▪ Active site leaching ▪ Complex synthesis ▪ Expensive

2 Animal bio-waste-based catalysts

2.1. Eggshells

CaO is amongst the most active and cost-effective of heterogeneous solid catalysts for biodiesel production [31][32][33]. However, its major source (limestone) is non-renewable, and its synthesis is lengthy and costly. Alternative approaches that harness natural waste materials have therefore attracted interest as the precursors are typically non-toxic, easy to handle, plentiful, low cost, and renewable [18][22]. Literature reveals that waste shells comprise 96-98 % $CaCO_3$ along with trace $MgCO_3$, $SrCO_3$, $Ca_3(PO_4)_2$, organic material and water. This high proportion of $CaCO_3$ in waste shells (and bones) makes them an excellent potential source of CaO, with high temperature calcination (750-1000 °C) [24] the most widely used process for making biomass-derived solid base catalysts. In particular, the exploitation of waste eggshells as a catalyst precursor solves major problems of waste dumping and recycling [24]. The calcination temperature alluded to above has a major impact on the synthesis and the evolution of the catalyst's surface morphology, and this can be correlated with activity [34]. A general flowchart for the different types of biomass-derived CaO, and modified CaO is presented in **Fig. 3**. In general, bare CaO obtained by calcination of waste shells is commonly used as a highly basic catalyst for biodiesel production by transesterification [35][36]. Nonetheless, bare CaO usually possesses low-surface area, and relatively low catalytic activity. Hence, attempts have been made to increase the basicity, stability and activity of waste shell-derived CaO by doping with active metals [37][38][39], by catalyst support [40] (**Fig. 3b**), and by hydration-dehydration [41][42][43][44] (**Fig. 3c**).

To date, a variety of waste eggshells have been used in biodiesel production (**Table 2**). Goli *et al.* [35] synthesized CaO from chicken eggshell and utilized it with soybean oil. Calcination at 500-1000 °C examined temperature effects on CaO production. Temperatures up to 800 °C failed to convert the major portion of the $CaCO_3$ to CaO (18.75 %), while an increase from 800-900 °C led to the much more complete generation of CaO (58.33 %). Further increasing temperature did not show any significant improvement. Theoretical and experimental procedures then displayed 92.32 % and 93 % biodiesel yield, respectively. Similarly, CaO derived from chicken eggshells at 800-1000 °C was used to transesterify waste cooking oil (WCO)[26][34][35]. A relatively brief (2-4 h) calcination at higher temperature (1000 °C) gave high conversion of $CaCO_3$ to CaO, while increasing calcination time (>4h) degraded the catalyst and suppressed active sites, and this was reflected in transesterification [45]. In spite of this, Tshizanga *et al.* [46] found that the calcination of eggshell at 800 °C for as much as 24 h resulted in increased surface area and allowed the resulting catalyst to show 91 % biodiesel yield. Whilst this performance might be surpassed by other catalysts, a demonstration that this catalyst could be reused in up to 10 consecutive cycles with no depreciation in activity, suggested excellent stability. After 10 cycles, the catalyst activity then dwindled, reaching 30 % yield in 18^{th} cycle. This decrease was possibly due to a combination of 1) leaching of Ca (in the form of CaO or calcium diglyceroxide) during methanolysis [47][48], 2) formation of $Ca(OH)_2$ in presence of water, and 3) calcium diglyceroxide (formed by reaction of CaO with glycerol byproduct) blocking active sites [49].

To offset the high energy consumption of conventional methods, microwave irradiation has been widely adopted in recent years as it enables faster reaction rates, thereby reducing the reaction time by using volumetric heating. Advantageously, apart from the economic benefit of reducing the reaction time, microwave-assisted reaction could enable better recovery and reusability of the CaO catalyst used in the methanolysis of triglyceride, because the amount of CaO solubilized in methanol increases with time. In an experiment, it was observed that after 3 h of immersion of CaO in methanol, leached Ca^{2+} amounted to 0.169 mg mL^{-1} and after 6 h it had increased to 0.532 mg mL^{-1}. Moreover, in the presence of glycerol, CaO forms calcium diglyceroxide, which is even more soluble [47]. Hence, reducing the reaction time should positively impact by preventing leaching of Ca^{2+} into the reaction mixture, helping retain the reactivity of CaO on repeated reuse. Owing to the advantages of microwave-assisted synthesis, several reports on microwave-assisted production of biodiesel have appeared [50][51][52][53]. Taking advantage of this trend, and with an intention to reduce the reaction time, thereby

making the synthesis procedure economical, chicken shell-derived CaO was used to produce biodiesel in 98.90 % yield from *C. inophyllum L.* oil in <13 mins [54]. The requirement of this short reaction time under microwave-irradiation could potentially endorse its wide application in industrial scale biodiesel production.

CaO is superior to other heterogeneous base catalysts in the methanolysis of vegetable oil to biodiesel. Yet, it is much slower than the homogeneous catalysts currently used in the biodiesel industry. To make it applicable on an industrial scale, the catalytic activity of waste shell-derived CaO has to be increased considerably by enhancing its basicity, surface area, and tolerance to ambient CO_2 and H_2O (which poison basic sites by the formation of $CaCO_3$ and $Ca(OH)_2$, respectively) as well as resistance to leaching [47]. In order to do this, numerous methods have been attempted; loading onto supports, formation of mixed oxide composites with other metal oxides and calcination-hydration-dehydration. Putra *et al.* [40] obtained CaO from eggshell and supported it on SiO_2 extracted from palm empty fruit branches (PEFB) for WCO transesterification. In comparison to CaO and CaO@PEFB, CaO@SiO_2 possessed a high surface area of 79.8 $m^2\ g^{-1}$, and this was reflected by an excellent 96 % biodiesel yield. In another study, a hybrid catalyst (CaO@SiO_2) derived from two waste materials (eggshell and rice husks) transesterified palm oil [55]

The surface area of CaO increased modestly from 6.83 to 12.29 $m^2\ g^{-1\ 1}$ after impregnation with silica from BET analysis, with the increased surface area attributed to a strong, stabilizing interaction of the CaO with the silica support reducing surface diffusion and sintering. The catalyst's porosity underwent examination through the N_2 physisorption method, with the pore size distribution of 0.0429 $cm^3\ g^{-1}$ showing the mesoporous nature of the catalyst determined via the adsorption branch. **Fig. 2** illustrates the nitrogen adsorption–desorption isotherms and the corresponding plots for pore size distribution. In these plots, all isotherm curves exhibited a type IV profile and type H3 hysteresis loop, except for silica, which notably lacked a hysteresis loop during the initial capillary condensation. SEM imaging revealed the agglomeration of silica particles and a heterogeneous distribution thereon of CaO. In CaO catalysts with 3 wt. % silica, there appeared to be greater room between agglomerates than was seen in those with 5, 7, and 10 wt. % silica. It was argued that this underpinned more efficient interaction with reactant molecules in this, the most active catalyst. Nevertheless, biodiesel yield was only 90 % and this dropped to 77.5 % after 7 cycles.

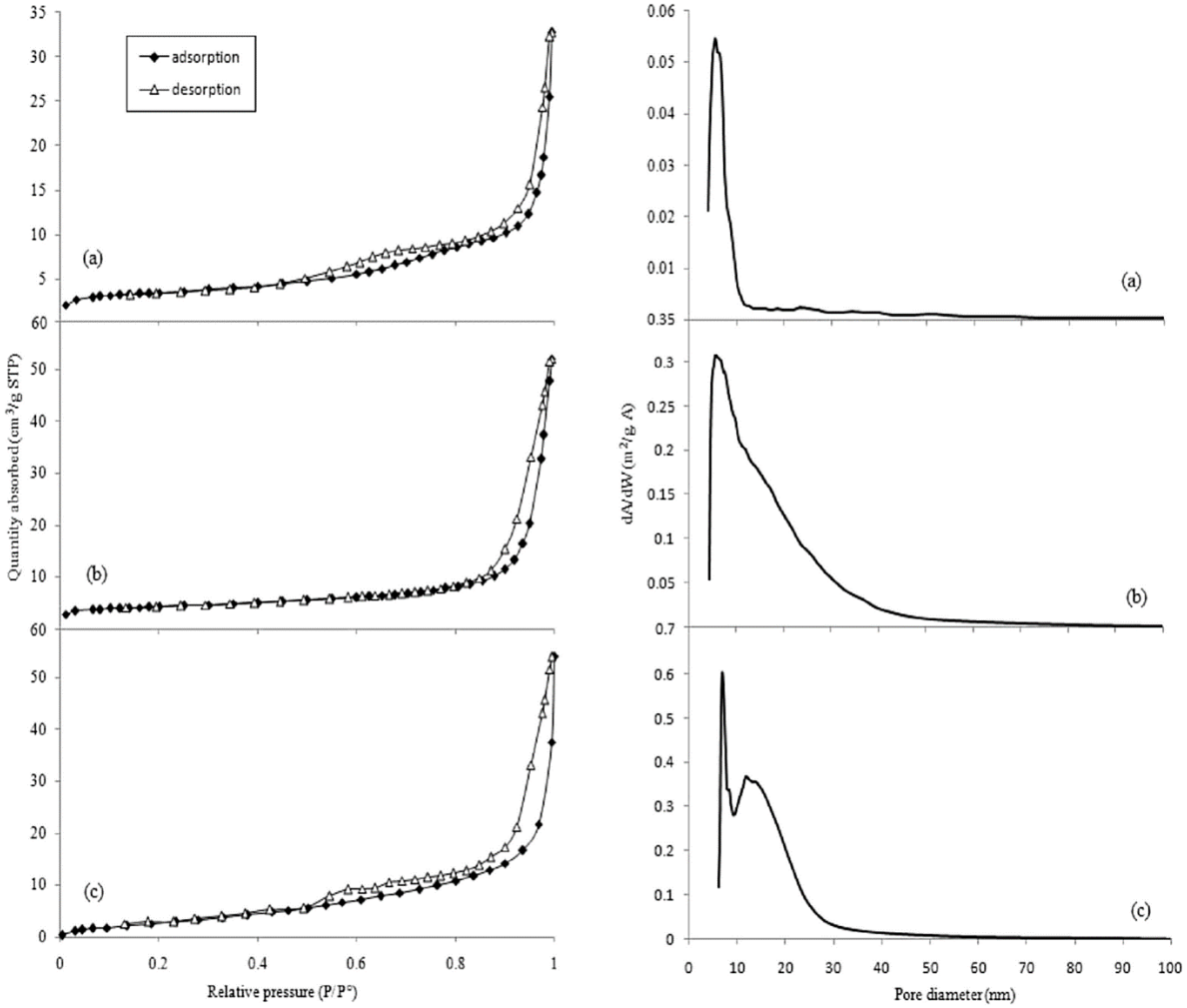

Fig. 2. N_2 adsorption–desorption isotherm and pore size distribution of the (a) CaO, (b) silica and (c) CaO impregnated with 3% silica; hybrid catalyst. Reproduced from Ref. [55].

Doping CaO with alkali metal species [37][38] to increase the basicity is another topic of research interest (**Fig. 3b**). This increase is believed to occur *via* the exchange of lattice M^{2+} for M^{+} upon calcination, leading to O^{-} vacancies [56][57]. With the intention of preparing highly basic metal doped CaO, Hossain *et al.* [37] treated eggshell-derived CaO with different concentrations of KOH to obtain K/CaO. Among several catalysts developed (1.25, 2.5, and 5 wt. % K^{+} doped), 5 wt. % K^{+} doping resulted in the high biodiesel yield of 98.46 % from waste soybean oil (WSO). In contrast, the bare eggshell-CaO afforded merely 88.1 % yield. The K^{+}-CaO catalyst was recycled by washing with hexane and dried overnight at 105 °C then calcined at 900 °C 4 h. In other work, Khatibi *et al.* [38] functionalized eggshell-derived CaO with Na-K *via* wet impregnation to obtain a doped Na-K/CaO catalyst for the transesterification of canola oil. The effect of Na:K molar ratio was studied using values of 3, 1 and 0.33, with Na:K

= 1 showing maximal biodiesel yield at 97.6 %. Interestingly, co-doped catalysts (Na-K/CaO) afforded much higher biodiesel yields than K/CaO (84.7 %) and Na/CaO (80.6 %).

Calcination-hydration-dehydration has also garnered attention for the development of CaO (abbreviated as $CaO_{C\text{-}H\text{-}D}$) with high surface area and basicity (**Fig. 3c**) [58][59][60]. The use of hydroxide precursor for the synthesis of CaO is effective in increasing the surface area and amount of basic sites [59]. Hence, waste shell ($CaCO_3$) was first calcined to produce CaO, which underwent hydration to form $Ca(OH)_2$ that was finally calcined to afford highly basic, high surface area $CaO_{C\text{-}H\text{-}D}$ (as detected by temperature programmed desorption of carbon dioxide, CO_2-TPD) [59]. In a pioneering work, Niju *et al.* [41] observed a remarkable difference in the transesterification yield of 67.57 %, 79.62 % and 94.52 % for commercial CaO, eggshell-derived CaO and eggshell-derived $CaO_{C\text{-}H\text{-}D}$ (eggshell- $CaO_{C\text{-}H\text{-}D}$), respectively. Eggshell-derived CaO had a surface area of 3.72 $m^2\ g^{-1}$, whereas that of eggshell-$CaO_{C\text{-}H\text{-}D}$ was 8.64 $m^2\ g^{-1}$, which accounted for its higher activity. Using Hammett indicator titration, the basicity of eggshell derived-CaO was found to be in the range $9.8<H<12.2$, whereas eggshell-$CaO_{C\text{-}H\text{-}D}$ was $12.2<H<15.0$. Similarly, Gupta *et al.* [58] reported eggshell-$CaO_{C\text{-}H\text{-}D}$ for the transesterification of WCO. The hydration-dehydration process involved two steps. Hydration of CaO with deionized water at 60 °C for 6 h formed $Ca(OH)_2$, followed by drying of the resultant mass at 80 °C followed by calcination at 600 °C for 3 h. The resulting eggshell-$CaO_{C\text{-}H\text{-}D}$ catalyst possessed a high surface area of 53.48 $m^2\ g^{-1}$, which was much higher than many reported commercial CaO systems (3-4 $m^2\ g^{-1}$) [61], and returned a 93.1 % biodiesel yield. Nano-eggshell-$CaO_{C\text{-}H\text{-}D}$ has also been used for the production of biodiesel using microalgal strain *A. obliquus* as a low-cost feedstock [62].

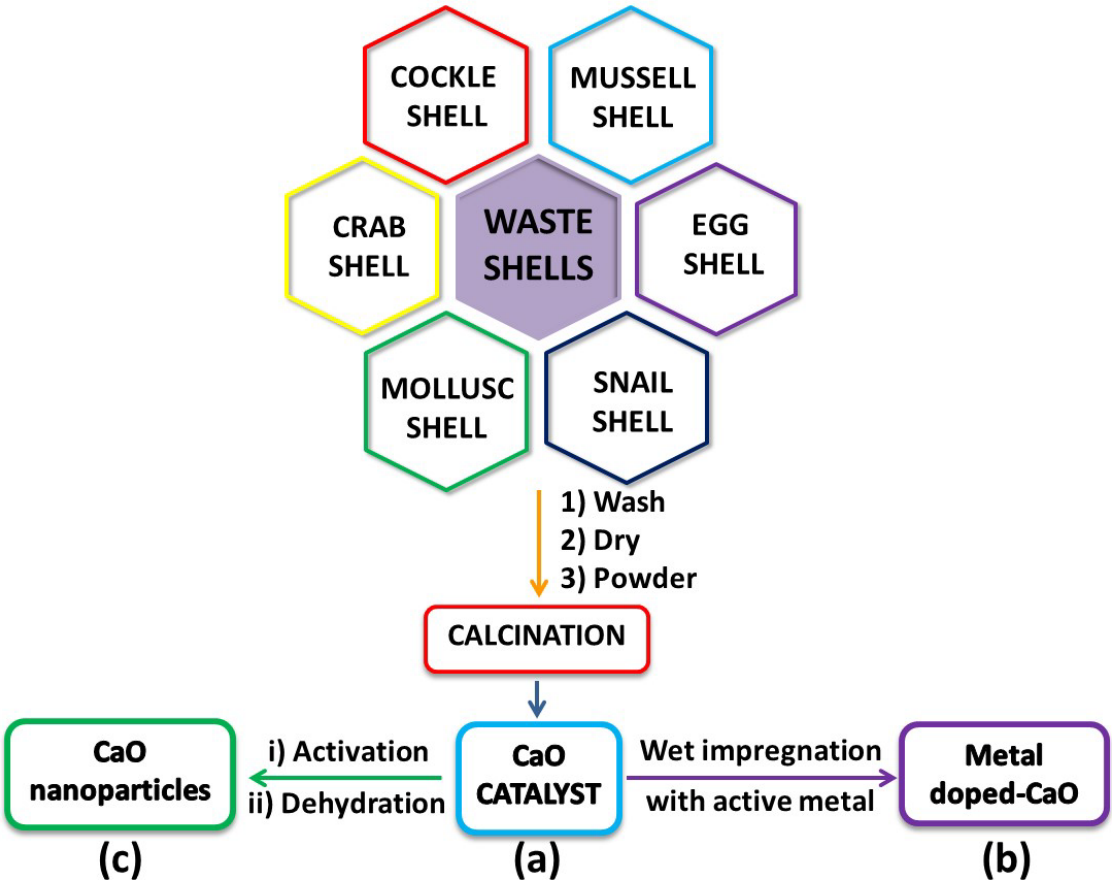

Fig. 3. Preparation of (a) CaO-derived catalysts, (b) metal-doped CaO, (c) CaO nanoparticles from shell-based biomass.

294

295 **2.2 River, sea and other shells**

296 A wide variety of river and seashells have been calcined to produce CaO transesterification
297 catalysts [63][64](**Table 2**). In a 2017 example, Kaewdaeng *et al.* [65] reported the synthesis
298 of biodiesel from used cooking oil (UCO) with river snail shell-derived CaO. Calcination of
299 the shell at 800 °C for 4 h resulted in efficient CaO formation (70.1 wt. %), and this then
300 showed good catalytic activity with 92.5 % oil conversion. Of course, different types of snail
301 shells are available, and a range have been utilized for the transesterification of feedstocks such
302 as palm oil [66], soybean oil [3] and WCO [42]. The effects of a range of co-solvents on
303 reaction kinetics and biodiesel yield have also been investigated [66], with 98.5 % ± 1.5
304 achieved using 10 % v/v THF in methanol. In this case, activation energy (E_a) was established
305 to have been reduced to 57.79 kJ mol^{-1} compared to 67.60 kJ mol^{-1} in pure methanol.

306 A 98 % biodiesel yield was obtained from soybean oil at ambient temperature using
307 snail shell (*Pila spp.*)-derived CaO. The authors systematically investigated the effect of

calcination temperature and observed that, at above 900 °C, essentially all the $CaCO_3$ was converted (CaO content 98.0 wt. %, **Fig. 4**). As with oxide prepared from egg shell, high yield was achievable in spite of only moderate catalyst surface area (7.0 m^2 g^{-1}). However, reusability tests saw a considerable depreciation in activity from 98 % to 77 %, and this was attributed to blocking of catalyst active sites with glycerol [3], moisture [56] and impurities [57]. In other work, mussel shell was also successfully calcined to obtain a highly basic CaO and employed for the transesterification of *Camelina sativa* oil, achieving 95 % biodiesel yield. The catalyst proved to be reusable in up to 10 reaction cycles, maintaining a biodiesel yield of ~ 93 %, suggesting the possibility of high stability catalysts of this type [67]. ASTM biodiesel standards were used to compare the fuel qualities of product made from *Camelina sativa* oil. Importantly, it was found that there would be no need to modify an engine to use this biodiesel because its viscosity was comparable to that of ordinary diesel fuel. Beneficially, the biodiesel produced showed a higher cetane number, which indicates improved fuel efficiency, better ignition quality, lessening of harmful emissions, and quicker pumping of protective lubricating fluids throughout the system. Similarly, Venus clam (*Tapes belcheri S.)* was used in a similar fashion, the resulting catalysts transesterified palm oil efficiently in the first instance (97 % yield). Interestingly, in CO_2-TPD analysis, commercial CaO catalyst displayed a basicity of only 294.20 µmol g^{-1}. In contrast, venus clamp calcined at 900 °C (CS-900) showed roughly 44 times higher basicity (13,156.80 µmol g^{-1}). However, reusability now proved disappointing (86 % yield after 3 cycles) [61].

Crab shell has been used for the synthesis of CaO catalyst. One study employed the resulting material to transesterify karanja oil. Interestingly, the catalyst exhibited a moderate surface area of 16.47 m^2 g^{-1} that was nevertheless high enough to show respectable activity (94 % yield). The catalyst was tested in up to 5 cycles, but with an almost 11 % decrease in activity, stability was suspect [68]. Finally, using ASTM standards, the characteristics of the biodiesel produced were described. It was found that the density decreased from 0.92 (for karanja oil) to 0.81 (for biodiesel), and the pour and flash points were both 184 °C. Given that density and viscosity are directly proportional, the kinematic viscosity at 40 °C was decreased from 43.6 (mm^2 s^{-1}) to 4.02 (mm^2 s^{-1}). Biodiesel had a calorific value of 3800 kcal kg^{-1} and a moisture content of 0.005 %. The synthetic biodiesel met US biodiesel criteria in full.

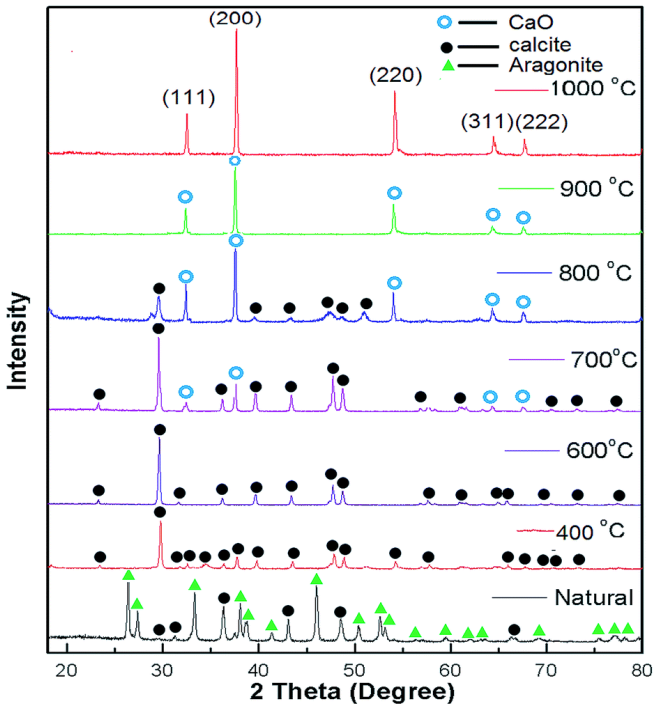

Fig. 4. XRD patterns showing the effect of 4 h calcination temperature on conversion of snail shells to CaO. Reproduced from Ref. [3]

Although snail shell-derived CaO has demonstrated respectable biodiesel production activity, it has frequently failed to achieve excellent yields due to its low basicity. Like for egg shells, to improve the basicity, doping with alkali metals has been attempted. An activated catalyst was therefore synthesized by combining ground snail shell-derived CaO and kaolin, doping with KBr. With a 20.5 wt. % K content, this catalyst (eggshell-CaO/kaolin) returned a 98.5 % biodiesel yield, which compared with 93.2 % without KBr activation [69]. In another study, waste mussel shell-derived CaO was combined with activated carbon prior to impregnation with NaOH. Calcination at 800 °C for 3 h finally produced C/CaO/NaOH for transesterification of WCO. The authors examined the effect of C:CaO mass ratio and concentration of NaOH and discerned that 2:3 C:CaO and 30 % NaOH concentration gave the best yield (95.1 %) [39]. In an effort to increase the catalytic activity, crab shell-derived CaO was doped on Na-ZSM-5 for the transesterification of neem oil. Expectedly, a very high surface area of 385 m^2 g^{-1} was observed for the supported CaO catalyst (CaO-Na-ZSM-5). This displayed good activity, with 95 % biodiesel yield obtained. However, a high methanol-to-oil ratio (MTOR, 12:1) and high catalyst amount (15 wt. %) were required to achieve the maximum biodiesel yield [70].

Generally speaking, CaO derived from snail shells has achieved reasonable yields but has possessed low surface area and reusability and, in this sense, is very much like chicken eggshell-derived CaO. This has led to augmentation by calcination-hydration-dehydration. Very recently therefore, Krishnamurthy *et al.* [71] synthesized CaO at 900 °C. The resultant mass then underwent hydration-dehydration to form nano-$CaO_{C\text{-}H\text{-}D}$. This catalyst still possessed a modest surface area (9.37 m^2 g^{-1}), but now showed excellent activity towards transesterification of *H. wightiana oil*, achieving a 98.9 % yield. The catalyst could be reused to some extent, but whilst C-H-D treatment aimed to make it more resilient, yield still dropped to 87.5 % after only 5 cycles.

Chicoreus brunneus [72] and *Polymedosa erosa* [42] sea shells were also utilized for the synthesis of nano-$CaO_{C\text{-}H\text{-}D}$ for the transesterification of rice bran oil and Jatropha oil, respectively. At only 1.56 m^2 g^{-1}, the surface area of the *Chicoreus brunneus* catalyst was very low, making it somewhat of an anomaly compared to the CaO nanocatalysts derived from snail shells and eggshells. Nevertheless, a promising biodiesel yield of 93 % using only 0.4 wt. % CaO nanocatalyst was achieved. However, this required a very high MTOR of 30:1 [72]. On the other hand, Brunauer-Emmett-Teller (BET) analysis established that *Polymedosa erosa* nano-$CaO_{C\text{-}H\text{-}D}$ possessed a diameter of 66 ± 3 nm, indicating macroporosity, and a high surface area of 90.61 m^2 g^{-1}. Correspondingly, it showed excellent catalytic activity (98.5 % yield) from Jatropha oil using a still low catalyst loading of 2 wt. %. Of particular appeal, this performance could be achieved at room temperature [42]. Cockle shell [43] was converted into nano-$CaO_{C\text{-}H\text{-}D}$ and was utilized in the transesterification of palm oil in 96.43 % yield. However, as direct comparison with only calcined CaO was not investigated, the extent of the effect of hydration-dehydration on CaO was not clearly elucidated.

Overall, shell-derived CaO has acted as a biogenic, cheap, widely available, renewable and strong base in the transesterification of triglyceride of vegetable oil and animal fats to biodiesel. At the same time, CaO rapidly hydrated (to $Ca(OH)_2$) and carbonated (to $CaCO_3$) by contact with H_2O and CO_2 present in the air has deactivated very quickly during transesterification reactions. Hence, reactivation by outgassing at temperatures 550-700 °C to revert the CO_2 poisoning and hydration, is essential for repeated reuse as a catalyst [73][74]. In some case, calcination at an elevated temperature (1100 °C) has been required to reactive the spent CaO, making the system uneconomical [72]. In addition, CaO has suffered deactivation due to the cloaking of active sites by adsorbed intermediates or byproducts. These have included monoglyceride, diglyceride, and glycerol. More so, leaching of CaO into

solution has drastically reduced catalyst efficacy. Hence, many attempts have been made to promote the activity, stability and recyclability of CaO by doping with metals, supporting on another metal oxide, and hydration-dehydration treatment to increase surface area and basicity.

2.3 Animal bones

The oxides of alkaline earth materials and other nonmetals are commonly found in animal bones. There is an excess of calcium and phosphorus in these bones, giving scope for producing highly basic calcium hydroxyapatite (Ca-HAP, $Ca_{10}(PO_4)_6(OH)_2$) *via* calcination. A flowchart outlining the preparation of waste bone-derived Ca-HAP catalyst, activated Ca-HAP, and supported CaO is given in **Fig. 5**. Khan *et al.* [75] used ostrich bone-derived Ca-HAP (**Fig. 5a**) to transesterify WCO. A decent yield of 90.56 % was achieved, albeit using a high MTOR (15:1). Similarly, Ca-HAP derived from cow [76] and goat [77] was employed for the conversion of WCO and microalgae, respectively, into biodiesel. Particularly timely, the use of a solar reactor for heating could represent an excellent way to reduce the cost of biodiesel production. Solar heating has returned a high FAME yield (96 %) using cow bone-derived Ca-HAP to esterify the FFA component in WCO. This required a more moderate MTOR (12:1) and the catalyst was reusable in up to 10 consecutive cycles, with only a very slight depreciation in activity [76]. A chicken and fish bone mixture (1:1 mass ratio), calcined at 1000 °C for 4 h to produce CaO and hydroxyapatite, was also employed as a catalyst for biodiesel production from WCO, giving an 89.5 % yield [78].

Despite the fact that waste bone-derived catalysts have demonstrated reasonable performance and consistency in biodiesel synthesis, these catalysts have tended – see above – to require high MTORs. In an attempt to overcome this, calcined waste animal bones were soaked in aqueous KOH (**Fig. 5b**). In one recent study, bones soaked in KOH solutions of different concentration were used to transesterify pretreated *Jatropha* oil. A high biodiesel yield of 96.1 % was achieved using a 9:1 MTOR and a 6 wt. % catalyst loading. The catalyst showed reasonable reusability, giving 86 % yield on 4^{th} cycle. The authors attributed the respectable reusability to high basicity in KOH-AB (potassium hydroxide-animal bone) that stopped the further decomposition of β-$Ca_3(PO_4)_2$ in the reaction mixture [79].

The low surface area of waste bone-derived catalysts is a perennial issue that effects biodiesel yield. Efforts to address this have led to the modification of calcined animal bones by hydrothermal treatment [80] and impregnation into a solid support [81] to improve surface area. Beef bone-derived Ca-HAP catalyst has been developed *via* a two-step process based on

calcination and hydrothermal treatment. The hydrothermal step underpinned the formation of a layered Ca-HAP structure. Calcination of this was claimed to then result in a slight increase in the surface area (8.63 $m^2 g^{-1}$) compared to that of the purely calcined bone (7.03 $m^2 g^{-1}$) with a pore volume of 0.042 cc g^{-1}. Here because of the small pore volume, 88 % and 96 % yield were recorded for the calcined and hydrothermally treated layered system, respectively. The higher yield of the latter catalyst was mainly attributed to enhanced surface area. Interestingly, a very low decrease (1 %) in yield was observed in the 5th catalytic cycle, confirming the satisfactory stability of the layered catalyst [80]. Similarly, fly ash was used as a catalyst support for Ca-HAP (**Fig. 5c**) derived from sheep bone. Again, the aim was to increase surface area, and the resulting composite was utilized for the transesterification of mustard oil. The surface area of the calcined catalyst increased drastically from 1.7 to 100 $m^2 g^{-1}$ upon depositing onto the support. The amount of composite needed to achieve maximal biodiesel yield was 20 wt. % (w.r.t. fly ash). Interestingly, a low MTOR (5.5:1) was sufficient to achieve a good oil conversion of 90.4 %. On the other hand, the maximum conversion achieved by using fly ash and calcined sheep bone were only 7.3 % and 85.4 %, respectively, suggesting the positive impact of increasing the surface area. A reusability investigation revealed a decline of 11.1 % oil conversion after the 7th run [81].

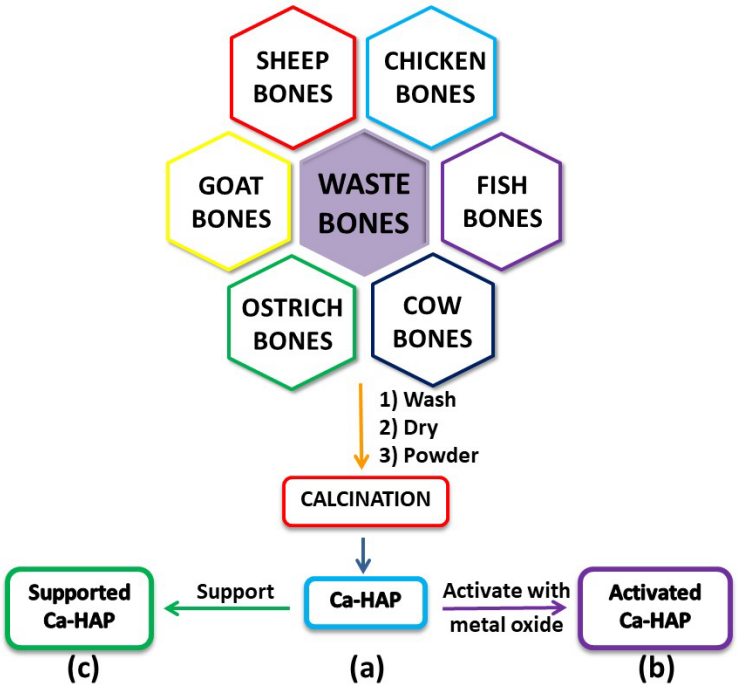

Fig. 5. Flowchart of the preparation of (a) Ca-HAP catalyst, (b) activated Ca-HAP, (c) supported Ca-HAP from a range of animal bone sources.

440

Table 2. Biodiesel production by transesterification using various shell- and animal bone-derived solid base catalysts and different feedstocks. NR = not reported. CRC (Y) = catalyst reusability cycles (yield %). RT = room temperature.

No.	Catalyst source	Calcination process[a]	Catalyst	Catalyst surface area ($m^2\ g^{-1}$)	Feedstock	Conditions[b]	Yield (%)	CRC (Y)	Ref.
1.	Chicken eggshell	900 °C, 3 h	CaO	NR	Soybean oil	10:1, 7, 57.5, 120	93	5 (75)	[35]
2.	Chicken eggshell	1000 °C, 2 h	CaO	NR	WCO	4:1, 2, 65, 120	NR	NR	[45]
3.	Chicken eggshell	900 °C, 1 h	CaO	5.20	WCO	12:1, 1.5, 60, 60	96.23	NR	[36]
4.	Chicken eggshell	800 °C, 24 h	CaO	30.7	WCO	22.5:1, 3.5, 65, 330	91	10 (91)	[46]
5.	Chicken eggshell	900 °C, 2.5 h	CaO	NR	*C. inophyllum* L oil	9:1, 3.88, MW, 12.47	98.90	NR	[54]
6.	Chicken eggshell	$CaCO_3$ (10% w/w) from eggshell impregnated with SiO_2 extracted from PRFB and calcined at 900 °C for 2 h	CaO/SiO_2	79.8	WCO	14:1, 8, 60, 90	96	3 (89)	[40]
7.	Chicken eggshell	Hybrid catalyst of calcined eggshell (900 °C, 6 h) and silca (extracted from rice husks) prepared by wet impregnation followed by calcination (800 °C, 3 h).	CaO/SiO_2	12.29	WCO	15:1, 3, 60, 120	90	6 (80)	[55]
8.	Chicken eggshell	900 °C, 5 h followed by treatment with KOH solution, dried and calcined (900 °C, 4 h)	K/CaO	12.14	WSO	12:1, 3, 65, 180	98.46	8 (68.52)	[37]
9.	Chicken eggshell	900 °C, 3 h followed by treated with $NaNO_3$ and K_2SO_4.	Na-K/CaO	12.6	Canola oil	9:1, 3, 50, 180	97.6	4 (66)	[38]
10.	Chicken eggshell	850 °C, 3 h followed by hydration (deionized water, 60 °C, 6 h) and dehydration (600 °C, 3 h).	CaO	48.35	WCO	10:1, 1.5, 60, 50	93.10	5 (81.15)	[58]
11.	Chicken eggshell	900 °C, 3 h followed by hydration (deionized water, 60 °C, 6 h) and dehydration (870 °C, 3 h).	Nano-CaO	16.4	Microalgal strain *A. obliquus*	10:1 (wt/vol), 1.7, 70, 3.6 h	86.41	6 (67.87)	[62]
12.	River snail shell	800 °C, 4 h	CaO	NR	UCO	9:1, 3, 65, 60	92.5[c]	NR	[65]
13.	River snail shell	800 °C, 3 h	CaO	3.45	Palm oil	12:1, 5, 65, 90	98.5	7 (54)	[66]
14.	River snail shell	900 °C, 4 h	CaO	7	Soybean oil	6:1, 3, RT, 420	98	9 (77)	[3]
15.	Crab shell	900 °C	CaO	16.47	Karanja oil	8:1, 2.5, 65, 120	94	5 (84)	[68]

16.	Mussel shell	900 °C for 2 h	CaO	NR	*Camelina sativa* oil	12:1, 1, 65, 120	95	10 (~93)	[67]
17.	Venus clam (*Tapes belcheri S.*)	850 °C for 6 h	CaO	11.6	Palm oil	15:1, 5, 65, 360	97	3 (86)	[61]
18.	Snail shell-kaolin	Calcined snail shell and kaolin mixed, soaked in KBr, then calcined at 450-650 °C for 3 h	CaO/KBr/kaolin	25.82	Soybean oil	6:1, 2, 65, 120	98.5	4 (73.6)	[69]
19.	Mussel shell (*Perna varidis*)	900 °C for 3 h, mixed with activated carbon (2:3 C:CaO), impregnated with NaOH (30%) and calcined at 500 °C for 5 h	C/CaO/NaOH	NR	Palm oil	0.5:1 (w/w), 7.5, 65, 180	95.12	NR	[39]
20.	Crab shell	900 °C and mixed with Na-ZSM-5.	CaO/Na-ZSM-5	385	Neem oil	12:1, 15, 75, 360	95	NR	[70]
21.	Snail shell	900 °C, 4 h, hydration (80 °C, 8h) and dehydration (860-900 °C, 3.5 h)	Nano-CaO	9.37	*H. wightiana* oil	12.4:1, 0.892, 61.6, 145.154	98.93	5 (87.46)	[71]
22.	*Chicoreus brunneus* shell	900 °C, 2.5 h followed by hydration (60 °C, 24 h), and dehydration (800-1100 °C, 3 h)	CaO	1.56	Rice bran oil	30:1, 0.4, 65, 120	93	7 (80)	[72]
23.	*P. erosa* seashells	900 °C, 2.5 h followed by hydration (60 °C, 6 h), and dehydration (600 °C, 3 h)	Nano-CaO	90.61	Jatropha oil	5.15:1, 2, RT, 133.1	98.54	6 (90.1)	[42]
24.	Waste cockle shells	900 °C, 3 h followed by hydration with deionized water (60 °C, 3 h) and dehydration (650 °C, 2 h)	Nano-CaO	13.91	Palm oil	8:1, 3, 60, 3	94.13	NR	[43]
25.	Ostrich bones	600-1000 °C, 4 h	Ca-HAP	3.61	WCO	15:1, 5, 60, 240	90.56	4 (87)	[75]
26.	Cow bones	400-800 °C, 8 h	Ca-HAP	3.25	WCO	12:1, 10. solar, 240	96	10 (94)	[76]
27.	Goat bone	900 °C, 3 h	CaO	NR	Microalgae	11:1, 2, 60, 180	92	NR	[77]
28.	Chicken-fish bone	1:1 chicken and fish bones calcined at 1000 °C for 4 h	CaO-HAP	34.73	WCO	NR, 1.98, 65, 94	89.5	4 (65)	[78]
29.	Waste animal bone	900 °C, then soaked in KOH solution	Ca-HAP/KOH	NR	Pre-treated Jatropha oil	9:1, 6, 70 ± 3, 180	96.1	4 (86)	[79]
30.	Beef bone	1000 °C for 4 h, followed by hydrothermal treatment at 200 °C for 12-48 h	Ca-HAP	8.636	Honge oil	12:1, 2.5, 65, 120	96	5 (96)	[80]
31.	Sheep bone/fly ash	900 °C, 2 h, followed by impregnation with fly ash.	Ca-HAP/fly ash	11.3	Mustard oil	5.5:1, 10, 65, 360	90.4[c]	7 (80.3)	[81]

[a]Calcination temperature unless otherwise stated

[b]MTOR, catalyst loading (wt. %), temperature (°C), reaction time (min unless otherwise stated)

[c]Conversion

3 Plant biomass-based catalysts

3.1 Plant-derived basic catalysts

3.1.1 Different parts of plants

Recent efforts to reduce the cost of biodiesel production have combined with environmental concerns to lead to the advent of plant biomass-derived material as a cheap, renewable, and environmentally benign catalyst source (**Table 3**). Simple burning of waste biomass to ash has provided active catalysts with high levels of (basic) oxides such as K_2O, CaO [82][83][84], K_2CO_3 [85][86] and KCl [84] as the major components. With an intent to produce a green, easy to synthesize and economical catalyst, Pathak *et al.* [82] have prepared *Musa acuminata* peel ash (MAPA) catalyst by simple burning in the open air. The MAPA yielded a catalyst estimated to have 65.11 % potassium (K_2O) and a total surface area of 1.45 $m^2 g^{-1}$. This yielded 98.85 % biodiesel from soybean oil (6:1 MTOR, 7 wt. % catalyst loading at room temperature for 4 h). However, the yield reduced significantly, to 52.16 %, after 4 cycles due to the loss of potassium and calcium and the accumulation of glycerol and esters on the surface of the catalyst, blocking the active sites. The product soybean biodiesel was tested for its physico-chemical characteristics and the result met the standards of both European and ASTM D 6751 criteria (EN 14214). In recent work, Rajkumari *et al*. [87] burned the trunk of banana to obtain *M. acuminate* banana trunk ash (MBTA) ash, before using it to obtain a free fatty acid conversion of 98.39 % from the transesterification of soybean oil. As detected by XPS, K_2O is the main basic site, contributing 58.72 wt. % of the ash catalyst. The catalyst showed a somewhat higher total surface area (39.067 $m^2 g^{-1}$) and pore volume (0.21 $cm^3 g^{-1}$) than in the MAPA work above. However, a high catalyst loading of 14 wt. % and longer reaction time of 360 mins were required for biodiesel generation. Hence, the K_2O content (higher in MAPA than MBPA) represented the major factor in determining the basicity of either catalyst. An orange peel ash catalyst obtained by simple burning of the precursor revealed potassium and calcium contents increased from 0.18 % and 0.03 % (in the dried peel) to 14.67 % and 7.34 % (orange peel ash). The ash showed high porosity (0.428 $cm^3 g^{-1}$) and total surface area (605.60 $m^2 g^{-1}$). It contained two highly basic components; K_2O (51.64 wt. %) and CaO (25.67 wt. %). Albeit a 7 wt. % catalyst loading was needed, a 98 % biodiesel was then obtained from soybean oil. This catalyst provided only modest stability though – returning an 85 % yield after 5 cycles [83].

Whilst open burning of biomass to produce ash catalyst is simple and economical, calcination drives up basicity by decomposing the carbon content of the ash catalyst [85][88] and often leads to an increase in surface area as well [89]. In the meantime, care has to be taken

over the temperature of calcination as too high a temperature can led to a decrease in surface area due to sintering [90]. In recent work, with the aim of increasing the concentration of the basic component (K) through decomposition of the carbon content by calcination of the biomass, an ash catalyst was prepared by calcining kola nut pod husk (KNPH) at 300-1100 °C. The potassium content, only 8.21 % in raw KNPH, was slightly increased to 12.22 % in the ash produced by its open-air burning. Interestingly, on calcining the ash at 500 °C, the K concentration increased to 47.14 %, mainly due to the decomposition of organic material during calcination. Potassium is now present mainly as $K_2Ca(CO_3)_2$ and $K_2CO_3 \cdot 1.5H_2O$, as recorded by PXRD. Compared to other studies, the optimal ash preparation temperature was relatively low. Most impressively though, at 96.28 % after 4 cycles, biodiesel yield was rather stable for a biomass-derived catalyst [85].

The positive impact of calcination on the basicity and surface area of an ash-based catalyst was reported by Gohain *et al.* [89], who calcined *Musa balbisiana* Colla (banana) ash (BPA) at 700 °C for 4 h to give CBPA. In this case, apart from increasing the basicity, calcination slightly enhanced catalyst porosity and total surface area (the latter from 10.176 (BPA) to 14.036 m^2g^{-1} (CBPA)) leading to improved catalytic potential. Another determinant of alkalinity and catalytic activity are potassium and calcium content, and these were estimated to be 41.37 and 36.08 %, respectively. A Hammett indicator test on both BPA and CBPA revealed $9.8<H<12.2$ and $9.8<H<18.4$ respectively, indicating higher basicity for CBPA. Under optimized conditions, the oil conversions using BPA and CBPA were 63.88 and 100 % respectively. The higher reactivity of CBPA was attributed to the combination of higher surface area and basicity. However, akin to many other studies, stability proved a problem and after just 5 transesterification cycles the yield was reduced to 50 %. This depreciation in yield was attributed to the loss of active species. Correspondingly, the potassium and calcium content of the CBPA catalyst after the fifth cycle was 30.11 % and 32.40 % respectively by EDX analysis.

One example of a heterogenous basic catalyst made by the same basic route as described above came from calcining the ash of dried banana peel at 700 °C for 4 h. The activity of the resulting catalyst was attributed to its K_2CO_3 content (potassium represented 99.73 wt. % of metal present). Morphologically, the catalyst was glossy and spongy in nature, with a total surface area of 4.442 $m^2\ g^{-1}$. Using Response Surface Methodology-Central Composite Design (RSM-CCD), which is a very useful statistical technique for calculating optimal reaction conditions, transesterification conditions of 7.6:1 MTOR, 2.75 wt. % catalyst loading at 65 °C for 69.02 mins were arrived at, with a 99.79 % theoretical yield expected. To validate

the accuracy of the model, the predicted optimum values were applied in laboratory experiments and a 98.5 % yield was observed, thereby showing the reliability of the model [86]. Etim *et al.* [91] produced ash catalysts from ripe plantain (*Musa paradisiacal*) fruit peels at different temperatures (500, 700, 900, and 1100 °C) to probe the effects of calcination temperature. Calcination at 700 °C produced the highest potassium (K_2CO_3) content (51.02 %). Using the RSM-CCD, a 99.2 % biodiesel yield was predicted, and a 99.3 % yield was observed. The closeness of the predicted and observed biodiesel yields again validated the reliability of the model. A leaching test was performed on the biodiesel, and it was observed that while the unwashed biodiesel had Na/K and Ca/Mg concentrations of 115.6 and 0.96 ppm respectively, these levels dropped to 1.8 and 0.42 ppm respectively after washing.

Moving from skins to husks and shells, powdered walnut shell was calcined at 800 °C for 2 h twice to yield a biochar. The potassium (K_2O) composition was observed to be 23.55 %, and a biodiesel yield of 98 % was achieved from soybean oil. However, like many basic biowaste catalysts, after 4 cycles of transesterification the yield was reduced to a very low 33.4 % [92]. In a similar study, a kola nut pod husk catalyst was combined with non-edible, low-cost biodiesel feedstock *Hevea brasiliensis* oil, whereupon a yield of 96.97 % biodiesel was obtained [93]. In similar research, waste *Brassica nigra* was calcined at 550 °C, which is a relatively low temperature for calcination [84]. The prepared catalyst had a potassium level of 56.13 % (in the forms of K_2O, K_2CO_3 and KCl), a total surface area of 7.3 $m^2 g^{-1}$ and showed a high yield of soybean oil biodiesel (yield 98.79 % in 25 mins). Interestingly, a low E_a of 27.87 kJ mol^{-1} was observed, explaining rapid product formation (transesterification of vegetable oil with excess methanol follows a pseudo-first order reaction rate law and the E_a usually ranges from 21 kJ mol^{-1} to 84 kJ mol^{-1}) [94]. Of further significance, the catalyst was reasonably stable, with only a 2 % decline in the yield, albeit this was measured up to only a third reaction cycle (where the yield was 96 % in a rather longer 135 mins). Leaching of active components from the recycled catalyst was recorded using AAS and XPS analyses. The AAS analysis of the three times-recycled catalyst showed a decrease in K from 343.89 ppm (fresh) to 320.93 ppm (after the 3rd cycle), but showed just a negligible decrease in Mg and Ca concentration. XPS analysis of the recycled catalyst confirmed the decrease in potassium content from 15.13 % to 10.19 % [84].

Remaining with modest preparation conditions, Nath *et al.* [95] synthesized a renewable catalyst by calcining waste *Sesamum indicum* plants at 550 °C. The resulting catalyst incorporated potassium (K_2CO_3 and K_2O) at 29.64 % and Ca (CaO and $CaCO_3$) at 33.80 % but

showed a modest total surface area of 3.66 m^2 g^{-1}. It still returned an impressive catalytic activity (yield 98.9 % biodiesel in 40 mins using sunflower oil). However, this required a high 12:1 MTOR and a 7 wt. % catalyst loading. The prepared catalyst was fairly reusable, maintaining a yield of 94.2 % (in 165 mins) in the 3rd cycle. XPS analysis was used to determine the leaching of active component K. The catalyst was probed after initial calcination and again sulfonated. The morphology and chemical composition of the catalyst was studied by TEM. The low resolution TEM image in **Fig. 6A** shows irregular cylindrical and hexagonal particles. Meanwhile, high-resolution TEM imaging revealed well-ordered, porous materials **(Fig. 6B–E)**. The SAED pattern (**Fig. 6F**) shows the presence of mixed polycrystalline components in the catalyst.

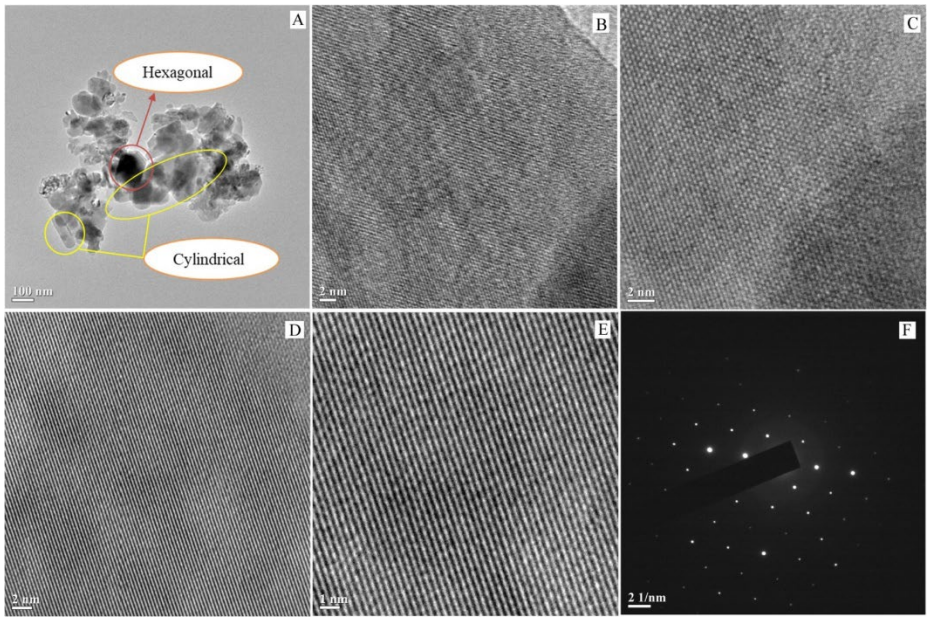

Fig. 6. TEM images (A–E) and the SAED pattern (F) of calcined *Sesamum indicum* catalyst. Scale bars: 100 nm (A), 2 nm (B–D), 1 nm (E) and 2 nm^{-1} (F). Reproduced from Ref. [95].

Banana peduncle constitutes approximately 13 % by mass of harvested banana clusters. Having no commercial value, it represents an attractive precursor for low-cost biocatalyst preparation. To test ash catalyst produced from banana peduncle, red banana peduncle has been calcined at 700 °C for 4 h to give a catalyst where potassium constituted a major percentage of the elemental composition (42.23 %). Calcination increased the total surface area from 24.46 m^2g^{-1} to 45.99 m^2 g^{-1} and the pore volume from 0.083 to 0.14 cm^3 g^{-1}. The catalytic activity of banana peduncle ash catalyst in transesterification was optimized by RSM-CCD, and the optimum reaction conditions recorded as 2.68 wt. % catalyst loading, MTOR 11.46:1 at 65 °C for 106 min, affording 98.73 % conversion from *Ceiba pentandra* oil [96]. The same research

group investigated *Musa spp*. "Pisang Awak" peduncle-derived ash calcined at 700 °C. Morphology studies using SEM imaging of uncalcined banana peduncle (UBP) are depicted in **Fig. 7** (a, b), with the calcined (CBP) variant in **Fig. 7** (c, d). Data indicates the effect of calcination temperature. UBP shows voids, cracks, and irregularly distorted rough surfaces, but few perforations or pores. After calcination, these latter features are much more evident. This porosity points to an increase in the surface area of the catalyst, which potentially enhances activity. Also, on calcination, the K contribution was found to increase from 63.64 (UBP) to 68.37 wt. % (CBP). RSM-CCD software predicted a FAME yield from *Ceiba pentandra* oil of 99.36 %, with the optimal conditions of 1.978 wt. % catalyst, 60 min reaction time, and 9.20:1 MTOR. Experimentally, 98.69 ± 0.18 % was observed. The requirement of a low catalyst loading and a short reaction time suggested the feasibility of using calcined banana peduncle specifically as a catalyst for biodiesel production [97].

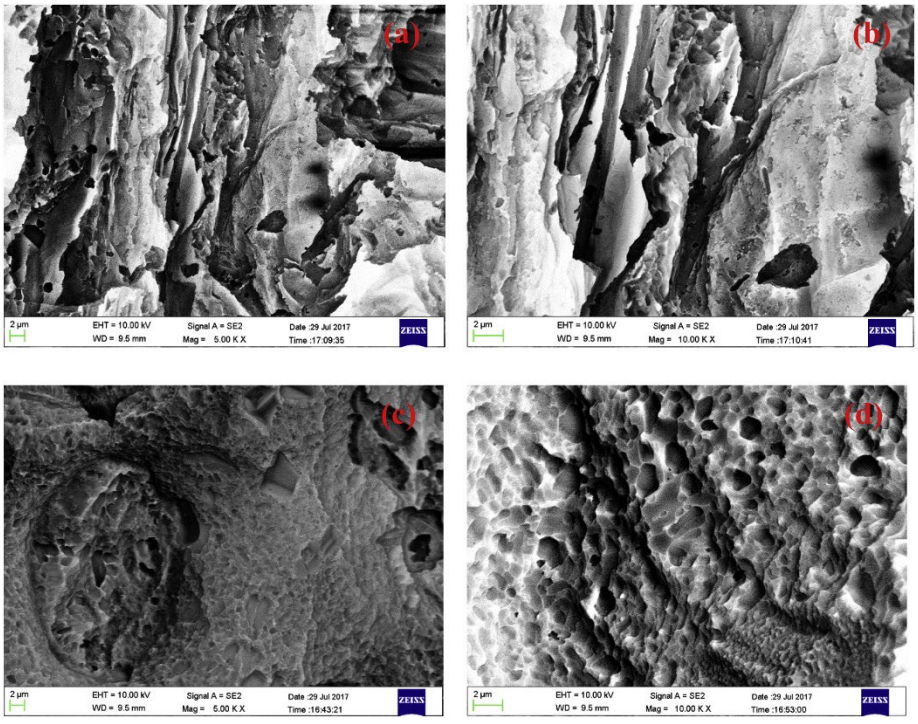

Fig. 7. SEM images of uncalcined (a, b) and calcined (c, d) banana peduncle revealing the development of porosity in the latter. Reproduced from Ref. [97].

In another study the catalytic activity of Cupuaçu (*Theobroma grandiflorum*) seed shell ash was evaluated by ethanolysis of soybean oil and the process was optimized using RSM and analysis of variance (ANOVA). The significance of the different process parameters and their combined effects were established through CCD. At 10:1 MTOR, 10 wt. % catalyst loading at 80 °C for 8 h, the optimal conditions were less compelling than for several other systems.

583 Nevertheless, using soybean oil as a feedstock gave 98.36 % oil conversion; in good agreement
584 with the predicted conversion of 97 %. Upon reusing the catalyst for two cycles, leaching of
585 active species was observed by Fourier transform infrared (FT-IR) spectroscopy. However, 98
586 % oil conversion to biodiesel was still achieved [98].

587 Another study has observed that calcination at the relatively modest temperature of 700
588 °C was optimal for producing catalyst from cocoa pod husk ash. Its efficacy was attributed
589 mainly to the high potassium content (59.2 %). Using statistical optimization RSM-CCD, the
590 best transesterification conditions for producing biodiesel from *Azadirachta indica* oil were
591 generated. In particular, an exceptionally low 0.65 wt. % catalyst loading was computed, which
592 nevertheless yielded an impressive 99.3 % biodiesel. However, recyclability of the catalyst was
593 not tested [99].

594 A cost-effective and eco-friendly heterogenous catalyst was prepared from Elephant
595 ear pod husk. It catalyzed a transesterification of blended rubber and neem oil under microwave
596 heating. While some husks were powdered without any further treatment, some were converted
597 to ash and calcined at 300-1100 °C. As expected, it was observed that the percentage of
598 potassium was highest in calcined biomass, and calcination at 700 °C once again produced the
599 highest percentage of potassium (K_2CO_3). Further alkalinity was provided magnesium, calcium
600 and iron. The K content of raw, burnt and calcined husk (700 °C) were 1.86, 17.55 and 50.01
601 wt. % respectively, showing a sequential increase in K content, and thereby basicity.
602 Interestingly, the transesterification of blended rubber and neem oil under microwave heating
603 at 150 W for only 5.88 min yielded 98.77 % biodiesel, which was close to the RSM-predicted
604 yield of 99.61 %. Though this opened up the possibility of short reaction times, after 4 cycles
605 the yield decreased to 74.68 % due to leaching of active sites [100].

606 In an attempt to boost the eco-friendly and cost-effective credentials of a new catalyst,
607 calcination of dried *Musa paradisiaca* peel, trunk and rhizome at 550 °C was attempted to
608 investigate the potential of using different parts of the plant. The percentage of potassium in
609 the calcined banana was highest in the trunk (36.31 wt. %), followed by rhizome (30.06 wt. %)
610 and peel (29.25 wt. %). However, basicity of catalyst increased in order 1.39 mmol g^{-1}
611 (rhizome) < 1.43 mmol g^{-1} (peel) < 1.59 mmol g^{-1} (trunk). In line with potassium content,
612 calcined catalyst prepared from the trunk afforded the highest biodiesel yield (97.65 %) under
613 optimized transesterification conditions using Jatropha oil. The rate constant and E_a for all three
614 catalysts were calculated using the Arrhenius equation. The slopes of peel, trunk, and rhizome

615 catalysts were found to be −5.8553, −5.7208 and −5.8848, and E_a was calculated as 48.68,
616 47.56, and 48.93 kJ mol^{-1} respectively (**Fig. 8**). Additionally, the burnt trunk (without
617 calcination) was also tested and found to yield less biodiesel under the conditions optimized
618 for calcined trunk. This was considered due to lower K content [101].

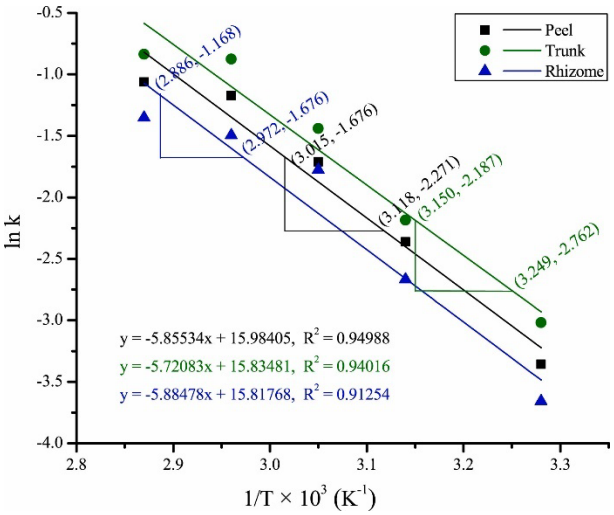

619

620 **Fig. 8.** Arrhenius plot of ln k versus 1/T (Reaction temperatures = 32, 45, 55, 65 and 75 °C).
621 Reproduced from Ref. [101]

622 Research by Gohain *et al.* [102] showed that in a dried, ground and calcined (700 °C)
623 *Carica Papaya* stem. potassium (as K_2CO_3) constituted the major component of its active sites.
624 Though perhaps most importantly, the surface area was 78.681 $m^2 g^{-1}$ and the pore volume was
625 0.349 $cm^3 g^{-1}$. Such an open structure was considered vital to enhancing effective mass transfer
626 during transesterification, though in the event, oil extracted from microalgal species
627 *Scenedesmus obliquus* achieved a modest 93.33 % conversion. Moreover, after 6 cycles this
628 had dropped somewhat, to 85.4 %. A study conducted on the viability of using waste sugar
629 beet as the source of a heterogenous catalyst revealed 93 % conversion [103]. Calcination
630 temperature varied between 600-1000 °C. A temperature of 800 °C generated the most efficient
631 catalyst. Interestingly, the active metal oxide in the calcined sugar beet waste is CaO (90.1 wt.
632 %) while in most other biomass waste, K (as K_2O, KCl, K_2CO_3) is found in large quantities.
633 With a moderately high total surface area of 27.9 $m^2 g^{-1}$, this Ca catalyst converted sunflower
634 oil, yielding 93 % biodiesel using a low 1 wt. % loading. Problematically, the catalyst showed
635 poor recyclability due to leaching of CaO into the glycerol by-product, leading to the formation
636 of calcium diglyceroxide [104]. This leaching was also commented on for many waste shell-
637 derived CaO systems in the above section. In another study, ash catalyst was derived from dried
638 and ground Tucuma peel calcined at 800 °C. On the positive side, the catalyst showed high K,

P, Ca, and Mg content as well as thermal stability up to 800 °C. However, its surface area was just 1.0 $m^2 g^{-1}$ and, while it promoted the transesterification of soybean oil, it gave just a 97 % yield [105].

In other interesting work, 100 % conversion of pre-treated WCO to biodiesel was achieved at room temperature using an ash catalyst prepared from calcined *Tectona grandis* leaves (CTGL). This material offered a high surface area of 116.83 $m^2 g^{-1}$, and XRD analysis revealed the presence of metal oxides and carbonates in abundance, with strong peaks observed for K_2O and K_2CO_3, as well as for CaO and $CaCO_3$. The quantitative activity of CTGL was attributed to this combination of elemental composition and the high surface area, with the latter argued to provide better interaction between the reactants and the active sites [106]. Another investigation, by Onoji *et al.* [88], showed the impact of calcination on the production of catalyst. Rubber seed shell was dried in an oven at 110 °C, powdered and calcined at the relatively low temperatures of 40-800 °C. In line with other work, thermogravimetric analysis revealed that the highest temperature tested was optimal. That done, it was then established that calcination above 800 °C did not have any significant effect on the nature of the catalyst. Lower temperature calcination did enhance the total surface area from 21.83 $m^2 g^{-1}$ (uncalcined) to 352.51 $m^2 g^{-1}$ (calcined at 800 °C). The latter had a pore volume of 0.1208 $cm^3 g^{-1}$. However, in spite of the impressive surface area, transesterification of rubber seed oil yielded just 83.06 % biodiesel. After 4 cycles, the yield had only reduced to 80 %. Nevertheless, it was clear that in this case raising surface area had failed to guarantee good performance. The low yield may have been due to the low density of K (9.38 wt. %) and Ca (10.43 wt. %) in the calcined catalyst

3.1.2 Blended catalyst sources

The previous section has highlighted the creation of bio-based catalysts from different parts of a range of plants, and this has led to research on mixing different types of lignocellulosic biomass. Recently, and for the first time, Falowa *et al.* [107] reported the application of blended agrowaste ash containing an equal mixture of cocoa pod husk, plantain peel and kola nut pod husk ashes (CPK). This was obtained by open combustion of each biomass in air followed by calcination at 500 °C for 4 h. The major constituents of calcined CPK proved to be potassium (47.67 %), calcium (5.56 %) and magnesium (4.21 %). A 98.45 % biodiesel yield was achieved with a low catalyst loading of 1.158 wt. % in only 6 min under microwave irradiation. In addition, a respectable biodiesel yield of 89.46 % was recorded on the 4^{th} cycle, which

suggested decent stability for the catalyst as compared to most biomass ash catalyst in pure form (not blended).

Similarly, Olatundun *et al.* [108] prepared ash catalyst by blending and calcining cocoa pod husk and plantain peel (CCPA). The biomasses were dried, then calcined at 300-1100 °C. As elsewhere in the review, calcination temperature significantly influenced the elemental constitution of the catalyst. In this work, calcination at 700 °C produced a catalyst with the highest percentage of potassium (51.94 %, as $K_2CO_3 \cdot 1.5H_2O$, K_2CO_3, KCl) but no calcium. In contrast, calcination at 500 °C resulted in 50.95 % potassium and 2.30 % calcium (CaO) and this was therefore chosen as the optimal calcination temperature based on economics. The surface area and pore volume were 18.86 $m^2\ g^{-1}$ and 0.04297 $cm^3\ g^{-1}$, respectively, and the catalyst yielded 99.03 % biodiesel from pre-treated Honne seed oil. The Taguchi method was used to derive optimal transesterification conditions. Impressively, reusing the catalyst for 3 cycles maintained a very stable biodiesel yield (98.98 %). Meanwhile, though stability was not probed, another study saw banana peel and cocoa pod husk blended and calcined at 700 °C to give a catalyst capable of promoting the transesterification of Palm kernel oil to yield ~99 % biodiesel [109]. In general, though, it can be concluded that blended ash catalysts show the potential for higher stability and reusability as compared to unblended biomass waste ash catalyst.

3.1.3 Magnetized biomass

Recent interest in the environmental and economic benefits of catalyst recovery has led to integrating magnetic compounds with the catalyst for the efficient reclamation and repeated reuse of the latter [110][111][112]. Magnetic catalysts offer the potential for easy and quantitative isolation and recovery using an external magnet, thereby reducing the time required for catalyst recovery (and reuse) compared to isolation by filtration or centrifugation. While the introduction of a magnetic component adds some synthetic complexity and deviates from pure biomass utilization, it is worth noting that one way in which the environmental credentials of this approach can be maintained is by fabricating nano-oxides from highly polluting fine-grained iron ore tailings [113] that result (as waste) from the excavation of iron ores.

In 2016, a magnetic catalyst, Na_2SiO_3@Ni/C was prepared and used for the production of biodiesel from soybean oil. [114] The catalyst was made by blending $Ni(NO_3)_2 \cdot 6H_2O$, solid urea and bamboo powders at 135 °C to generate $Ni(OH)_2$. The composite was then dried and

calcined at 700 °C to form a carbonaceous solid loaded with Ni nanoparticles. A second step was then required, in which the Ni/C composite was mixed with aqueous Na_2SiO_3 and calcined at 400 °C for 2 h to afford Na_2SiO_3@Ni/C. The total surface area and pore volume of the Ni/C after the first stage were 76.1 $m^2\ g^{-1}$ and 0.101 $cm^3\ g^{-1}$, respectively. After blending with Na_2SiO_3, these were reduced to 8.24 $m^2\ g^{-1}$ and 0.047 $cm^3\ g^{-1}$. Using a 9:1 MTOR and a 7 wt. % catalyst loading, soybean oil could be used to generate a respectable biodiesel yield of 98.1 %. In spite of the need for relatively high MTOR and catalyst loading and the good but unexceptional yield, the catalyst was easily recovered using a magnet. However, after 5 cycles the yield had dropped to the region of 80 %. The catalyst deactivation might, it was suggested, be attributed to leaching of the Na_2SiO_3 component in methanol [115]. Though efficacy had dropped, it was argued that simple and fast recoverability of the catalyst significantly enhanced the green credentials of the work.

In another study, magnetic solid base Na_2SiO_3@Ni/JRC catalyst (JRC = *Jatropha curcas* residue) was reported to afford a respectable biodiesel yield of 96.7 % from Jatropha oil. While the magnetic catalyst was easily recovered, after 5 cycles its effectiveness still dropped off (yield 75.3 %), meaning that the same problems of retaining activity seen above still remained [116]. Very recently, work looked at palm kernel shell (PKS)-supported KOH, denoted as Fe-KOH-PKS, but containing 23.0 wt% potassium as K_2O and in which the Fe phase existed as magnetite. The catalyst yielded 99.4 % biodiesel initially. However, recovering the catalyst by magnet led to just 70.1 % biodiesel after 4 cycles. This decline was attributed to active site loss (dissolution of K_2O under methanolic conditions is well documented in [82][92][95], though the authors also speculated about difficulties with magnetic recovery of the catalyst [117].

Finally, in this section therefore, lignocellulosic biomass derived from *Citrus sinensis* peel ash was straightforwardly magnetized using nano-Fe_3O_4 at 65 °C for 30 mins. The total specific surface area (SSA) of the thus derived catalyst was 15.55 $m^2\ g^{-1}$ and, while a low MTOR could be used, a 6 wt. % catalyst loading was needed to produce a respectable 98 % biodiesel yield from WCO. Importantly, the E_a of the transesterification reaction was found to be 34. 41 kJ mol^{-1}, which is well within the E_a required for transesterification. An external magnet was used to easily recover the catalyst, which showed excellent stability and was reused for several catalytic cycles, affording a high yield of 91 % even in the 9^{th} cycle [118]. It may be worth noting that non-magnetic orange peel (*Citrus sinensis*) ash hardly afford 85 % biodiesel yield in 5^{th} cycle of catalyst reuse [83]. In conclusion, magnetic catalysts are already

735 establishing themselves as having great potential to replace many conventional catalysts used
736 in biodiesel synthesis, largely due to their straightforward recycling, and often nearly
737 quantitative recovery (easily monitored but also inferred from performance retention). They
738 are therefore potentially very economical and can be environmentally benign. In the long-run
739 however, bringing down the cost involved in their more complex synthesis and reliably
740 preventing separation of magnetic and catalytic species represent major challenges.

741

742

743

744

745

746

747

748

749

750

751

752

753

Table 3. Different basic plant-derived ash catalysts used in biodiesel production. NR = not reported. CRC (Y) = catalyst reusability cycles (yield %). RT = room temperature.

No.	Catalyst source	Catalyst preparation	Catalyst surface area (m^2 g^{-1})	Feedstock	Conditions[a]	Yield (%)	CRC (Y)	Ref.
1.	*M. acuminata* peel	Burn in the open air	1.45	Soybean	6:1, 0.7, RT, 240	98.95	4 (52.16)	[82]
2.	*M. acuminata* trunk	Burn in the open air	39.07	Soybean oil	6:1, 14, RT, 360	98.39[b]	5 (61)	[87]
3.	Orange peel	Burn in the open air	605.60	Soybean oil	6:1, 7, RT, 420	98[b]	5 (85)	[83]
4.	*Musa balbisiana* Colla peel	Burn in the open air. Calcine at 700 °C, 4 h	14.036	WCO	6:1, 2, 60, 180	100[b]	5 (50)	[89]
5.	Musa'Gross Michel' banana peel	Burn in the open air. Calcine at 700 °C, 4 h	4.44	Napoleon's plume seed oil (*Bauhinia monandra*)	7.6:1, 2.75, 65, 69.02	98.5	NR	[86]
6.	Ripe Plantain peel	Burn in open air. Calcine at 700 °C, 4 h	18.80	Neem oil	0.2:1[c], 2.2, 65, 57	99.2	NR	[91]
7.	Walnut shell	Burn in open air. Calcine at 800 °C, 2 h	8.80	Soybean oil	12:1, 5, 60, 10	98	2 (33.4)	[92]
8.	Kola nut pod husk	Burn in open air. Calcine at 300-1000 °C, 4 h	5.21	Kariya seed oil (KSO)	6:1, 3, 65, 75	98.67±0.01	4 (96.28)	[85]

9.	Kola nut pod husk	Burn in open air. Calcine at 300-1000 °C, 4 h	NR	*Hevea brasiliensis* oil (HBO)	6:1, 3.5, 65, 75	96.97	NR	[93]
10.	*Brassica nigra* plant	Burn in open air. Calcine at 550 °C, 2 h	7.3	Soybean oil	12:1, 7, 65, 25	98.79	3 (96)	[84]
11.	*Sesamum indicum* plant	Burn in open air. Calcine at 550 °C, 2 h	3.66	Sunflower oil	12:1, 7, 65, 40	98.87	3 (94.2)	[95]
12.	*Cupuaçu* seeds shell	Calcine at 800 °C, 4 h	NR	Soybean oil	10:1, 10, 80, 480	98.36[b]	2 (98)	[98]
13.	*Musa spp* "Pisang Awak" peduncle	Calcine at 700 °C, 4 h	NR	*Ceiba pentandra* oil	9.20:1, 1.978, 65, 60	98.69 ± 0.18	NR	[97]
14.	*Musa acuminata* peduncle	Calcine at 700 °C, 4 h	45.99	*Ceiba pentandra* oil	11.46:1, 2.68, 65, 106	98.73±0.50[b]	3 (>90)	[96]
15.	Cocoa pod husk	Calcine at 700 °C, 4 h	2.76	*Azadirachta indica* oil	0.73:1[c], 0.65, 65, 57	99.3	NR	[99]
16.	Elephant ear pod husk	Calcine at 700 °C, 4 h	1.29	Blend of rubber and neem oils	11.44:1, 2.96, 150 W[d], 5.88,	98.77	4 (74.68)	[100]
17.	*Musa paradisiaca* trunk, peel, and rhizome	Calcine at 550 °C, 2 h	6.4, 4.1, 7.0	Jatropha oil	9:1, 5, 65, 9	97.65	3 (91.23)	[101]
18.	*Carica papaya* stem	Calcine at 700 °C, 4 h	78.68	*Scenedesmus obliquus*	9:1, 2, 60, 180	93.33[b]	6 (85.4)	[102]

19.	Sugar beet waste	Calcine at 800 °C, 2 h	27.9	Sunflower oil	4.5:1, 1, 75, 60	93[b]	5 (NR)	[103]
20.	Tucumã peels	Calcine at 800 °C, 4 h	1.00	Soybean oil	15:1, 1, 80, 240	97.3[b]	4 (80.75)	[105]
21.	*Tectona grandis* leaves	Calcine at 700 °C, 4 h	116.83	WCO	6:1, 2.5, RT, 180	100[b]	5 (NR)	[106]
22.	Rubber seed shell	Calcine at 800 °C, 3 h	352.51	Rubber seed oil	0.20:1[c], 2.2, 60, 60	83.06	4 (80)	[88]
23.	Cocoa pod husk, plantain peel and kola nut pod husk blend	Burn in air. Calcine at 500 °C, 4 h	16.871	Honne, rubber seed and neem oils	12:1, 1.158, 150 W[d], 6	98.45	4 (89.46)	[107]
24.	Cocoa pod husk-plantain peel blend	Calcine at 500°C, 4 h	18.86	*Honne seed oil*	15:1, 4.5, 65, 2.5	99.03	3 (98.98)	[108]
25.	Banana peel/ cocoa pod husk	Calcine at 700 °C, 4 h	NR	Palm kernel oil	0.80:1[c], 4, 65, 65	99.5/99.3	NR	[109]
26.	Bamboo powder (Na_2SiO_3@Ni/C), magnetic	$Ni(NO_3)_2·6H_2O$, urea, bamboo powders (700 °C, 2 h). Mix with Na_2SiO_3 and calcine (400 °C, 2 h)	8.24	Soybean oil	9:1, 7, 65, 100	98.1	5 (80.9)	[114]
27.	Jatropha residue (hulls) (Na_2SiO_3@Ni/JRC), magnetic	$Ni(NO_3)_2·6H_2O$, urea, Jatropha residue (700 °C, 2 h). Mix with $Na_2SiO_3·9H_2O$ (400 °C, 2 h)	12.2	Jatropha oil	9:1, 7, 65, 120	96.7	5 (75.3)	[116]

28.	Palm kernel shell. Fe-KOH-PKS, magnetic	Palm kernel shells, $FeCl_3$ (800 °C, 2 h). Immerse in 2 M KOH, dry at 120 °C	5.323	Palm oil	9:1, 7.5, 65, 120	99.43	4 (70.1)	[117]
29.	Citrus sinensis peel@ Fe_3O_4, magnetic	CSPA, $FeSO_4 \cdot 7H_2O$, $FeCl_3$ in deionized water, 65 °C. Stir 3 h and concentrate	15.5	WCO	6:1, 6, 65, 180	98	9 (91)	[118]

[a]MTOR, catalyst loading (wt. %), temperature (°C unless otherwise stated), reaction time (min).

[b]Conversion

[c]v/v

[d]Watts

3.2 Sulfonated biomass-based catalyst

3.2.1 Sulfonated carbonaceous material

Diverse reports exist of the use of abundant biomass for the synthesis of heterogeneous acid-functionalized catalysts for the simultaneous esterification-transesterification activity that produces biodiesel from low cost biodiesel feedstocks with high FFA. These catalysts have usually been synthesized by a two steps method: 1) biomass was converted to carbonaceous materials (CAMs) by pyrolysis or hydrothermal treatment at elevated temperature, 2) CAMs were heat-treated in the presence of sulfonating agents such as fuming H_2SO_4 [119], concentrated H_2SO_4 [120], *p*-toluenesulfonic acid (PTSA) [121] or 4-benzenediazonium sulfonate (4-BDS) [122] to increase surface acidity [123]. The resultant sulfonic acid-functionalized CAMs (SAFCAMs) contain polycyclic aromatic carbon sheets decorated with $–SO_3H$, –COOH, and –OH functional groups that work cooperatively to increase catalytic activity [124]. Problematically, however, high temperature is typically needed for stable CAM formation while a lower sulfonation temperature favors improved attachment of the acidic groups –COOH and –OH. The presence of these groups is well documented as increasing catalyst hydrophilicity and enhancing access to active sites for hydrophilic reactants like methanol. These types of catalyst also exhibit efficient absorption of long-chain organic molecules (e.g. fatty acids), eliminate water (the by-product of esterification), and demonstrate good adjustability of microstructure of the carbon material on which they are based [125]. In recent years, with the aim of making their preparation more economical, the one-pot synthesis of SAFCAMs at an intermediate temperature has been explored [126][127]. Recently developed SAFCAMs used in biodiesel production from inedible oils with high FFA are listed in **Table 4**.

Generally, pure cellulosic biomass such as xylose [128], sucrose [129] and glucose [130] are the precursor of choice for the synthesis of SAFCAMs. This is on account of the known resistance of lignocellulosic biomass to hydrothermal thermal carbonization (HTC, this involves the hydrothermal decomposition of carbohydrates in aqueous solution at elevated temperature) to form the CAM. Moreover, they remain unaffected by sulfonation conditions [131][132]. Recently, Tran *et al.* [128] used xylose as a precursor to develop pseudospherical SAFCAMs with high surface area (86 $m^2\ g^{-1}$) by sequential hydrothermal carbonization and sulfonation using H_2SO_4. The second step led to a slight decrease in surface area from the CAM (95 m^2g^{-1}), with particle size increasing. Sulfonation was confirmed by FT-IR and XPS

measurements and an increase in acid density from 0.05 to 1.38 mmol g^{-1}. However, transesterification of untreated WCO yielded only 89.6 % biodiesel, due to the presence of oligomers of triglyceride and other impurities in the oil. This decreased to 70.2 % after reusing the catalyst for 3 cycles, mainly due to the leaching of sulfonic groups ($–SO_3H$), as detected by NH_3-TPD analysis. The leaching was attributed to a combination of active site solubility in polar solvents [133][134] and the formation of sulfonate esters [133]. In addition, the decrease in acidity (activity) of the recycled catalyst may be attributed to the esterification of the –COOH and –OH groups with methanol and FFA respectively [132][11].

In order to minimize steps involved, time, energy consumed, complexity and capital cost required for preparation of catalyst, *simultaneous* sulfonation and carbonization in 'one-pot' has been carried out using glucose as a substrate to obtain an irregularly-shaped SAFCAM [11]. The sulfur content was recorded as 4.14 wt. % using ICP-OES analysis and the total acid content of the catalyst determined by titration was 5.31 mmol g^{-1}. The performance of this catalyst was tested in the esterification of oleic acid (a free fatty acid whose esterification can be employed as a model for biodiesel production) with methanol. Esterification under the optimal conditions yielded 97.7 % conversion to biodiesel. The catalyst proved to remain moderately stable; still affording 80.1 % conversion in the 5^{th} cycle. The decrease in catalytic activity was investigated using ss-NMR (solid-state nuclear magnetic resonance) spectroscopy, with data displaying a major difference between fresh and recovered catalysts in the 10-60 as well as 30-55 ppm regions. These were considered to be due to methoxy group formation by methanol-induced reversible decomposition of active sulfonic acid groups to sulfonate esters [133] and also esterification of carboxyl groups [132]. Interestingly, the acidity, and thereby catalytic activity, of the recovered catalyst could be regenerated by H_2SO_4 treatment. Thus-treated (used) catalyst showed an impressive 97.4 % oleic acid conversion. Another research group used 'one-pot' synthesized irregularly-shaped SAFCAMs to yield 93.04 % biodiesel under optimal conditions. The catalyst proved to remain stable after 3 cycles of transesterification [129].

Nata *et al.* [130] successfully converted glucose to pseudospherical SAFCAMs by using aqueous hydroxyethylsulfonic acid and citric acid in a 'one-pot' HTC. It was observed that, apart from increasing the acidity, hydroxyethylsulfonic acid played a highly significant role in stabilizing the size of the particles such that the SAFCAMs could be gradually grown to give 50-100 μm carbon spheres late in the process [135]. Compared to CAMs (11.28 $m^2 g^{-1}$) synthesized in the absence of hydroxyethylsulfonic acid, the surface area of these SAFCAMs

(25.72 $m^2 g^{-1}$) was rather higher. The catalyst had a total acidity of 1.99 mmol g^{-1} (by EDX, sulfur content amounted to 1.18 mmol g^{-1} assuming only $–SO_3H$). It achieved a ~95 % conversion of FFA to ester using WCO as a feedstock and acid-pretreated WCO was also converted to biodiesel in a modest 87 % yield using NaOH catalyst. Although it was hoped that citric acid would impart the catalyst with additional –COOH groups and so boost its activity, it largely failed to do this. Indeed, many SAFCAMs produced without using citric acid have total acidities higher than the one observed in this report.

In spite of the resistance of lignin to HTC, attempts to reduce the cost of biodiesel production have encompassed the use of lignocellulosic biomass waste as a cheap and abundant catalyst precursor. Biochar was therefore made from lignocellulosic biomass (oat hull) by partial carbonization (600 °C for 3 h). Sulfonation using concentrated H_2SO_4 at two somewhat lower temperatures (100 and 140 °C) showed that a sulfonation temperature of 140 °C (for 30 mins) under microwave irradiation resulted in the highest level of sulfur (S) attachment (7.55 wt. %) in the form of $–SO_3H$ groups. At the same time, the SSA of the biochar was reduced from 49.32 $m^2 g^{-1}$ to 5.43 $m^2 g^{-1}$, and this was attributed to the breakdown of biochar pores because of oxidation, condensation and/or carbonization of its structure during sulfonation. The most sulfonated form of this catalyst yielded ~90 % biodiesel in only 15 mins at 140 °C. The reusability of the catalyst was tested with and without a hexane wash before subsequent cycles of transesterification. Unwashed catalyst only yielded ~14 % biodiesel after three cycles while hexane-washed catalyst maintained a more respectable, yet clearly still rather depleted, 60 % biodiesel even after 6 cycles. The difference in the performance after 3 cycles of transesterification implied that pores on the surface of the catalyst were becoming blocked with biodiesel and/or glycerol after the initial transesterification and that washing with hexane effectively prevented clogging of these pores [51].

Waste *Jatropha curcas* seed cake has been used as a SAFCAM catalyst precursor, with carbonization at 350 °C for 4 h followed by sulfonation with H_2SO_4 at 90 °C for 5 h [136]. A biodiesel yield of 99.13 % was achieved which, for a SAFCAM, is notably high. However, after 4 cycles of transesterification, this was reduced to 81.03 % and the acidity was also reduced. However, a leaching test using barium chloride showed a negative result, indicating that any lost sulfur sites were not present in the reaction mixture in the form of sulfuric acid. As recently as 2020, Behera *et al.* [137] applied SAFCAMs to the production of biodiesel using algal feedstock. CAMs (or biochar) were prepared from peanut shell, sugarcane bagasse, corncob, and coconut shell, and were sulfonated with concentrated H_2SO_4. Out of the three

biomasses tested the highest sulfonic acid density (of 0.837 mmol g^{-1}, having a 6.616 m^2 g^{-1} surface area) was observed for peanut shell. Using this catalyst, algal oil was transesterified and a yield of 94.91 % was obtained, albeit with a high MTOR of 20:1. That notwithstanding, a more normal 5 wt. % catalyst loading was used at 65 ºC after 240 min. The reusability of the catalyst was tested and over 5 cycles, after which the biodiesel yield was observed to be 79.85 %, with the decline due to the leaching of sulfonic acid sites. Endut *et al.* [138] used coconut shell as a catalyst precursor in work that saw it carbonized and sulfonated at different temperatures and for different durations. The effect of catalyst preparation was analyzed using RSM. Optimization revealed that carbonization at 422 °C for 4 h, and sulfonation at 100 °C for 15 h should result in the highest yield of biodiesel. However, this was only 88.03 % and, even then, needed an MTOR of 30:1 MTOR. Using 6 wt. % catalyst loading at 60 °C for 6 h, palm oil was converted.

Again, in an attempt to minimize steps involved, time, and energy consumed on catalyst preparation, 'one-pot' *simultaneous* sulfonation and carbonization of coconut meal residue (CMR) was carried out using H_2SO_4 at a mild temperature for a very short time (100 °C for 1 h). Nevertheless, the sulfur content of the resulting catalyst was found to be relatively high; 3.89 wt. % (elemental analysis) corresponded to 1.215 mmol g^{-1} acid density. In the meantime, the total acid content of the catalyst was recorded as 3.8 mmol g^{-1}. This was much higher than was explicable by its sulfonic acid content and was attributed to the presence of –COOH and phenolic groups. The catalyst had a low surface area of 1.33 m^2 g^{-1} and a biodiesel yield of 93.7 % was achieved from waste palm oil (WPO) [139]. In other work, sugarcane bagasse-derived SAFCAM was reported to afford 85.1 % conversion from oleic acid. A 17 % decrease in catalytic activity after the first cycle was observed as sulfur content decreased from 0.59 to 0.56 mmol g^{-1}. Though the decrease in sulfur content was small, these findings still offered some insight into the catalyst's stability throughout the course of a 24-hour reaction. Further, reusability tests revealed that the catalyst retained only 76.5 % of its original efficiency and 86 % of its initial acid density after 5 esterification cycles [140].

Other work focused on corncob as a catalyst precursor. It was sulfonated with either H_2SO_4 or PTSA at 110 °C for 5 h [141]. PTSA proved more effective in removing cellulose and hemicellulose from the substrate biomass. This was of interest as the removal of cellulose and decomposition of hemicellulose while maintaining the lignin composition of the biomass was considered a route to increasing the thermal stability of the subsequently formed catalyst. The high thermal stability of PTSA-sulfonated catalyst can be seen in thermal gravimetric

analysis (TGA) where it decomposed at above 400 °C, whereas H_2SO_4-sulfonated catalyst started to decompose at 200 °C. Also, sulfonation with PTSA represented a less hazardous and greener option than using volatile, concentrated H_2SO_4. Higher SSA (297.5 $m^2 g^{-1}$) and pore volume (0.28 $cm^3 g^{-1}$) were observed in PTSA-sulfonated catalyst. In contrast, the acidity (1.93 mmol g^{-1}) and levels of FAME production were higher in H_2SO_4-sulfonated catalyst. Although these comparisons were interesting, at 86.5 % the yield of FAME using sulfuric acid was modest while that obtained using PTSA was just 80.4 %. This work showed how FAME production not only depends on total surface area and pore volume but also on the acidity of the catalyst. Overall, taking these data together and, of significant practical importance, considering biosafety, PTSA was argued to be a preferred sulfonating agent.

Wang *et al.* [142] prepared a sulfonated catalyst by heating chitosan powder with chlorosulfonic acid. Reaction proved possible under remarkably facile conditions (25 °C for 6 h), making the preparation of the catalyst extraordinarily simple and eco-friendly. A drop in the total specific area from 2.18 to 1.21 $m^2 g^{-1}$ post-sulfonation was attributed to the presence of surface sulfonic groups and acidity was observed as 3.81 mmol g^{-1}. This was on a par with other studies, but benefitted from rather more straightforward catalyst production conditions. Oleic acid esterification using a 15:1 MTOR, 3 wt. % catalyst loading at 75 °C for 3 h resulted in 95.7 % conversion. Meanwhile, after 4 cycles of esterification this had dropped to 85.7 %. Overall, while the spent catalyst showed respectable stability, this drop was significant, leaving the facile mode of catalyst production as the main interesting facet of this work.

A generalized method for the preparation of biomass-derived acid-functionalized CAMs is depicted in **Fig. 9**. In brief, the biomass is first converted to biochar (**Fig. 9a**) by hydrothermal or pyrolytic processes, before undergoing chemical activation using KOH [143][144], H_3PO_4 [145][146], $ZnCl_2$ [147] etc. to produce activated carbon (AC) with high SSA (**Fig. 9b**). In order to increase the acidity of a catalyst, the AC finally is sulfonated using H_2SO_4 [119], PTSA [121] or 4-BDS [122] to yield sulfonic acid-functionalized CAMs (**Fig. 9c**). Nonetheless, the biochar produced by carbonization also can be directly sulfonated to afford sulfonic acid-functionalized CAMs, although with a relatively lower SSA (**Fig. 9c**) [134] [11].

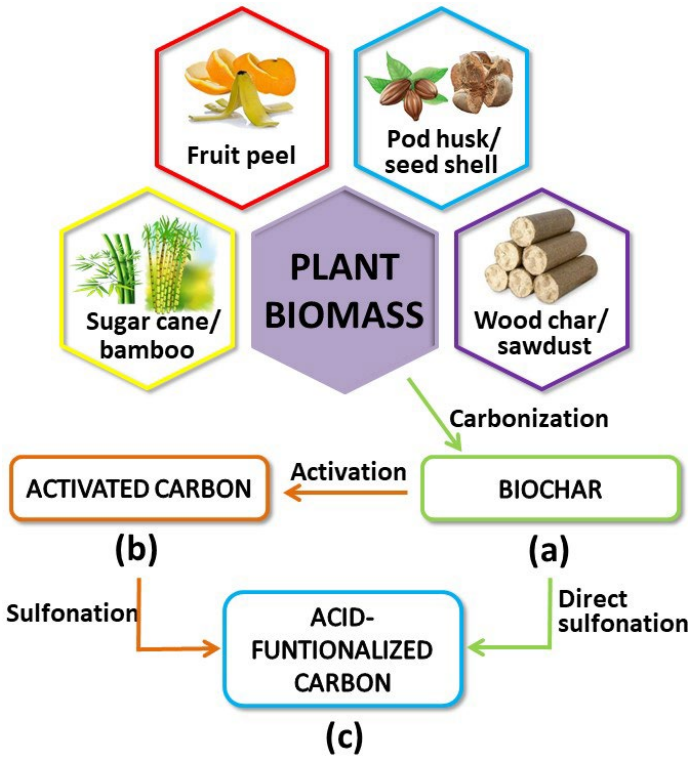

Fig. 9. General flowchart for the synthesis of biomass-derived sulfonic acid-functionalized carbonaceous materials (SAFCAMs)

915

916 **3.2.2 Sulfonated, pre-activated carbonaceous material**

917 The promising scope of sulfonated carbonaceous biomass in renewables catalysis has
918 highlighted the need for further research to enhance catalyst efficiency and, more particularly,
919 stability. Typical carbon-based materials have low surface areas and pore volumes and the
920 potential of pre-activation has been recognized for addressing these issues.

921 In this domain, waste orange peel was activated using KOH at 180 °C for 6 h, after
922 which sulfonation was carried out using H_2SO_4 at 200 °C for 24 h [143]. During the
923 hydrothermal carbonization, KOH acted as an activation agent and template for formation of a
924 mesoporous structure [148]. The activated catalyst had a 44 m^2 g^{-1} surface area, which is higher
925 than most SAFCAMs. Conditions of transesterification were optimized using the statistical tool
926 Box-Behnken Design (BBD), yielding 91.68 % biodiesel from corn acid oil feedstock at 20:1
927 MTOR and 5 wt. % catalyst loading at 65 °C for 275 min. Disappointingly though, after 4
928 cycles of transesterification the yield was reduced drastically to 16.43 %. This sudden decline
929 could be attributed mainly to the severe leaching of S content from 3.68 wt. % (fresh) to 1.58

930 wt. % (4th recycling) [143]. Similarly, through a 'one-pot' carbonization-sulfonation process
931 [149], orange peel (OP) was employed to create carbon-based solid acid catalysts. Model
932 reagent oleic acid was then converted to methyl oleate, giving 96.51±0.4 % yield in the first
933 cycle. Further catalytic cycles were then investigated, returning a conversion of 83.29±0.5 %
934 in the 5th cycle. The authors reported that leaching of sulfur from 1.96 mmol g^{-1} in fresh catalyst
935 to 0.99 mmol g^{-1} on 5th use was mainly responsible for the drop in yield.

936 The study of an activated bamboo sulfonated with benzylsulfonic acid at 30-80 °C for
937 2-60 min showed that maximum acid density and catalytic efficiency (90 %) could be achieved
938 under the fairly undemanding conditions of 50 °C for 10 min. After sulfonation, the surface
939 area of the catalyst was reduced. But having dropped from 919.04 to 225.71 $m^2 g^{-1}$, it was still
940 significant. The optimized catalyst yielded 96 % biodiesel using oleic acid as a feedstock in a
941 7:1 ethanol/oleic acid mixture at 85 °C for 180 min. However, a high 12 wt. % catalyst loading
942 was needed. Moreover, establishing something of a theme for sulfonated activated carbons,
943 after 5 cycles of transesterification, the yield dropped catastrophically to 28 % [125]. In a
944 similar study that aimed to diversify the source of sulfur, palm seed cake was activated using
945 orthophosphoric acid (H_3PO_4) followed by calcination (400 °C for 2 h) and sulfonation (H_2SO_4
946 at 150 °C under nitrogen for 12 h). The SSA of the emerging catalyst was significantly
947 increased by orthophosphoric acid treatment (from 107 to 658 $m^2 g^{-1}$), consistent with the view
948 that H_3PO_4 assists in the creation of porosity. At the same time, the pore volume increased from
949 0.15 to 1.18 $cm^3 g^{-1}$. Activation meant that when, after sulfonation, the SSA and the pore
950 volume were both reduced (to 483.07 $m^2 g^{-1}$ and 0.84 $cm^3 g^{-1}$, respectively), the catalyst still
951 had a somewhat open and accessible structure. The acid density of palm seed cake, activated
952 palm seed cake and sulfonated activated palm seed cake were 5.44, 8.35 and 12.08 mmol g^{-1}
953 respectively. Transesterification of palm fatty acid distillate feedstock using the catalyst
954 produced biodiesel in an impressive 97.8 % yield. Apart from the requirement of low catalyst
955 loading (2.5 wt. %), the catalyst showed a modest improvement in stability on repeated reuse,
956 given its use of a pre-activated CAM. It produced a biodiesel yield after 8 cycles of 68.2 %
957 [145].

958 Tang and Niu [146] tested different temperatures and durations for the carbonization
959 and H_2SO_4 sulfonation of bamboo-derived carbon catalysts with a surface area of 1208 $m^2 g^{-1}$.
960 Carbonization temperatures of 220-550 °C and durations of 0.5-4 h were interrogated, as were
961 sulfonation temperatures of 75-135 °C over 0.5-8 h. Carbonization at 350 °C for 2 h generated
962 the largest SSA, which enabled the attachment of more sulfonic acid groups. Meanwhile,

963 sulfonation at 105 °C for 4 h gave the highest acid density (1.28 mmol g^{-1}). The catalyst was
964 activated by increasing the pore size with phosphoric acid. Free fatty acid conversion gave
965 product in 97.3 % yield using a 10:1 methanol-to-oleic acid ratio but, again, needed a high (10
966 wt. %) catalyst loading. The reaction was conducted at 65 °C for 2 h and, as in line with the
967 previous report, after 6 cycles of esterification the yield stood at a more modest 57.2 %. That
968 said, the same research group had earlier synthesized a bamboo-derived carbon catalyst
969 (without activation) that showed low recyclability on repeated use (27.84 % yield after 5
970 cycles) [134]. Hence, activation by phosphoric acid plainly helped.

971 In a study conducted by Hussein *et al.* [147] potato peel was activated using $ZnCl_2$, then
972 subjected to sulfonation using H_2SO_4 at 180 °C for 8 h. The SSA and total pore volume of
973 potato peel were found to be 15.7 $m^2 g^{-1}$ and 0.016 $cm^3 g^{-1}$, respectively, which were drastically
974 increased to 1027 $m^2 g^{-1}$ and 1.34 $cm^3 g^{-1}$ after activation. It was posited that $ZnCl_2$ achieved
975 this by eroding the carbon microstructure of the biomass. Though reduced in the next step, the
976 total SSA after sulfonation was still very high, at 827 $m^2 g^{-1}$. The catalyst was then used for the
977 esterification of oleic acid and methanol at a 12:1 MTOR using a 5 wt. % catalyst loading at
978 80 °C for 2.5 h. The first-time yield of 97.2 % fell to just over 70 % after five catalytic runs,
979 again demonstrating a good direction of travel for this research even if stability was still
980 modest.

981 Sulfonation using aryl diazoniumsulfonates has enabled the demonstration of similar
982 efficiencies as those seen when e.g. H_2SO_4 was used. This being so, they clearly represent
983 potentially interesting sulfonating agents. Moreover, they offer benefits including nonoxidative
984 sulfonation conditions, the requirement for only low concentrations of sulfonating agent,
985 retention of catalyst precursor structure and texture and high chemical and thermal stability.
986 Efficient sulfonation with aryl diazoniumsulfonates can be achieved after carbonization [150].
987 Konwar *et al.* [122] activated pogamia seed cake using phosphoric acid (500 °C for 1 h),
988 sulfonated the biochar using 4-benzenediazoniumsulfonate and used it as a catalyst for
989 conversion of *Mesua Ferrea* Linn oil with high FFA content to biodiesel. The composition the
990 feedstock was found to heavily influence optimal MTOR. The highest biodiesel yield (91 %)
991 was obtained from oil when transesterification was optimized at 20:1 MTOR and 5 wt. %
992 catalyst loading at 120 °C for 24 h.

993 Another catalyst precursor, corncob, was activated using phosphoric acid at 500 °C for
994 1 h and sulfonated using 4-benzenediazoniumsulfonate at 3-5 °C for 1 h. Sulfonation now

decreased SSA to a relatively lesser extent; from 793.4 $m^2 g^{-1}$ to 730 $m^2 g^{-1}$. The presumed attachment of sulfonic groups was confirmed by the increase in acidity between activated catalyst (0.843 mmol g^{-1}) and activated sulfonated catalyst (0.890 mmol g^{-1}). Biodiesel yield was estimated as 88.7 % from soybean oil using a 6:1 MTOR and 20 wt. % catalyst loading. Though the latter was somewhat high, it was noteworthy that reaction proceeded at 75 °C in a mere 2 mins using microwaves. Moreover, this diazoniumsulfonate-based system performed well upon reuse, maintaining 80 % efficiency after 5 cycles [52].

3.2.3 Magnetic sulfonated material

As mentioned earlier, the use of magnetic compounds in catalyst preparation can introduce some significant advantages [111][151]. In the context of SAFCAMs, a mesoporous, double-shelled magnetic catalyst was prepared by mixing chitosan and Fe_3O_4 in the presence of CTAB, tetraethyl orthosilicate and KOH. The double-shell of the resulting Fe_3O_4@chitosan@hollow-chitosan (FCHC) nanoparticles was observed to both prevent the core from being etched and increase the SSA of the catalyst. The double-shelled FCHC system was sulfonated with *p*-toluenesulfonic acid monohydrate at 25 °C overnight (giving FCHC-SO_3H), as shown in **Fig. 10**, where upon it was found that the SSA (54.3 $m^2 g^{-1}$) was higher than that of chitosan magnetic sulfonated catalyst (41.4 $m^2 g^{-1}$). This suggested the successful loading of sulfonic acid groups. A maximum biodiesel yield of 96.7 % was observed for FCHC-SO_3H at an albeit high MTOR of 15:1 using 4 wt. % catalyst dosage at 80 °C for 3 h and with oleic acid as a feedstock. This was still 84.3 % after 5 cycles of esterification. The decline in yield was attributed to a reduction in the number of active sites (stability) rather than loss of catalyst material through ineffective recovery. In addition, kinetic studies on the esterification showed that with FCHC-SO_3H the reaction benefitted from a relatively low E_a of 37.5 kJ mol^{-1} [151].

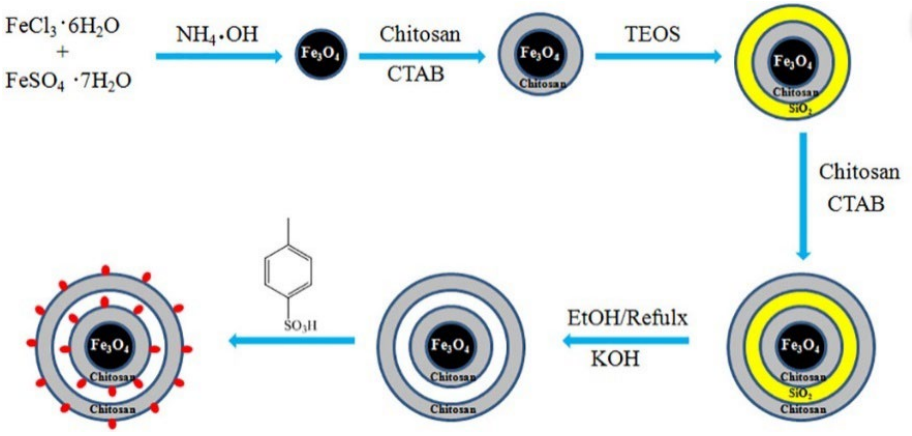

Fig. 10. Synthesis of the magnetic mesoporous chitosan-based catalyst FCHC-SO_3H. Reproduced from Ref. [151].

In another study, a magnetic cellulose catalyst was prepared by precipitation of cellulose microspheres with Fe_3O_4. Heteropolyacid $H_3PW_{12}O_4$ was immobilized thereon to produce a magnetic heterogeneous acid catalyst. Out of different transesterification parameters tested, the highest biodiesel yield of 93.1 % was achieved at an MTOR of 10:1 but requiring a 15 wt. % catalyst loading at 60 °C for 80 min. Recovery of catalyst was simple and proved highly efficient and the catalyst was reused in 4 cycles of biodiesel production, albeit with yield depleting to 80.7 % [152]. Another study focused on the effective recovery of magnetic sulfonated catalyst wherein jatropha hull was hydrothermally precipitated under optimal condition of 180 °C for 12 h, before being carbonized at 600 °C for 1.5 h, magnetized with Fe_3O_4, and finally sulfonated with H_2SO_4 at 180 °C for 12 h. The surface area of the catalyst decreased from an already low 2.37 to 1.92 $m^2\ g^{-1}$ after this last step, and the pore volume and pore diameter were also lowered. The best conditions for esterification required a slightly elevated MTOR of 18:1, 7.5 wt. % catalyst loading, 180 °C, and 7.5 h to afford a good biodiesel yield (95.9 %). Impressively, a drop of only 1 % in yield (94.3 %) was observed upon 5 cycles of reuse, highlighting the potential of efficient catalyst recovery [153].

Waste palm kernel shell has been used as a magnetic catalyst precursor. It was magnetized with Fe_3O_4 and sulfonated with H_2SO_4, whereupon a drastic decrease in Fe content from 64.00 wt. % to 19.31 wt. % (EDX analysis) after sulfonation was observed. This was accompanied by a drastic fall in magnetic properties as seen in the magnetization hysteresis loop. Interestingly however, the resulting magnetic sulfonated catalyst was observed to be very thermally stable. A biodiesel yield of 90.2 % was observed, which reduced to 73.6 %, after 4 cycles [154]. Meanwhile, a highly efficient heterogenous magnetic sulfonated catalyst was prepared from acai seed and red mud. A maximum biodiesel yield of 88 % was obtained under optimal reaction conditions [155]. Ibrahim *et al.* [156] used empty fruit bunch (EFB) as a catalyst precursor that was magnetized using $FeCl_3$ and sulfonated with chlorosulfonic acid (HSO_3Cl) to obtain the desired magnetic catalyst. Palm fatty acid distillate was then used as a feedstock, resulting in 98.6 % free fatty acid conversion efficiency. The catalyst was easily recovered, but after 6 cycles of esterification the conversion was reduced to ~79 %. The authors speculated that this was due to loss of iron species and acid active sites into the reaction medium as detected by elemental analysis and ICP-OES results.

Pyrolyzed cassava peel biochar, sulfonated and impregnated with Fe_3O_4, has been reported as a magnetic catalyst for the production of biodiesel using *Millettia pinnata* seed oil as a feedstock. The catalyst demonstrated a high surface area of 423.89 $m^2 g^{-1}$ and a 0.21 $cm^3 g^{-1}$ pore volume. It also showed three functional acidic sites (–OH, –COOH and $–SO_3H$). The S 2p spectrum in XPS analysis revealed peaks at 168.1, 168.9 and 169.9 eV that were attributed to S–C, S–O, and S=O bonds respectively. These data were taken as confirmation that sulfur was mainly present as $–SO_3H$ groups bonded to the aromatic carbon structure. Transesterification yielded 98.7 % biodiesel under optimum reaction conditions. The magnetic nature of the catalyst contributed to easy recovery, though reuse up to 5 times only allowed a 75 % yield [157]. Lastly, a palm oil EFB-derived magnetic catalyst with acid density of 0.28 mmol g^{-1} was reported to convert oleic acid to biodiesel in 97.6 % yield [158].

Table 4. Biomass derived sulfonated acid catalysts used for biodiesel production. NR = Not reported. CRC (Y) = catalyst reusability cycles (yield %).

No.	Sulfonated catalyst	Preparation	Catalyst surface area ($m^2\ g^{-1}$)	Feedstock	Conditions[a]	Yield (%)	CRC (Y)	Ref.
1.	Xylose	HTC at 190 °C, 24 h sulfonation with H_2SO_4 at 150 °C, 15 h	86	WCO	10:1, 10, 110, 240	89.6	3 (70.78)	[128]
2.	Sucrose	Sulfonate with H_2SO_4 at 250 °C, 2 h	NR	Oleic acid	10:1, 1.5, 67, 120	93.04	6 (~84)	[129]
3.	Glucose	Sulfonate with aq. $C_2H_6O_3S$ at 180 °C, 4 h	25.72	WCO	20:1, 10, 60, 180	95	5 (not affected)	[130]
4.	Glucose	Sulfonate with H_2SO_4 at 80 °C, 18 h	7.364	Oleic acid	20:1, 5, 80, 120	97.7	5 (80.1)	[11]
5.	Lignocellulosic biomass	Pyrolyze at 600 °C, 3 h, then sulfonate with H_2SO_4 at 140 °C, 30 min	5.43	WCO	10:1, 10, 140, 15	90	6 (60)	[51]
6.	Bamboo	Carbonize at 350 °C, 2 h, then sulfonate with H_2SO_4 at 105 °C, 2 h	0.25	Oleic acid	7:1[c], 2, 90, 360	98.4	5 (27.84)	[134]

7.	Peanut shell	Pyrolyze at 300 °C, 1 h, then 400 °C, 1h, then 600 °C, 30 min, sulfonate with H_2SO_4 at 100 °C, 1h, agitate at 50 °C, 24 h	6.616	Algal oil	20:1, 5, 65, 240	94.91	5 (79.85)	[137]
8.	Coconut shell	Carbonize at 422 °C, 4 h, sulfonate with H_2SO_4 100 °C, 15 h	24.17	Palm oil	30:1, 6, 60, 360	88.03	NR	[138]
9.	Jatropha curcas seed	Carbonize at 350 °C, 4h, sulfonate using H_2SO_4 at 90 °C, 5 h	1.92	JCO	12:1, 7.5, 60, 60	99.13[b]	4 (81.03)	[136]
10.	Sawdust biochar	Pyrolyze at 600 °C, 4 h, sulfonate with H_2SO_4 at 90 °C, 1 h	3.3	*Pongamia pinnatta* oil	9:1, 2, 85, 120	95.6	4 (85.7)	[159]
11.	Sugarcane bagasse	Simultaneous carbonization and sulfonation using H_2SO_4 at 150 °C, 8 h	NR	Oleic acid	20:1, 10, 65, 360	85.1	5 (76.5)	[140]
12.	CMR-DS-SO_3H	Sulfonate with H_2SO_4 at 100 °C, 1 h	1.33	Waste palm oil	12:1, 5, 65, 72	92.7	5 (>80)	[139]

13.	Corncob	Dry and pretreate with 2 wt. % H_2SO_4 for 120 °C, 5 min, sulfonate with H_2SO_4 and TsOH for 110 °C, 5 h	14.1	Oleic acid	15:1, 5, 60, 480	>80	3 (28.76)	[141]
14.	Chitosan	Sulfonate with chlorosulfonic acid at 25 °C, 6 h	1.21	Oleic acid	15:1, 3, 75, 180	94.4	4 (85.7)	[142]
15.	Orange peel	Activate using KOH at 180 °C, 6 h, sulfonate with H_2SO_4 at 200 °C, 24 h	44	Corn acid oil	20:1, 5, 65, 275	91.68	4 (82)	[143]
16.	Orange peel	Sulfonate with H_2SO_4 at 100 °C, 18 h	3.617	Oleic acid	15:1, 7, 60, 80	96.51±0.4	5 (83.29)	[149]
17.	Bamboo	Activate at 105 °C, overnight, sulfonate with sulfanilic acid at 80 °C, 1 h	225.71	Oleic acid	7:1[c], 12, 180, 85	96[b]	5 (28)	[125]
18.	Palm seed cake	Pyrolyze at 400 °C, 2 h, activate using phosphoric acid, calcine at 400 °C, 2 h and sulfonate with H_2SO_4 at 150 °C, 12 h	483	Palm fatty acid distillate	9:1, 2.5, 60, 120	97.8	8 (68.2)	[145]

19.	Pongamia seed cake	Activate using phosphoric acid at 500 °C, 1 h, sulfonate using BDS at 3-5 °C	483	*Mesua Ferrea* Linn oil	40:1, 5, 120, 1440	97.79	4 (62)	[122]
20.	Corncob	Activate with phosphoric acid at 500 °C, 1 h, sulfonate with BDS at 3-5 °C, 1 h	730.8	Soybean oil	6:1, 20, 75, 20	88.7	5 (88)	[52]
21.	Bamboo	Carbonize at 350 °C, 2 h, phosphoric acid activation, sulfonation with H_2SO_4 at 105 °C, 4 h	1208	Oleic acid	10:1, 10, 65, 120	97.3	6 (57.2)	[146]
22.	Potato peel	Activate using $ZnCl_2$, sulfonate with H_2SO_4 at 180 °C, 8 h	827.7	Oleic acid	12:1, 5, 80, 150	97.2	5 (68 %)	[147]
23.	Chitosan, magnetic	Magnetize using Fe_3O_4 at 80 °C, 1.5 h, sulfonate with *p*-toluenesulfonic acid at 25 °C, overnight	41.4	Oleic acid	15:1, 4, 80, 180	96.7	5 (84.3)	[151]
24.	Cellulose (cotton)	Precipitate with Fe_3SO_4 and sulfonate with $H_3PW_{12}O_{40}$	NR	P. chinensis seed oil	10:1, 15, 60, 80	93.1	4 (80.7)	[152]

25.	Jatropha hulls, magnetic	Precipitation at 180 °C, 12 h, carbonize at 600 °C, 1.5 h, magnetize with Fe_3O_4, sulfonate using H_2SO_4 at 180 °C, 12 h	46.7	Jatropha oil	18:1, 7.5, 180, 450	95.9	5 (94.3)	[153]
26.	Palm kernel shell, magnetic	Magnetize using Fe_3SO_4 at room temperature, 4 h, sulfonate with H_2SO_4 at 120 °C, 12 h	59.8	Used cooking oil	13:1, 3.66, 65, 102	90.2	4 (73.63)	[154]
27.	Acai seeds and red mud, magnetic	Carbonize at 400 °C, 3 h, sulfonate using H_2SO_4 at 80 °C, 3, h magnetized using red mud	60	Oleic acid	12:1, 5, 100, 60	88	4 (55.4)	[155]
28.	EFB, magnetic	Carbonate at 700 °C, 2 h, sulfonate using H_2SO_4 at 150 °C, 2 h, magnetize using $FeCl_3$	20.425	PFAD	16:1, 4, 199, 180	98.6[b]	6 (79)	[156]
29.	Cassava peel biochar, magnetic	Pyrolyze at 400 °C, 1 h, magnetize using nano-Fe_3O_4 at room temp, 8 h)	424	Millettia pinnata oil	11:1, 3, 65, 45	98.7	5 (75)	[157]

30.	Oil palm EFB, magnetic	Magnetize with $FeCl_3$ at room temperature, 5 h, sulfonate with H_2SO_4 at 150 °C, 10 h, carbonize at 500 °C, 1 h	38.51	Oleic acid	8:1, 5, 150, 90	97.6	NR	[158]

[a]MTOR, catalyst loading (wt. %), temperature (°C), reaction time (min)

[b]Conversion

[c]Ethanol:oil molar ratio

1062

3.3 Biomass-based bifunctional catalysts

As explained in Section 1, the cost and ethical implications of deploying edible oil as a biodiesel precursor has meant that inedible oils with their high FFA content have come to the fore in biodiesel production [160][161]. The unsuitability (on account of saponification reactions) of the basic catalysts that dominate TRIG transesterification for treating FFA-rich systems [162], has previously necessitated two-step processing whereby acid-promoted FFA esterification was followed by base-promoted TRIG reaction. The commercially unappealing prospect of conducting more complex, multistage synthesis has recently led to the advent of *bifunctional* catalysts that offer one-pot reactions and limit product extraction and separation steps [163]. These catalysts contain both acid *and* base active sites. Additionally, Brønsted acids help esterify the FFAs while Lewis acids can contribute to transesterification, introducing further potential control through the synthesis of catalysts with tunable Brønsted/Lewis acid ratios. Most recently, these catalysts have been combined with heterogeneous catalysis [164] through the development of solid-state bifunctional systems [163].

Maintaining the theme of developing more sustainable catalysts, researchers have started using biomass in bifunctional biodiesel production catalysis. Neem oil was used in an attempt to overcome the persistent need for high MTOR as well as elevated temperature and reaction duration. In so doing, researchers acknowledged the high FFA content of their starting material (4.43 %). To treat this, they generated a composite from corncobs modified using phosphoric and sulfuric acids (SCC) and KOH-loaded poultry droppings (KPD) [144]. Analysis verified the inclusion of acidic (P_2O_5), amphoteric (Al_2O_3) and basic (CaO) oxides. Whilst a high biodiesel yield of 92.89 % was subsequently achieved from NSO with respectable temperature and reaction time, a high MTOR ratio of ~15:1 was still required. Moreover, catalyst recycling revealed problems like those that have more widely bedeviled biodiesel catalysis. A drop in performance to 76 % after 4 cycles was speculated to be due to a combination of sulfate leaching and poisoning. In spite of these problems, more robust protection of catalyst integrity is emerging, albeit by diluting the bio-based content of the bifunctional catalyst.

In one report, CaO was combined with a tungsten molybdenum support by wet impregnation [165]. The CaO was derived from egg shell, though its wet impregnation into a support created by calcining $H_3PO_4 \cdot 12WO_3 \cdot xH_2O$ and $(NH_4)_6Mo_7O_{24} \cdot 4H_2O$ added complexity and lowered sustainability. Nevertheless, the power to vary the W/Mo intermetallic ratio

provided options. Transesterification was improved as W:Mo molar weight ratio was increased, with CaO-$W_{0.6}Mo_{0.4}$ giving the highest biodiesel yield (96.2 %). Interestingly, a high surface area was not required for effective reaction. However, a high 15:1 MTOR was needed. Reusability was strong by the standards of biomass-derived bifunctional catalysts; a 90 % biodiesel yield after 5 cycles was attributed to catalyst stability (reduced leaching) on account of Ca^{2+} replacing W(III) and/or Mo(VI) in the support [166]. However, the inorganic nature of this support makes accurate comparison with other biomass-derived catalysts difficult.

A similar approach to that outlined in [144] generated a simple system in which corncob alone was KOH-activated. The substrate was treated with sulfuric acid under various conditions, enabling a systematic assessment of SSA [167]. Unlike thermal treatment alone, pyrolysis in the presence of sulfuric acid increased this significantly. Hence, an SSA of 211 m^2 g^{-1} (600 °C for 4 h) rose to 877 m^2 g^{-1} (including 5:1 H_2SO_4:biomass). From an economic perspective, 600 °C for 1 h was used (SSA 627 m^2 g^{-1}) for subsequent KOH loading. While this catalyst returned a 97.8 % yield of biodiesel from WCO at an impressively low 45 °C, a high (18:1) MTOR was required. Reusability tests also revealed a complex but ultimately problematic picture. Though FFA esterification was maintained over 5 cycles, a dramatic loss of transesterification performance (to 35 %, proposed to be due to K^+ loss) offset the benefits of single-stage biodiesel production. Similar work by Brar et al. [168], intended to evaluate the technological viability of in situ transesterification using a bifunctional KOH/rice bran-derived activated heterogeneous carbon catalyst to produce microalgae-based biodiesel. Under optimized conditions, the direct transesterification approach resulted in a modest 80.9 % conversion to biodiesel after a reaction period of 1.5 h, with a biomass to S+CS (solvent and co-solvent) molar ratio of 1:10, a catalyst loading of 5 wt. %, and a temperature of 70 °C. GC-MS was used to analyze the biodiesel that was produced, and it was found to contain high unsaturated fatty acids (53.82 %) which reduce viscosity, allowing better functionality in adverse weather conditions. Here a co-solvent (hexane) helped in the miscibility and formation of a single phase between methanol (solvent) and the biodiesel feedstock (micro-algae), thereby improving the biodiesel yield [169][170].

The modification of CaO has been explored via a two-step process; the high temperature thermolytic generation of CaO in angel wing shell (AWS) was followed by sulfonation using sulfuric acid (3-11 M) under facile conditions [171]. The resulting catalysts (CAWS-$_{(3\text{-}11)}SO_4$) revealed $CaSO_4$ with diminishing levels of hydration as a function of sulfuric acid molarity. As evidenced by biodiesel yield (97.8 % from PFAD), CAWS-$_{(7)}SO_4$ optimally

balanced acid and base sites, albeit none of the composites prepared showed high SSAs and relatively high (5 wt. %) catalyst loadings were needed. In common with most other bifunctional catalysts reported, problems of stability remained, with only 46 % yield obtained from the 4th cycle. In other work, a bifunctional catalyst of crab shell-plantain peel-Al_2O_3, was used for a 'one-pot' simultaneous esterification and transesterification to produce biodiesel [172]. The catalyst's large surface area (260.35 m^2 g^{-1}) and pore volume (0.65 cm^3 g^{-1}) helped produce the a biodiesel yield of 93 % at a reaction temperature of 60 °C which, while not very high, was appreciably better than comparable catalysts [173][174]. In this case, crab shell-derived CaO, and metal oxides such as MgO and K_2O from the plantain contributed to the basicity, while Al_2O_3 offered acidic sites. After six cycles, a yields of still >80 % was maintained, demonstrating reasonable reusability of catalyst. It was argued that unreacted TRIGs poisoning the catalyst surface could be to blame for the decrease in biodiesel yield.

Moving completely away from CaO, which has dominated attempts to fabricate basic transesterification catalysts from biomass (i.e. from $CaCO_3$ [31]), K_2O-doped composites continue to be a source of interest. Waste palm kernel (WPK), with or without H_3PO_4 activation, was hydrothermally converted to the char PKSHAC . Wet impregnation with K_2CO_3 and $Cu(NO_3)_2$ gave catalysts described as PKSHAC-K_2CO_3-CuO, which showed acceptable biodiesel production but significantly lacked robustness [175][176]. In contrast, other advances have been underpinned by the second metal introducing more distinct ancillary functionality than was offered by Cu. Hence, VSM established the superparamagnetism of RHC-K_2O(20 %)-Fe_2O_3(5 %), prepared by drying rice husk to give the corresponding char (RHC) and then introducing K_2O and hematite (optimally 20 and 5 wt. %, respectively). This catalyst returned a biodiesel yield of 98.6 % from WCO with a slightly improved MTOR of 12:1. However, not only SSA (modest in even fresh catalyst) but also, crucially, magnetic susceptibility both dropped dramatically over 5 subsequent cycles. This led to a last-cycle biodiesel yield of 44.1 %, reflecting a need for further work on recyclability measures [177]. In this vein, similar work with nickel recently afforded RHC-K_2O (20 %)-Ni(X %) (X = 1, 5, 10). Increasing Ni content raised magnetic susceptibility but decreased catalyst basicity, with X = 5 proving a decent compromise, yet still affording just a modest 80.8 % biodiesel yield. Moreover, catalyst deactivation properties were essentially as for the earlier hematite work (45.9 % yield after 6 cycles) [178]. These data reinforce the urgency of addressing the protection of both catalytically and magnetically active sites.

Remaining with magnetically recoverable composites, refined bamboo charcoal (BC) particles have been wet impregnated with Fe salts to incorporate γ-hematite. After drying, the magnetic carrier was exposed to K_2O-source KNO_3 (10-40 wt. %) prior to calcination at 300-700 °C (**Fig. 11**) [179]. BC-Fe_2O_3 characterization, ostensibly by TGA/DSC, revealed that O-containing functions at the composite surface facilitated KNO_3 decomposition, promoting the low temperature formation of intermediate potassiated surface functions. These then rearranged at higher temperature to give K_2O active sites in a sequence the authors described as low temperature radial activation followed by high temperature transverse activation. Optimized preparation conditions (30 wt. % KNO_3, 500 °C, 3 h) enabled a biodiesel yield from soybean oil (SO) of 98 % using an impressively low 8:1 MTOR. Additionally, the catalyst proved robust by the standards of the other biomass-derived bifunctional catalysts, with only the substantially more engineered inorganic composite CaO-W_xMo_y [165] showing similar resilience. K_2O-BC-Fe_2O_3 still achieved a respectable ~85 % biodiesel yield after the catalyst had been magnetically reclaimed in 9 experiments, hinting that simply modified sustainable resources may yet offer chemically resilient catalytic solutions in biodiesel production.

Similarly a 'one-pot' transesterification/esterification was used to synthesize biodiesel from a low-quality oil (WCO) with a high FFA level using bifunctional CaO-Fe_2O_3/AC catalyst from EFB (empty fruit bunch) [180]. Using the impregnation approach with $FeCl_3$ solution, the acid-base bifunctionality and magnetization were introduced into the powder. Calcination was done at 900 ^oC to obtain the catalyst. A significant C=O absorption band at 1774 cm^{-1} and a singlet methoxy proton signal at 3.7 ppm were observed confirming the presence of biodiesel using FT-IR and ^1H NMR spectroscopy, respectively. A biodiesel yield of 98.3 % was achieved and reusability tests showed that the catalyst was relatively stable for at least six successive cycles (FAME yield > 80%). The authors suggested that an abundance of basic (2.65 mmol g^{-1}) and acidic (1.85 mmol g^{-1}) active sites on the catalyst surface explain the good activity i.e, with just 3 wt. % a high biodiesel yield was obtained. Recently, Wang et al. [181] impregnated blast furnace dust (BFD) using either Na_2CO_3 (to give Na-BFD_T after 300-900 °C (= T) calcination) or $CaCO_3$ (giving Ca-BFD_T after similar calcination), with these catalysts both used for the efficient generation of biodiesel. Both systems performed well, with the sodium analogue slightly more impressive in terms of yield and showing notable stability. Hence, though Ca-BFD_{600} achieved a good yield of 98.30 ± 0.75 wt. % initially and maintained a 94.12 ± 0.66 wt. % yield on cycle 7, performance was lost catastrophically in the 8th cycle. Conversely, the transformation of Na_2CO_3 to nanocrystals of $NaFeO_2$ (29.9 nm) in Na-BFD_{500}

enabled quantitative biodiesel yields in cycles 1-3 (also achieved for Na-BFD_{600} in cycles 1-2) and maintaining an excellent 98.23 ± 0.53 wt. % in cycle 15, before dropping to <80 wt. % in cycle 17. These data served to highlight the effectiveness of simple magnetic recovery, though the catalyst was calcined at 500 °C between cycles. Biowaste-derived bifunctional catalyst performance is summarized in **Table 5**.

Table 5. Different biomass-derived solid bifunctional catalysts for biodiesel production. NR = not reported. CRC (Y) = catalyst reusability cycles (yield %). RT = room temperature. DI = de-ionized.

No	Catalyst	Preparation	Catalyst surface area ($m^2 g^{-1}$)	Feedstock	Conditions[a]	Yield (%)	CRC (Y)	Ref.
1.	SCC-KPD	Treat CC with H_3PO_4, calcined at 450 °C, 6 h. Adding H_2SO_4 (150 °C, 2 h). Carbonize PD at 280 °C, 72 h, treat with KOH, heat at 900 °C, 6 h. Combine SCC and KPD in water at 100 °C, 4 h.	NR	NSO	15:1, 2.6, 73, 62	92.9	3 (89.3) 5 (<76)	[144]
2.	KOH-ACC	Treat refined CC with mineral acid. After water, KOH and calcine at 500-800 °C, 1-4 h. KOH treatment, calcine at 450 °C, 2 h.	627	WCO	18:1, 1, 60, 45	97.8	2 (35)	[167]
3.	KOH/Rice bran/AC	Mix RB and KOH. Treat RBP with H_2SO_4, 1 h. Calcine at 700 °C, 4 h. Subject AC to KOH, 4 h.	-	Algal biomass	10:1, 5, 90, 70	81.8	-	[168]

4.	CaO-W_xMo_y	Obtain CaO at 900 °C, 4 h. Add to W_xMo_y aq., calcine at 650 °C, 4 h.	9.4	WCO	15:1, 2, 120, 70	96.2	3 (93) 5 (90)	[165]
5.	Crab shell-plantain peel-Al_2O_3	Calcine CS at 900 °C. Carbonize PP at 500 °C, 3 h. Mix CCS, CPP, Al_2O_3 at 80 °C, 2 h. Calcine at 900 °C.	260.35	WCO	13.03:1, 5, 149.9, 60	93.0	5 (>80)	[172]
6.	CAWS-$_{(7)}SO_4$	Calcine AWS at 900 °C, 2 h. Immerse in H_2SO_4, 2 h. Dry at 150 °C.	6.53	PFAD	15:1, 5, 180, 80	97.4[b]	4 (46)	[171]
7.	RHC-K_2O(20%)-Fe_2O_3(5%)	Calcine RH at 450 °C, 3 h. Wet impregnation with K_2CO_3 and $FeCl_3·6H_2O$. Calcine at 700 °C, 3 h.	57.89	WCO	12:1, 4, 240, 75	98.6	3 (88.7) 6 (44.1)	[177]
8.	RHC-K_2O(20%)-Ni(5%)	Calcine RH at 450 °C, 3 h. Wet impregnation with K_2CO_3 and $Ni(NO_3)_2·6H_2O$. Calcine at 600 °C, 3 h.	32.40	WCO	12:1, 4, 120, 65	98.2	4 (81.8) 6 (45.9)	[178]
9.	PKSHAC-K_2CO_3(30%)-CuO(5%)	Treat PKS with H_3PO_4 then carbonize at 700 °C, 3 h. Treat with NaOH, K_2CO_3, $Cu(NO_3)_2$	438.08	WCO	12:1, 5, 240, 80	95.0	3 (93.3) 6 (55.3)	[118]

		at RT, 6 h. Carbonize at 700 °C, 3 h.						
10.	PKSHAC-K_2CO_3(20%)-CuO(5%)	Activate PKS with NaOH, neutralize with HCl, add K_2CO_3 and $Cu(NO_3)_2$ by wet impregnation. Heat at 105 °C, 24 h.	3368.60	WCO	12:1, 4, 120, 70	95.4	3 (>90) 6 (<60)	[176]
11.	K_2O-BC-Fe_2O_3	Treat BC with $FeCl_2 \cdot 4H_2O$, $FeCl_3 \cdot 6H_2O$. Add NH_3. Wet impregnate using KNO_3. Calcine at 300-700 °C.	28.7	SO	8:1, 2.5, 60, 60	98.0	5 (>94) 10 (~85)	[179]
12.	CaO-Fe_2O_3/AC	Add EFB powder to $FeCl_3$ and $Ca(NO_3)_2 \cdot 6H_2O$. Calcine at 900 °C, 4 h.	106.2	WCO	18:1, 3, 180, 65	98.3	6 (>80)	[180]
13.	Na-BFD_{500}	Mix Na-BFD and sodium carbonate in DI water at 75 °C, 2 h). Calcine at 500 °C.	3.19	SO	15:1, 7, 120, 65	100	16 (95.8)	[181]

[a]MTOR, catalyst loading (wt. %), time (min), temperature (°C)

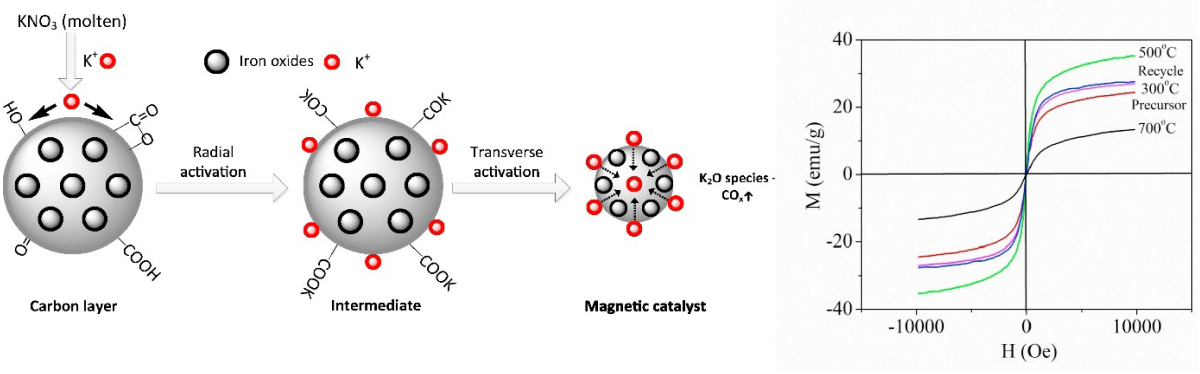

Fig. 11. Left: Proposed K_2O-BC-Fe_2O_3 formation mechanism, with surface functions (–OH, –COOH, etc.) promoting the lower temperature decomposition of KNO_3 followed by higher temperature rearrangement of metalated surface groups to give K_2O.
Right: Despite good retention of catalyst properties, magnetic saturation drops after use. Reproduced from Ref. [179].

4 Challenges of using biomass-derived catalysts

As discussed above, biomass-derived catalysts can effectively, sustainably, and efficiently replace chemical catalysts. However, biomass-derived catalysts suffer multiple drawbacks that currently compromise their commercial application in biodiesel production. The main downsides of these catalysts are discussed here. They include active site leaching, low surface area, sensitivity to moisture, solvents and heat, and saponification. To identify the elements that influence the end-product quality requires investigation of catalyst synthesis and operation. Challenges and probable solutions are highlighted in **Table 6**.

4.1 Active site leaching

As discussed in Section 2.1, a range of animal biowaste has been used to source basic metal oxide (mainly CaO) catalysts for biodiesel production. Although several examples have proved highly active, they have generally suffered sometimes profuse leaching of active metal sites. One of the major reasons for this on repeated reuse is the partial solubility of CaO in methanol [47][104]. This recognition has driven attempts to minimize reaction times [47]. However, this is intrinsically difficult for multi-use catalysts such as one reported by Tshizanga et al. [46]. They noted that the decrease in biodiesel yield after 18 successive cycles was due to leaching of Ca^{2+} (as CaO or calcium diglyceroxide) [47][48]. Kouzu and Hidaka's research also indicated that wet reaction

media promoted Ca^{2+} leaching [48], with the consequent need to remove Ca^{2+} ions from the biodiesel product. Taken together, these observations led to studies involving the deliberate leaching of Ca^{2+}, with CaO forming calcium diglyceroxide upon washing. This calcium diglyceroxide is not only more soluble than CaO itself [47], but it has been shown to inhibit reactant access to the CaO catalyst [49]. In other work, Etim et al. [91] used AAS (Atomic Adsorption Spectroscopy) to investigate possible leaching, and observed that washed biodiesel product had $Na^+ + K^+$ and $Ca^{2+} + Mg^{2+}$ concentrations of 1.8 and 0.42 ppm respectively, while unwashed biodiesel product had corresponding concentrations of 115.6 and 0.96 ppm, respectively, confirming leaching. In order to try and limit leaching of Ca^{2+}, doping of CaO with metal ions such as Na^+ [38] and K^+ [37] has been attempted. For example, CaO has been impregnated with Na-ZSM-5. [70] Alternatively, supporting CaO on scaffolds such as SiO_2 [40], Fe_3O_4 [117], and Al_2O_3 [172], have given impressive results.

As discussed in Section 3, the high basicity of catalysts based on calcined plant biomass is attributed to the presence mainly of potassium in various forms; K_2O, $K_2Ca(CO_3)_2$ and K_2CO_3. Again though, leaching of metal ions on repeated reuse has been reported in several plant biomass studies [82][83] to decrease catalytic activity and contaminate the biodiesel product. The potentially dramatic extent of this was shown using SEM-EDX analysis, with Pathak et al. [82] observing a sharp decline in K concentration in the catalyst from 65.11 % (fresh) to 27.99 % (used four times). Concomitantly, soybean oil conversion decreased from 98.95 % to just 52.16 % in the fourth cycle, with SEM-EDX and XRD data showing a dramatic reduction in the potassium oxide intensity, the primary basic site. More recently, waste *Brassica nigra* was calcined at the relatively low temperature of 550 °C [84]. The prepared catalyst had a potassium level of 56.13 % (in the form of K_2O, K_2CO_3 and KCl, the first two representing the primary active ingredients), and showed a high yield of biodiesel (98.79 %). However, leaching of K content was recorded. The AAS analysis of the catalyst after being recycled 3 times showed a decrease in K-content from 343.89 ppm (fresh) to 320.93 ppm. XPS analysis of the recycled catalyst confirmed the decrease of potassium content from 15.13 % in fresh catalyst to 10.19 %. Changmai et al. [118] magnetized *Citrus sinensis* peel ash (CSPA) using nano-Fe_3O_4. EDX analysis was used to study the changes in the elemental composition of core@shell Fe_3O_4@CSPA for the fresh as well as reused catalyst (9 cycles). The resulting data showed a decline in K concentration to be the key reason for a concurrently observed decrease in biodiesel yield (from 98.7 to 91.0 %). Work by Abdelhady et

al. [103] involved calcining sugar beet waste. In this, the active metal oxide was CaO (90.1 wt. %); this contrasts with most other reported cases of plant biomass waste, where potassium is dominant. With just a 1 % catalyst loading, conversion of sunflower oil to biodiesel reported was 93.0 %. Subsequently, a steep decline in conversion of oil to biodiesel was reported due to a combination of leaching and formation of calcium diglyceroxide.

Moving away from the persistently problematic leaching of Ca^{2+} and K^{+} from biomass-derived catalysts, that of sulfonic groups was also reported in several plant biomass derived SAFCAMs [118][133]. This leaching of $–SO_3H$ is attributed to solubility in polar solvents [134][182]. Although obtaining acidic carbocatalysts with a high level of $–SO_3H$ functionalization through simultaneous carbonization and sulfonation with H_2SO_4 has recently been developed as an effective and straightforward synthetic method, the materials produced by this process have low porosity, a high density of oxygen functional sites (1.0-7.3 mmol g^{-1}), and poor thermal stability, which limits their effectiveness in hydrophobic media and/or at high temperatures [183]. Besides these points, the carbon frameworks have a soft (less rigid) graphitic structure due to polycondensation, and high-pressure treatments in the presence of water, or upon repeated reuse can cause mechanical exfoliation, inducing the detachment of aryl fragments. The consequence of this is that loosely held polycyclic aromatic carbon networks containing $–SO_3H$ groups cleave from the bulk during liquid-phase reactions, desulfonating it (**Fig. 12**) [150][182][183]. Such loss of $–SO_3H$ groups was proved by Mo et al. [182] using ^{1}H NMR analysis of liquid reaction mixtures after reaction. They observed weak signals characteristic of polycyclic aromatics at ca. 7.4-7.8 ppm in the corresponding spectra [184][185]. Correspondingly, the activity of the catalyst decreased drastically on repeated use [182]. Seeking to address one of the problems associated with SAFCAM stability, thermally and chemically stable polycyclic aromatic carbon networks have been produced by high temperature pyrolysis (823 K). This approach has afforded more rigid graphite-like carbon materials [186]. Subsequent sulfonation has then been used to produce SAFCAMs. In one report, due to the presence of a chemically stable graphite-like sulfonated structure, rigid carbon materials functionalized by strong sulfonating reagents like $ClSO_3H$ and by the chemical reduction of 4-benzenediazoniumsulfonate did not exhibit any detectable leaching of SO_3H-containing polyaromatic moieties [150].

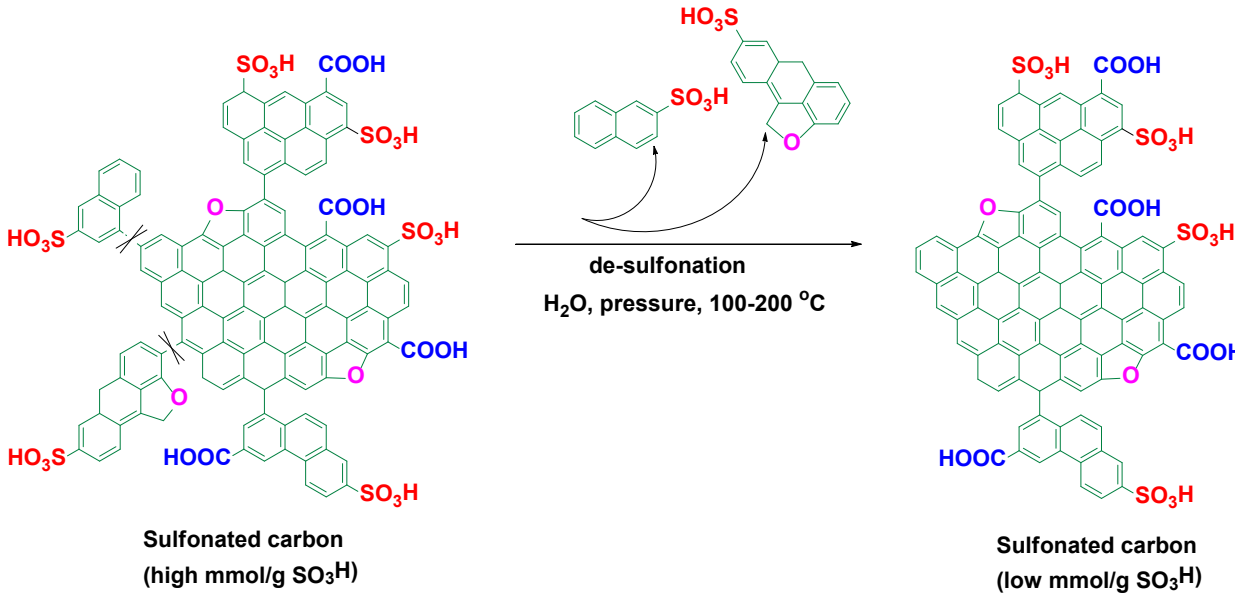

Fig. 12. Examples of leaching of S-containing fragments from a SAFACAM

Leaching of sulfonated species in fact only plays a limited part in SAFCAM deactivation. Instead, primary deactivation is produced by direct alcohol treatment [150]. The effectiveness of this depends greatly on the type of alcohol used, with methanol being the most effective. Solid state NMR shows the presence of chemically bound alkyl groups coming from the alcohol, emphasizing the difference from strongly physisorbed species obtained by pretreatment at room temperature [133]. The strongly deactivating effect of alcohol lies in the formation of sulfonate esters, which results from the reaction of the sulfonic groups in the solid with the alcohol at high temperature. Due to the lack of mobility of the surface species, the spectrum of the sample that was processed under heating to reflux only exhibited very broad signals. Very narrow signals, including those of the hydroxyl group, clearly demonstrated the existence of highly mobile liquid propanol in the sample that was processed at ambient temperature. The NMR study, together with the deactivation results, pointed to a general picture at room temperature of the formation of hydrogen bonds between the alcohol and the different protic groups of the material (sulfonic and carboxylic acids, hydroxyls of alcohols and phenols), whereas under heating those species evolved into alkyl esters (sulfonic and carboxylic) or alkyl ethers. Fraile et al. [133] confirmed this thesis by reaction of the sulfonic groups in the solid with alcohol at high temperature (**Fig. 13a**). The solid pretreated with methanol, as well as the catalyst recovered after esterification, presented a prominent signal at 52 ppm, showing the formation of sulfonate esters. Rokhum et al. [11] recently

confirmed the same through ^{13}C-CP NMR spectroscopy (**Fig. 13b**), establishing that the formation of aliphatic signals in the 30-55 ppm region of a spent SAFCAM (5 cycles of oleic acid esterification) is the result of a mixture of methanol-induced breakdown of active sulfonic acid groups into sulfonate esters [133][181] and the esterification of carboxyl groups. However, the production of sulfonate ester (as well as carboxyl ester/ether) is a completely reversible deactivation process, and the acid sites have been shown to be readily regenerable through the hydrolysis of ester bonds with water [133] or through treatment of sulfonate esters with weak acids (**Fig. 14**) [150]. Resulfonating the catalyst by the same preparation method after five esterification cycles using conc. H_2SO_4 (1:10 recovered catalyst:sulfuric acid (wt./vol.), 80 °C, 18 h) has been done to essentially recover leached –SO_3H groups, as shown in **Fig. 13b** (green line) [150][187]. The solvent is another key factor that can significantly affect the nature and extent of active site leaching. Polar solvents are usually more aggressive in their dissolution [188]. Therefore, one of the simplest methods that has emerged to prevent leaching is to use less polar solvents, such as hexane or dimethylether (DME) in approximately 25 % volume [170][189].

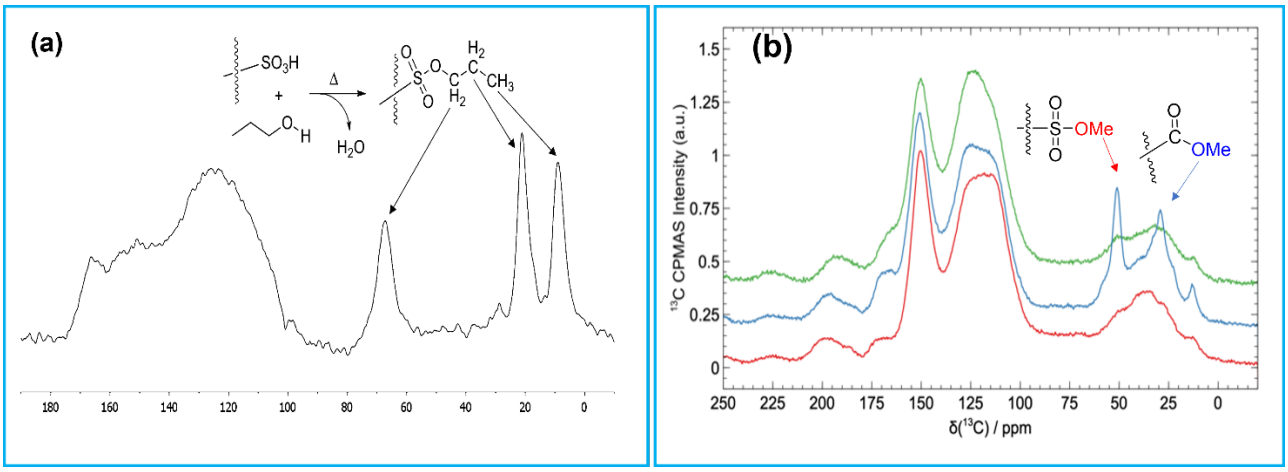

Fig. 13. a) ss-NMR analysis showing the formation of sulfonate esters in a SAFCAM. Reproduced from Ref. [133]. b) ^{13}C-CP NMR spectra of a fresh SAFCAM (red), and the same recovered after 5 oleic acid esterification cycles (blue) and after re-sulfonation (green). Reproduced from Ref. [11]

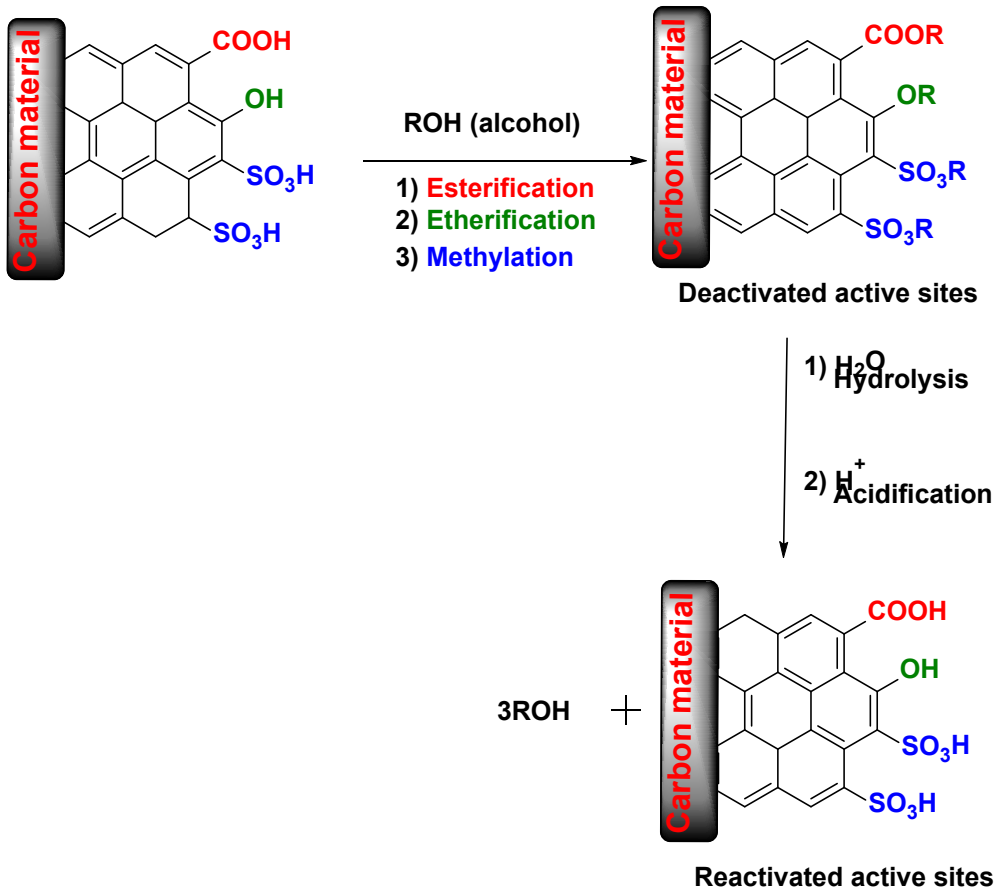

Fig. 14. Reaction scheme for the regeneration of surface acid sites of sulfonated carbons deactivated in alcoholic media.

4.2 Fouling/coking

Reactants' ability to interact with the active sites of a catalyst directly or indirectly is inhibited by fouling. In biodiesel production, inhibition can be caused by the blockage of mesopores [190] as well as active sites themselves [191]. When transesterification is being conducted using acid catalysts, the danger of organic molecules fouling or poisoning the acid sites is significant. Indeed, the deposition of coke produced by methanol and glycerin has been seen in acid catalyzed biodiesel synthesis [48]. Many metal oxides also suffer deactivation due to cloaking by adsorbed intermediates or byproducts, such as monoglyceride, diglyceride, and glycerol [47][48], or renewable feedstock contaminants, as noted by Malaguti et al. [192]. Copeland et al. [193] confirmed the strong interaction of the 2° alcohol of glycerol with metal oxide surfaces (β interaction in **Fig. 15**) through strong hydrogen bonding, following the trend

Al_2O_3>TiO_2>ZrO_2>CeO_2>MgO. The same work also identified a Lewis acid/base interaction through the remaining 1° alcohol group of the chemisorbed glycerol (γ interaction). Carbonaceous species can also block access to the catalyst active sites by pore plugging, encapsulation of the active phase, and binding on or near the active phase via chemisorption or physisorption [194]. ICP-OES and SEM-EDX mapping results reported by Zhu et al. [195] showed the external coating of the catalyst pellets on the top of their reactor by inorganic contaminant deposition. Meanwhile, carbonaceous species deactivated the catalyst by mainly binding near the sulfide active phase. This blocked access to the active edge sites, explaining a significant loss of desulfurization activity together with a minor loss of hydrogenation activity by the catalyst. Pore blocking was also observed on spent catalysts after co-processing raw biocrude, owing to the formation of a large amount of carbonaceous species [195]. One way to solve this is by using hexane, which can effectively prevent clogging of pores by forming a single phase between solvent and feedstock (oil). Reactivating the catalyst by heating can also open up the pores [178].

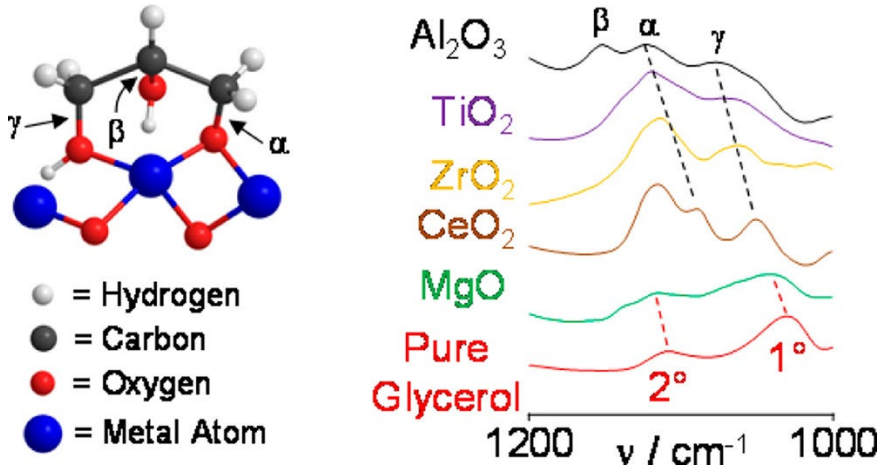

Fig. 15. Selected FT-IR data, explaining the surface interaction of chemisorbed glycerol with a metal oxide via three different O-centres; deprotonated (α) and 2° (β) and 1° (γ) alcoholic. Reproduced from Ref. [193]

4.3 Wastewater treatment

Wastewater from biodiesel washing is the major residue created by the biodiesel industry. It has a high organic content and cannot be disposed of directly into the sewage system [196]. The source

of this waste is post-synthetic washing, which is vital for removing soap, catalyst, free glycerol, residual alcohol, water, and FFAs from the product [196][197]. The large amounts of wastewater generated by washing (often 4-5 cycles thereof) has drawn researchers to look for more straightforward and affordable remedies to the issue of biodiesel purification. The use of membrane extraction has proved advantageous in reducing the amount of water used by effectively avoiding the occurrence of emulsification during the washing step. This results in a reduction of methyl ester loss during refining [198]. Dry washing is another method that has been looked at to solve water management problems. This uses an ion exchange resin to remove impurities [199]. The benefits of this treatment are an absence of wastewater production and a reduction of the wash tank's overall surface area coverage [200]. The membrane extraction method is another advantageous technique in reducing the amount of water utilized. This avoids the occurrence of emulsification during the washing stage, resulting in a decrease in methyl ester loss during the refining process [201]. Tubular α-Al_2O_3/TiO_2 membranes with average pore diameters of 0.2, 0.1, and 0.05 μm and 20 kDa were used by Gomes et al. [202]. In their investigation, acidified water with a mass concentration of 10 % had glycerol separated from it effectively. Hence, the permeate achieved a free glycerol content of below 0.02 %.

4.4 Biomass residue treatment

The intensive production of biodiesel results in the generation of residues or by-products that cannot be utilized [203]. The most significant are glycerol, wastewater, methanol, and solid residues [204]. The by-product that sparks the most attention is crude glycerol, since it has commercial potential. Produced glycerol is regarded as a residue because it is combined with ethanol or methanol, fatty acid ethyl (or methyl) esters, and residual fatty acids. Their removal suggests a raw material for the food and pharmaceutical sectors or a precursor to solketal and glycerol carbonate, which are used as fuel additives, surfactants and lubricants [205][206]. Additionally, failure to treat biodiesel washes before their release into the environment can reduce the biological activity of sewage treatment plants as this wastewater contains grease and oil (G&O) and exhibits high COD (Chemical Oxygen Demand) [196][207]. Chemical pretreatment involves using strong acids such as H_2SO_4, HNO_3 and HCl to extract residual FAME/FFA from wastewater by protonation. Generally, adding acid directly to biodiesel wastewater induces separation into two phases, in the upper of which oil and soap coalesce [208]. Verification of the composition of this

upper layer has come from FT-IR and ^{1}H NMR spectroscopic analysis [196]. As an alternative strategy, electrocoagulation involves wastewater being put into a reactor. This is used to create an electric field that generates flocculating agents (associated with cationic aluminum, iron and magnesium species). These are capable of removing G&O or COD particles [196]. Lastly, methanol, which is used in excess, is another residue of biodiesel production. It is typically recovered by flash or vacuum distillation [204][208].

4.5 Lower reaction rates and diffusion limitations

Heterogeneous catalysts contribute to three phase systems (reactant, solvent, catalyst), resulting in decreased mass transfer rates [55][102]. The immiscibility of hydrophobic triglycerides with alcohol (methanol) and the intraparticle diffusion resistances of oil molecules also represent significant causes of lower catalytic activity linked to reduced mass transfer [102]. A boost in reaction temperature can increase solubility, although this requires energy and only results in a 2-3 wt. % increase in solubility with a temperature rise of 10 °C [209]. A possible approach to improve heterogeneous catalysis is the addition of a co-solvent such as hexane, acetone, tetrahydrofuran (THF), or dimethylether (DME). Under certain circumstances, this can yield a one-phase system, which lowers reaction E_a. The joint solubility of methanol and oil can be enhanced at lower reaction temperatures by using co-solvents, and it is also anticipated that using a co-solvent will increase the rate of a heterogeneously catalyzed transesterification.

To solve mass transfer constraints in biodiesel synthesis, techniques for the use of triglycerides and methanol, careful catalyst functionalization and, in some cases, pore size customization are required [3][170]. Several studies have shown that a co-solvent can significantly increase reaction rate by the polar and non-polar sites in the co-solvent lowering the surface tension between the methanol and oil phases [210][211], so encouraging formation of a single phase [169][170]. However, while it can reduce mass transfer limitations, the introduction of a co-solvent is not risk-free. Polar solvents such as THF and acetone have a tendency to promote the leaching of active sites [188]. Moreover, water solubility of each solvent varies and must be taken into account. When co-solvent that is miscible with both methanol and triglyceride is used, it can overcome initial phase separation. However, it has been reported that while the polarity and boiling point of THF are adequate to speed up the dissolution of methanol, the presence of feedstocks (oils) can lead to a decrease in biodiesel production on account of the co-solvent polarity. These

findings were reported by Roschat et al. [66], who used THF as a co-solvent in the NaOH-catalyzed transesterification of Jatropha curcas seed oil. Overall, methanol-miscible solvents such as toluene, benzene, chloroform, and dichloromethane are preferred for transesterification. In an alternative approach, using higher reaction temperature and pressure (above 130 °C and 90 bar) and a stoichiometric ratio of methanol with respect to feedstocks, it has proved possible to enhance the transesterification activities of sulfonated carbons for large triglycerides [55].

4.6 Sensitivity towards moisture and air

It is well documented that many shell-derived highly basic CaO systems can potentially catalyze conversion of vegetable oil and animal fats to biodiesel. Yet, shell-derived CaO is highly sensitive to moisture and air. On contact with moisture (water), it rapidly hydrates to $Ca(OH)_2$ and becomes inactivate. Further, it is easily carbonated ($CaCO_3$) by contact with CO_2 present in air [32]. Owing to these effects of moisture and CO_2, CaO catalysts lose their activity on repeated reaction cycles, thereby increasing the overall cost of biodiesel production. Hence, to reactivate the spent CaO catalyst, outgassing at elevated temperatures of 550-700 °C is used to reverse the CO_2 poisoning and effects of hydration. However, this introduces extra expense and complexity to the biodiesel production process [73][74].

Moving to plant biomass-derived acid-functionalized catalysts, affinity towards moisture can permit easy accessibility to hydrophilic solvents, enabling their interaction with active acidic sites and resulting in high catalytic performance [186]. However, several drawbacks exist. It is well known that a CAM catalyst prepared at low pyrolysis temperature (<400 °C) bears significant numbers of –OH and –COOH functional groups. These allow more water by-product from catalyzed esterification to be adsorbed at the catalyst surface. In one sense, this drives the reaction. However, it also gives a water layer that prevents hydrophobic long-chain FFAs from accessing active sites, thereby deactivating the catalyst [212]. The effects of these surface functions are non-trivial though; seminal reports have detailed how the same –COOH and –OH groups promote adsorption of reactants to sulfonated catalysts through the formation of hydrogen bonds and enhance access to active sites for hydrophilic reactants like methanol [213]. Hence, balancing the catalyst's hydrophilicity/hydrophobicity is critical for their successful application.

In general CAMs prepared at a lower pyrolysis temperature exhibit relatively less rigid (lowly carbonized) and thermally unstable structures. The framework of these catalysts can be

easily hydrolyzed (by water produced during esterification). The result is emulsification (dissolution) and active site leaching [125]. This has been detected by ^{1}H NMR spectroscopy by Mo et al. [182]. To retain the activity of functionalized CAMs, increasing the hydrophobicity has therefore emerged as a strategy for retaining activity [214][215][216]. Two main potential routes have been suggested; 1) High temperature pyrolysis to produce highly rigid graphitic CAMs, and 2) surface functionalization with water repellant groups such as $–CF_3$, $–CH_3$ [217] and –Ph [215]. This last strategy gives rise to a wettability-selective adsorbent that can capture organic molecules whilst completely resisting water [217].

The two strategies outlined above can be considered in more detail. In the washing process, soap, catalyst, free glycerol, leftover alcohol, water, and FFAs are among the unwanted materials eliminated. Contaminants that aren't eliminated will lower the quality of biodiesel and have an impact on engine performance. Low carbonization temperatures (< 400 °C) only provide complex polymers containing aromatic compounds. Thus, sulfonation results in soluble sulfonated species. In contrast, high carbonization temperatures (> 400 °C) yield hydrophobic, thermally stable, rigid graphitic CAMs due to growth of the polyaromatic carbon network by sequential dehydration, decarboxylation, decarbonylation and aromatization reactions [218]. However, highly hydrophobic CAMs produced at very elevated temperatures (> 550 °C) are difficult to sulfonate due to their excessively rigid, planer structure [123]. Hence, producing highly carbonized hydrophobic CAMs with high surface area from biomass remains a significant challenge. A potential solution to this problem could be sequential production of highly carbonized CAMs, then using chemical or physical activation of the produced CAMs to increase their surface area, and finally sulfonation to obtain SAFCAMs [219].

4.7 Low surface area

The low surface area of biomass-derived catalysts is a perennial issue that effects biodiesel production [220][221] on account of the corresponding reduction in numbers of active sites [222]. In response, hydration-dehydration treatment has been reported to increase surface area and with it activity [28][223]. In pioneering work, Niju et al. [41] observed a remarkable difference in the transesterification yields of commercial eggshell (67.57 %), eggshell-derived CaO (79.62 %) and eggshell-derived $CaO_{C\text{-}H\text{-}D}$ (94.52 %; C-H-D = calcination-hydration-dehydration), showing the benefit of this post-synthetic modification [59]. More recently, the two-step calcination and

hydrothermal treatment of beef-bone biomass underpinned an improvement in biodiesel yield [80]. In similar work, the hydrothermal treatment of CaO led to the formation of a layered Ca-HAP structure that was claimed to induce an increase in catalyst surface area from 1.7 to 100 $m^2\ g^{-1}$. [81] The synthesized catalyst showed improved activity when compared to the parent species (cf. conversions of 90.4 % and 71.7 %, respectively) [81]. Krishnamurthy et al. [71] also synthesized CaO at 900 °C. The resultant mass was then subjected to hydration-dehydration to form nano-$CaO_{C\text{-}H\text{-}D}$. Under optimized conditions of MTOR (12.4:1), catalyst loading (0.892 wt. %), temperature (61.6 °C) and time (145.154 min), a high yield of 98.3 % was obtained. Reddy et al. [42] reported a nano-$CaO_{C\text{-}H\text{-}D}$ catalyst obtained from *Polymedosa erosa* seashells, which gave a surface area of 90.61 $m^2\ g^{-1}$ and showed excellent activity (98.5 % yield).

Chemical activation can also be used to increase the surface area of biomass-based systems [128][143]. Activation may see a metal salt ($ZnCl_2$) being used to cleave glycosidic linkages in the biomass, leading to accelerated decomposition [224]. This induces the creation of micro- and mesopores, yielding a high surface area support for plentiful active sites [225]. In this vein, Tang and Niu [146] tested bamboo-derived biomass for carbonization and H_2SO_4 sulfonation, resulting in a catalyst with a surface area of 1208 $m^2\ g^{-1}$. This was activated by increasing the pore size (to 0.68 $m^2\ g^{-1}$) with phosphoric acid. Free fatty acid conversion using the activated material initially stood at 97.3 %. However, after 6 cycles of esterification, the yield was a modest 57.2 %. This contrasted with the earlier synthesis of a bamboo-derived carbon catalyst (without activation) having a surface area and pore size of 71 $m^2\ g^{-1}$ and 0.25 $cm^3\ g^{-1}$ that showed low recyclability on repeated use (27.84 % yield after 5 cycles) [134]. Decrease in sulfur content (6.069 % to 4.217 %) largely accounted for deactivation through leaching of $–SO_3H$ sites by breakdown of the polycyclic support, possibly also accompanied by formation of sulfonate esters. Hence, activation by phosphoric acid plainly helped recyclability. Recently, waste orange peel activated by KOH through hydrothermal carbonization and then sulfonated using H_2SO_4 at 200 °C for 24 h achieved a surface area of 44 $m^2\ g^{-1}$, which is higher than for most reported SAFCAM catalysts [143]. This was attributed to KOH acting both as an activation agent and template for the formation of a mesoporous structure during the hydrothermal carbonization step. Similarly, using KOH as activating agent, Naeem et al. [167] pyrolytically (600 °C for 4 h) activated corncob in the presence of sulfuric acid, increasing the SSA from 211 $m^2\ g^{-1}$ to 877 $m^2\ g^{-1}$. The composite catalyst promoted esterification and transesterification simultaneously and returned a 97.8 % yield of biodiesel from

WCO at an impressively low 45 °C, albeit a high (18:1) MTOR was required. Hussein et al. [147] studied potato peel activation using $ZnCl_2$. The resulting material was subjected to sulfonation using H_2SO_4 at 180 °C for 8 h. This dual process of activation and sulfonation raised the SSA and total pore volume from 15.7 $m^2 g^{-1}$ and 0.016 $cm^3 g^{-1}$, respectively, to 1027 $m^2 g^{-1}$ and 1.34 $cm^3 g^{-1}$. It was posited that $ZnCl_2$ erodes the biomass microstructure. The catalyst maintained over 70 % of its initial catalytic activity after five consecutive catalytic runs. Lastly, in other work by Chellappan et al. [157], modulation of surface area has been combined with the introduction of magnetic properties. Pyrolyzed cassava peel biochar was sulfonated and impregnated with Fe_3O_4. The resulting magnetic catalyst produced biodiesel using *Millettia pinnata* seed oil as a feedstock. The catalyst demonstrated a surface area of 423.89 $m^2 g^{-1}$ and a 0.21 $cm^3 g^{-1}$ pore volume, and gave a 98.7 % biodiesel yield.

Table 6. Major limitations, reasons and potential solutions associated with using biomass-derived catalysts for biodiesel production. G&O = grease and oil. COD = chemical oxygen demand.

No.	Challenges	Reasons	Potential solutions
1.	Leaching of active sites [47][104]	1. Partial solubility of metals/CAMs 2. Partially carbonized material is sulfonated with conc. H_2SO_4 3. Sulfonate ester and carboxylic acid ester formation	1. Prevent adsorption of organic reactants using catalysts with high hydrophobic surface areas. Metal doping or provision of a catalyst support helps prevent leaching [37][38] 2. Hydrolyze ester linkages. Resulfonate to partially recover lost $–SO_3H$ [150][187] 3. Use less polar solvents [3][170].
2.	Fouling/coking [115][178]	Accumulation of triglyceride, by-product, or side-product in catalyst pores/on active sites by adsorption of alcohol or oxygenated molecules upon repeated reuse	1. Wash with hexane to prevent pore clogging and form a single phase between solvent and the feedstock [51]. 2. Reactivate the catalyst before reuse [73][74]
3.	Wastewater formation [200][226]	Water needed to remove residual catalyst, glycerol, soap, oil, and alcohol requires disposal	1. Dry washing with ion-exchange resins and silica powder [200] 2. Membrane extraction [198]

4.	Biomass residue disposal [196]	By-product of oil extraction from plants includes large hydrocarbons requiring treatment and removal	1. Electrocoagulation pretreatment can remove G&O or COD particles [196] 2. Strong acid pretreatment [141][208]
5.	Side-product formation [227][228]	High water and FFA levels in raw materials cause the production of soaps, lowering ester yield	1. Separation and neutralization to remove high FFA content [228] 2. Use acid catalysts to prevent the formation of soap [227]
6.	Low reaction rates [229][230]	1. Poor mass transfer 2. Low temperature reactions	1. Increase pore diameter and tailor surfaces (e.g. for hydrophobicity, exterior catalytic sites, etc.) [3][170] 2. Raise reaction temperature and pressure 3. Use of co-solvents [169][170]
7.	Diffusion limitations [55][102]	Three phase systems show poor mass transfer	1. Careful surface functionalization and pore size customization [125][170] 2. Use of co-solvents [66]
8.	Sensitivity to moisture [231][232] and air [32]	Water adsorbs on hydrophilic solid acids, causing partial deactivation and framework hydrolysis	1. High temperature carbonization [186] 2. Surface functionalization with water-repellant groups [215]

9.	Low surface area [51][142]	Breakdown of biochar pores because of oxidation, condensation and/or carbonization	1. Chemical activation by H_3PO_4, KOH, NaOH to increase surface area and porosity [128][143] 2. Hydrothermal treatment and impregnation [80][81]

1511

5 Biodiesel production from biomass as a renewable energy carrier

Biomass was the first fuel used by humans and served as the foundation of the global fuel economy until the mid-eighteenth century. The annual global generation of electricity from biomass was about 750 TWh (about 2.5 % of total demand) in 2021 and is estimated to reach about 1,350 TWh (about 3.5% of total demand) in 2030. Of this, solid biomass (agricultural and animal waste) accounts for nearly three-quarters, biogas (CH_4) 14 %, and municipal solid waste 12 %. Fuelwood (firewood, charcoal, sawdust) and other forms of 'traditional biomass', that is, renewable biomass, generated up to 12.5 % of produced energy in 2021 [233], and is estimated as having contributed around 64 % of the total world supply of combustible renewables to date. More than two thirds of the renewable energy mix is currently made up of energy from biomass, making it the leading renewable energy resource globally [234]. It is a resource that can be found in a wide range of materials, including timber, sawdust, straw, paper, seeds and manure, municipal waste, and effluent. In addition, there is massive annual agricultural production, the by-products of which can be used as a source of energy. This has led to the development of so-called energy crops which, in turn, has allowed biomass resources to develop significance on account of their intrinsic economic potential for the energy sector. The international trade in biomass fuels has grown recently as a result of the rising use of biomass; the major fuels traded globally being wood pellets, biodiesel, and ethanol. The database in **Fig. 16**. shows the rising trend in usage of biomass as a feedstock for biodiesel production over the years. The authors have collected data in the month of April 2023 from Scopus Database using the keywords "Biodiesel production from biomass" and also from google scholar within the custom range of "2010-2022". From a merger of 208 publications in the year 2010 it has exponentially increased to 715 publications to its peak in the year 2022.

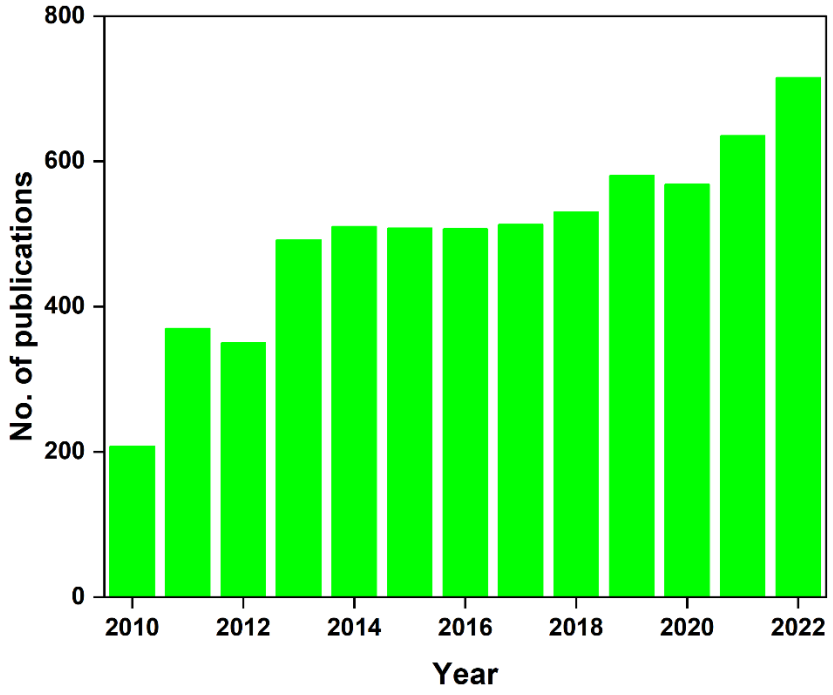

Fig. 16. Increasing trends of research publication during the period 2010 to 2022 (data collected from Scopus database).

Of the range of biomass-derived fuels available, such as biodiesel, bioethanol, and biomethane, the first represents the non-fossil fuel that is most frequently used today in place of traditional motor fuel. As the primary source of energy and chemicals in the world, oil is currently consumed at a rate of roughly 12 million tonnes per day (84 million barrels per day), with expectations that this rate will rise to 16 million tonnes per day (116 million barrels per day) by 2030 [235]. Importantly, when compared to petroleum diesel, biodiesel has less of an influence on the environment in terms of emission characteristics. Biodiesel emits less CO (4-16 %), hydrocarbons (45-67 %), and particulate matter (53-69 %) as compared to petroleum fuel. Moreover, the use of a huge range of different feedstocks (waste or specifically generated biomass) has already been developed and utilized in the manufacturing of biodiesel in order to achieve economically feasible sustainability, and to make energy access easier and more reliable/secure. Resource management is important here, producing feedstocks more locally, taking control of resource exploitation, reducing dependence on energy produced elsewhere, and using less water for cultivation [21][236]. In order to cut greenhouse gas emissions, many nations have embraced biodiesel-based policies and this trend will necessarily continue as fossil fuel reserves are further

depleted and the environmental consequences of their use become increasingly clear. One unambiguous manifestation of this appetite for change, is the growth in government subsidies aimed at advancing the sustainable generation of biofuels and associated feedstocks [237]. These incentives are often given for the planting of crops on fallow and abandoned agricultural lands, for better water management, and for practicing conservation.

6 Conclusions and outlook

The exploration of biomass-derived catalysts for biodiesel production represents a promising move towards sustainable and eco-friendly fuel generation. This review has sought to bring up-to-date our understanding of the potential of using biomass-derived catalysts for the production and post-synthetic treatment of biodiesel. Research on repurposing of animal and plant bio-waste has been critically analyzed with a focus on source sustainability and ease, reliability and resilience of catalyst preparation and catalyst reusability. In particular, efforts at more efficient catalyst recovery and the avoidance of deactivation by active site leaching, blockage or corruption have been discussed with the help of various analyses. For example in sulfonated systems, the leaching of $–SO_3H$ is attributed to graphitic structure polycondensation, and the fact that high-pressure treatments in the presence of water, or else repeated reuse can cause mechanical exfoliation, inducing the detachment of aryl fragments. Meanwhile, ^{13}C-CP NMR spectroscopy has established the formation of aliphatic signals in spent SAFCAMs are the result of a mixture of methanol-induced breakdown of active sulfonic acid groups into sulfonate esters [133][181] and the esterification of carboxyl groups [11]. Magnetic catalysts have also begun to establish themselves as having great potential to replace many conventional catalysts used in biodiesel synthesis, largely due to their straightforward recycling, which is often nearly quantitative (easily monitored but also inferred from performance retention). They are therefore potentially very economical and can be environmentally benign. In the long-run however, bringing down the cost involved in their more complex synthesis and reliably preventing separation of magnetic and catalytic species represent major challenges. The review has sought to address these technical hurdles, offering an outlook on potential solutions, thereby paving the way for the pragmatic utilization of biomass-derived catalysts in commercial applications.

Looking to the future, continued investigation of the potential of widely available yet underutilized animal and plant biomass waste will continue. However, the role of biomass-based

catalyst modification as a basis for overcoming existing limitations to reported catalysts will necessarily focus on the robustness and stability upon repeated reuse of catalysts and composites. The ability to recycle active sites either by harnessing support properties (e.g. magnetic recovery) or ensuring site retention (e.g. inhibiting desulfonation) represent current research vectors where advances would potentially significantly reshape the field. The latter line of research feeds into improving the effectiveness with which active sites are supported through the development of reliable, high surface area supports, and in particular the creation of simpler (more economical, atom-efficient) routes to multifunctional activated carbons. Additionally, and remaining with the theme of multifunctional catalysts, their robust catalytic activity in biodiesel production from inedible waste oils makes bifunctional biomass-derived catalysts economically very appealing. Not only do these catalysts, containing as they do both acid and base active sites, offer the possibility of utilizing inexpensive feedstocks (typically high in FFAs), but they exhibit enhanced efficiencies such as one-pot reactivity and easier product extraction and separation steps. The insights provided herein serve as a guiding beacon for identifying the most promising routes to propel these groundbreaking technologies toward widespread adoption, thereby fostering a more sustainable future in fuel synthesis and energy utilization.

6 Acknowledgement

7 References

[1] T. Kushwaha, S. Ao, K. Ngaosuwan, S. Assabumrungrat, B. Gurunathan, S.L. Rokhum, Esterification of oleic acid to biodiesel using biowaste-based solid acid catalyst under microwave irradiation, Environ. Prog. Sustain. Energy. 42 (2023) e14170. https://doi.org/10.1002/EP.14170.

[2] M.V.L. Chhandama, J.V.L. Ruatpuia, S. Ao, A.C. Chetia, K.B. Satyan, S.L. Rokhum, Microalgae as a sustainable feedstock for biodiesel and other production industries: Prospects and challenges, Energy Nexus. 12 (2023) 100255. https://doi.org/10.1016/J.NEXUS.2023.100255.

[3] I.B. Laskar, K. Rajkumari, R. Gupta, S. Chatterjee, B. Paul, L. Rokhum, Waste snail shell

derived heterogeneous catalyst for biodiesel production by the transesteri fi cation of soybean oil †, RSC Adv. 8 (2018) 20131–20142. https://doi.org/10.1039/C8RA02397B.

[4] B. Changmai, C. Vanlalveni, A.P.A.P. Ingle, R. Bhagat, L. Rokhum, Widely used catalysts in biodiesel production: A review, RSC Adv. 10 (2020) 41625–41679. https://doi.org/10.1039/d0ra07931f.

[5] S. Ao, L.A. Alghamdi, T. Kress, M. Selvaraj, G. Halder, A.E.H. Wheatley, S. Lalthazuala Rokhum, Microwave-assisted valorization of glycerol to solketal using biomass-derived heterogeneous catalyst, Fuel 345 (2023) 128190. https://doi.org/10.1016/J.FUEL.2023.128190.

[6] M. Van Lal, A. Chumpi, K. Belur, S. Ao, J. Vl, S. Lalthazuala, Bioresource Technology Reports Valorisation of food waste to sustainable energy and other value-added products : A review, Bioresour. Technol. Reports. 17 (2022) 100945. https://doi.org/10.1016/j.biteb.2022.100945.

[7] A. Bayat, M. Baghdadi, G.N. Bidhendi, Tailored magnetic nano-alumina as an efficient catalyst for transesterification of waste cooking oil: Optimization of biodiesel production using response surface methodology, Energy Convers. Manag. 177 (2018) 395–405. https://doi.org/10.1016/j.enconman.2018.09.086.

[8] M. Hajjari, M. Tabatabaei, M. Aghbashlo, H. Ghanavati, A review on the prospects of sustainable biodiesel production: A global scenario with an emphasis on waste-oil biodiesel utilization, Renew. Sustain. Energy Rev. 72 (2017) 445–464. https://doi.org/10.1016/j.rser.2017.01.034.

[9] P. Nair, B. Singh, S.N. Upadhyay, Y.C. Sharma, Synthesis of biodiesel from low FFA waste frying oil using calcium oxide derived from Mereterix mereterix as a heterogeneous catalyst, J. Clean. Prod. 29–30 (2012) 82–90. https://doi.org/10.1016/j.jclepro.2012.01.039.

[10] F. Toldra-Reig, L. Mora, F. Toldra, Trends in Biodiesel Production from Animal Fat Waste, Appl. Sci. 2020, 10(10), 3644; https://doi.org/10.3390/app10103644

[11] S.L. Rokhum, B. Changmai, T. Kress, A.E.H. Wheatley, A one-pot route to tunable sugar-

derived sulfonated carbon catalysts for sustainable production of biodiesel by fatty acid esterification, Renew. Energy. 184 (2022). https://doi.org/10.1016/j.renene.2021.12.001.

[12] M. Zabeti, W.M.A.W. Daud, M.K. Aroua, Activity of solid catalysts for biodiesel production: a review, Fuel Process. Technol. 90 (2009) 770–777. https://doi.org/10.1016/j.fuproc.2009.03.010.

[13] I.M. Atadashi, M.K. Aroua, A.A. Aziz, Biodiesel separation and purification: A review, Renew. Energy. 36 (2011) 437–443. https://doi.org/10.1016/j.renene.2010.07.019.

[14] S. Ao, M.V.L. Chhandama, H. Li, S.L. Rokhum, Microwave-Assisted Sustainable Production of Biodiesel: A Comprehensive Review, Current Microwave Chemistry 10 (2023) 3-25(23). https://doi.org/10.2139/SSRN.4389157.

[15] A.P.S. Chouhan, A.K. Sarma, Modern heterogeneous catalysts for biodiesel production: A comprehensive review, Renew. Sustain. Energy Rev. 15 (2011) 4378–4399. https://doi.org/10.1016/j.rser.2011.07.112.

[16] I.M. Atadashi, M.K. Aroua, A.R. Abdul Aziz, N.M.N. Sulaiman, The effects of catalysts in biodiesel production: A review, J. Ind. Eng. Chem. 19 (2013) 14–26. https://doi.org/10.1016/j.jiec.2012.07.009.

[17] A. Alagumalai, O. Mahian, F. Hollmann, W. Zhang, Environmentally benign solid catalysts for sustainable biodiesel production: A critical review, Sci. Total Environ. 768 (2021) 144856. https://doi.org/10.1016/j.scitotenv.2020.144856.

[18] Z.Q. Zhang, M.C. Liao, H.Y. Zeng, S. Xu, L.H. Xu, X.J. Liu, J.Z. Du, Mg–Al hydrotalcites as solid base catalysts for alcoholysis of propylene oxide, Fuel Process. Technol. 128 (2014) 519–524. https://doi.org/10.1016/j.fuproc.2014.08.015.

[19] N. Shibasaki-kitakawa, H. Honda, H. Kuribayashi, T. Toda, Biodiesel production using anionic ion-exchange resin as heterogeneous catalyst, 98 (2007) 416–421. https://doi.org/10.1016/j.biortech.2005.12.010.

[20] A. Alrobaian, V. Rajasekar, A. Alagumalai, Critical insight into biowaste-derived biocatalyst for biodiesel production, Environ. Prog. Sustain. Energy. 39 (2020). https://doi.org/10.1002/ep.13391.

[21] S.P. Gouda, J.M. H. Anal, P. Kumar, A. Dhakshinamoorthy, U. Rashid, S.L. Rokhum, J.M. Jasha, P. Kumar, A. Dhakshinamoorthy, U. Rashid, S.L. Rokhum Microwave-Assisted Biodiesel Production Using UiO-66 MOF Derived Nanocatalyst: Process Optimization Using Response Surface Methodology, Catalysts. 12 (2022) 1312. https://doi.org/10.3390/CATAL12111312/S1.

[22] S. Nawaz, M. Ahmad, S. Asif, J.J. Klemeš, M. Mubashir, M. Munir, M. Zafar, A. Bokhari, A. Mukhtar, S. Saqib, K.S. Khoo, P.L. Show, Phyllosilicate derived catalysts for efficient conversion of lignocellulosic derived biomass to biodiesel: A review, Bioresour. Technol. 343 (2022) 126068. https://doi.org/10.1016/J.BIORTECH.2021.126068.

[23] J. Escalante, W.H. Chen, M. Tabatabaei, A.T. Hoang, E.E. Kwon, K.Y. Andrew Lin, A. Saravanakumar, Pyrolysis of lignocellulosic, algal, plastic, and other biomass wastes for biofuel production and circular bioeconomy: A review of thermogravimetric analysis (TGA) approach, Renew. Sustain. Energy Rev. 169 (2022) 112914. https://doi.org/10.1016/J.RSER.2022.112914.

[24] S.H.Y.S. Abdullah, N.H.M. Hanapi, A. Azid, R. Umar, H. Juahir, H. Khatoon, A. Endut, A review of biomass-derived heterogeneous catalyst for a sustainable biodiesel production, Renew. Sustain. Energy Rev. 70 (2017) 1040–1051. https://doi.org/10.1016/j.rser.2016.12.008.

[25] A. Sarwer, S.M. Hamed, A.I. Osman, F. Jamil, H. Al-Muhtaseb, N.S. Alhajeri, D.W. Rooney, Algal biomass valorization for biofuel production and carbon sequestration: a review, 20 (2022) 2797–2851. https://doi.org/10.1007/s10311-022-01458-1.

[26] Z.E. Tang, S. Lim, Y.L. Pang, H.C. Ong, K.T. Lee, Synthesis of biomass as heterogeneous catalyst for application in biodiesel production: State of the art and fundamental review, Renew. Sustain. Energy Rev. 92 (2018) 235–253.

[27] S.Y. Chua, L.A. Periasamy, C.M.H. Goh, Y.H. Tan, N.M. Mubarak, J. Kansedo, M. Khalid, R. Walvekar, E.C. Abdullah, Biodiesel synthesis using natural solid catalyst derived from biomass waste — A review, J. Ind. Eng. Chem. 81 (2020) 41–60. https://doi.org/10.1016/J.JIEC.2019.09.022.

[28] S. Parida, M. Singh, S. Pradhan, Biomass wastes: A potential catalyst source for biodiesel production, Bioresour. Technol. Reports. 18 (2022) 101081. https://doi.org/10.1016/J.BITEB.2022.101081.

[29] A. Galadima, O. Muraza, Waste materials for production of biodiesel catalysts: Technological status and prospects, J. Clean. Prod. 263 (2020) 121358. https://doi.org/10.1016/J.JCLEPRO.2020.121358.

[30] M. Hamza, M. Ayoub, R. Bin Shamsuddin, A. Mukhtar, S. Saqib, I. Zahid, M. Ameen, S. Ullah, A.G. Al-Sehemi, M. Ibrahim, A review on the waste biomass derived catalysts for biodiesel production, Environmental Technology & Innovation 21 (2021) 101200. https://doi.org/10.1016/j.eti.2020.101200.

[31] D.M. Marinković, M. V. Stanković, A. V. Veličković, J.M. Avramović, M.R. Miladinović, O.O. Stamenković, V.B. Veljković, D.M. Jovanović, Calcium oxide as a promising heterogeneous catalyst for biodiesel production: Current state and perspectives, Renew. Sustain. Energy Rev. 56 (2016) 1387–1408. https://doi.org/10.1016/j.rser.2015.12.007.

[32] N.A. Zul, S. Ganesan, T.S. Hamidon, W. Da Oh, M.H. Hussin, A review on the utilization of calcium oxide as a base catalyst in biodiesel production, J. Environ. Chem. Eng. 9 (2021) 105741. https://doi.org/10.1016/j.jece.2021.105741.

[33] R. Chakraborty, S. Chatterjee, P. Mukhopadhyay, S. Barman, Progresses in Waste Biomass Derived Catalyst for Production of Biodiesel and Bioethanol: A Review, Procedia Environ. Sci. 35 (2016) 546–554. https://doi.org/10.1016/j.proenv.2016.07.039.

[34] J.S.J. Ling, Y.H. Tan, N.M. Mubarak, J. Kansedo, A. Saptoro, C. Nolasco-Hipolito, A review of heterogeneous calcium oxide based catalyst from waste for biodiesel synthesis, SN Appl. Sci. 1 (2019) 1–8. https://doi.org/10.1007/s42452-019-0843-3.

[35] J. Goli, O. Sahu, SC, Development of heterogeneous alkali catalyst from waste chicken eggshell for biodiesel production, Renew. Energy. 128 (2018) 142-154. https://doi.org/10.1016/j.renene.2018.05.048.

[36] G. Santya, T. Maheswaran, K.F. Yee, Optimization of biodiesel production from high free

fatty acid river catfish oil (Pangasius hypothalamus) and waste cooking oil catalyzed by waste chicken egg shells derived catalyst, SN Appl. Sci. 1 (2019). https://doi.org/10.1007/s42452-018-0155-z.

[37] M. Hossain, N. Muntaha, L.K.M. Osman Goni, M.S. Jamal, M.A. Gafur, D. Islam, A.N.M. Fakhruddin, Triglyceride Conversion of Waste Frying Oil up to 98.46% Using Low Concentration K + /CaO Catalysts Derived from Eggshells , ACS Omega. 6 (2021) 35679–35691. https://doi.org/10.1021/acsomega.1c05582.

[38] M. Khatibi, F. Khorasheh, A. Larimi, Biodiesel production via transesterification of canola oil in the presence of Na–K doped CaO derived from calcined eggshell, Renew. Energy. (2021). https://doi.org/10.1016/j.renene.2020.10.039.

[39] H. Hadiyanto, A.H. Afianti, U.I. Navi'A, N.P. Adetya, W. Widayat, H. Sutanto, The development of heterogeneous catalyst C/CaO/NaOH from waste of green mussel shell (Perna varidis) for biodiesel synthesis, J. Environ. Chem. Eng. (2017). https://doi.org/10.1016/j.jece.2017.08.049.

[40] M.D. Putra, Y. Ristianingsih, R. Jelita, C. Irawan, I.F. Nata, Potential waste from palm empty fruit bunches and eggshells as a heterogeneous catalyst for biodiesel production, RSC Adv. 7 (2017) 55547–55554. https://doi.org/10.1039/c7ra11031f.

[41] S. Niju, M.M.M.S. Begum, N. Anantharaman, Modification of egg shell and its application in biodiesel production, J. Saudi Chem. Soc. (2014). https://doi.org/10.1016/j.jscs.2014.02.010.

[42] R. Anr, A.A. Saleh, M.S. Islam, S. Hamdan, M.A. Maleque, Biodiesel Production from Crude Jatropha Oil using a Highly Active Heterogeneous Nanocatalyst by Optimizing Transesterification Reaction Parameters, Energy and Fuels. 30 (2016) 334–343. https://doi.org/10.1021/acs.energyfuels.5b01899.

[43] C.Y. Chooi, J.H. Sim, S.F. Tee, Z.H. Lee, Waste-Derived Green Nanocatalyst for Biodiesel Production : Kinetic-Mechanism Deduction and Optimization Studies, Sustainability 13 (2021), 5849. https://doi.org/10.3390/su13115849.

[44] Y.H. Tan, M.O. Abdullah, C. Nolasco-Hipolito, N.S. Ahmad Zauzi, Application of RSM

and Taguchi methods for optimizing the transesterification of waste cooking oil catalyzed by solid ostrich and chicken-eggshell derived CaO, Renew. Energy. 114 (2017) 437–447. https://doi.org/10.1016/j.renene.2017.07.024.

[45] Y.C. Wong, R.X. Ang, Study of calcined eggshell as potential catalyst for biodiesel formation using used cooking oil, Open Chem. 16 (2018) 1166–1175. https://doi.org/10.1515/chem-2018-0127.

[46] N. Tshizanga, E.F. Aransiola, O. Oyekola, Optimisation of biodiesel production from waste vegetable oil and eggshell ash, South African J. Chem. Eng. 23 (2017) 145–156. https://doi.org/10.1016/j.sajce.2017.05.003.

[47] M.L. Granados, D.M. Alonso, I. Sádaba, R. Mariscal, P. Ocón, Leaching and homogeneous contribution in liquid phase reaction catalysed by solids: The case of triglycerides methanolysis using CaO, Appl. Catal. B Environ. 89 (2009) 265–272. https://doi.org/10.1016/j.apcatb.2009.02.014.

[48] M. Kouzu, J.S. Hidaka, Transesterification of vegetable oil into biodiesel catalyzed by CaO: A review, Fuel. 93 (2012) 1–12. https://doi.org/10.1016/j.fuel.2011.09.015.

[49] A. Buasri, N. Chaiyut, V. Loryuenyong, C. Wongweang, S. Khamsrisuk, Application of eggshell wastes as a heterogeneous catalyst for biodiesel production, Sustain. Energy. 1 (2013) 7–13. https://doi.org/10.12691/rse-1-2-1.

[50] B. Sajjadi, A.R. Abdul Aziz, S. Ibrahim, Investigation, modelling and reviewing the effective parameters in microwave-assisted transesterification, Renew. Sustain. Energy Rev. 37 (2014) 762–777. https://doi.org/10.1016/j.rser.2014.05.021.

[51] M.E. González, M. Cea, D. Reyes, L. Romero-Hermoso, P. Hidalgo, S. Meier, N. Benito, R. Navia, Functionalization of biochar derived from lignocellulosic biomass using microwave technology for catalytic application in biodiesel production, Energy Convers. Manag. (2017). https://doi.org/10.1016/j.enconman.2017.01.063.

[52] P.D. Rocha, L.S. Oliveira, A.S. Franca, Sulfonated activated carbon from corn cobs as heterogeneous catalysts for biodiesel production using microwave-assisted transesterification, Renew. Energy. 143 (2019) 1710–1716.

https://doi.org/10.1016/j.renene.2019.05.070.

[53] B. Khedri, M. Mostafaei, S.M. Safieddin Ardebili, A review on microwave-assisted biodiesel production, Energy Sources, Part A Recover. Util. Environ. Eff. 41 (2019) 2377–2395. https://doi.org/10.1080/15567036.2018.1563246.

[54] A. Ansori, S.A. Wibowo, H.S. Kusuma, D.S. Bhuana, M. Mahfud, Production of Biodiesel from Nyamplung (Calophyllum inophyllum L.) using Microwave with CaO Catalyst from Eggshell Waste: Optimization of Transesterification Process Parameters, Open Chem. 17 (2019) 1185–1197. https://doi.org/10.1515/chem-2019-0128.

[55] N.S. Lani, N. Ngadi, N.Y. Yahya, R.A. Rahman, Synthesis, characterization and performance of silica impregnated calcium oxide as heterogeneous catalyst in biodiesel production, J. Clean. Prod. (2017). https://doi.org/10.1016/j.jclepro.2016.06.058.

[56] H. Matsuhashi, M. Oikawa, K. Arata, Formation of superbase sites on alkaline earth metal oxides by doping of alkali metals, Langmuir. 16 (2000) 8201–8205. https://doi.org/10.1021/la000346n.

[57] X. Yu, X. Chen, W. Meng, M. Zhu, Research progress on supported solid superbase and its catalytic application, Chem. Pap. 75 (2021) 4445–4463. https://doi.org/10.1007/s11696-021-01669-w.

[58] A.R. Gupta, V.K. Rathod, Waste cooking oil and waste chicken eggshells derived solid base catalyst for the biodiesel production: Optimization and kinetics, Waste Manag. (2018). https://doi.org/10.1016/j.wasman.2018.07.022.

[59] B. Yoosuk, P. Udomsap, B. Puttasawat, P. Krasae, Modification of calcite by hydration-dehydration method for heterogeneous biodiesel production process: The effects of water on properties and activity, Chem. Eng. J. 162 (2010) 135–141. https://doi.org/10.1016/j.cej.2010.05.013.

[60] B. Yoosuk, P. Udomsap, B. Puttasawat, P. Krasae, Improving transesterification acitvity of CaO with hydration technique, Bioresour. Technol. 101 (2010) 3784–3786. https://doi.org/10.1016/j.biortech.2009.12.114.

[61] O.N. Syazwani, S.H. Teo, A. Islam, Y.H. Taufiq-Yap, Transesterification activity and

characterization of natural CaO derived from waste venus clam (Tapes belcheri S.) material for enhancement of biodiesel production, Process Saf. Environ. Prot. 105 (2017) 303–315. https://doi.org/10.1016/j.psep.2016.11.011.

[62] P.R. Pandit, M.H. Fulekar, Egg shell waste as heterogeneous nanocatalyst for biodiesel production: Optimized by response surface methodology, J. Environ. Manage. (2017). https://doi.org/10.1016/j.jenvman.2017.04.100.

[63] J. Sani, F. Agada, F. Agada, Production and Characterization of Heterogeneous Catalyst (CaO) from Snail Shell for Biodiesel Production Using ... Related papers, (n.d.) 2–6. https://doi.org/10.4172/2576-1463.1000162.

[64] E. Science, Biodiesel Production From Waste Cooking Oil Using Catalyst CaO Derived From Strombus canarium shells Biodiesel Production From Waste Cooking Oil Using Catalyst CaO Derived From Strombus canarium shells, (2019) 8–13. https://doi.org/10.1088/1755-1315/353/1/012012.

[65] S. Kaewdaeng, P. Sintuya, R. Nirunsin, Biodiesel production using calcium oxide from river snail shell ash as catalyst, Energy Procedia. 138 (2017) 937–942. https://doi.org/10.1016/j.egypro.2017.10.057.

[66] W. Roschat, T. Siritanon, T. Kaewpuang, B. Yoosuk, V. Promarak, Economical and green biodiesel production process using river snail shells-derived heterogeneous catalyst and co-solvent method, Bioresour. Technol. 209 (2016) 343–350. https://doi.org/10.1016/j.biortech.2016.03.038.

[67] A. Perea, T. Kelly, Y. Hangun-Balkir, Utilization of waste seashells and Camelina sativa oil for biodiesel synthesis, Green Chem. Lett. Rev. (2016). https://doi.org/10.1080/17518253.2016.1142004.

[68] D. Madhu, S.B. Chavan, V. Singh, B. Singh, Y.C. Sharma, An economically viable synthesis of biodiesel from a crude Millettia pinnata oil of Jharkhand, India as feedstock and crab shell derived catalyst, Bioresour. Technol. (2016). https://doi.org/10.1016/j.biortech.2016.04.055.

[69] H. Liu, H. shuang Guo, X. jing Wang, J. zhong Jiang, H. Lin, S. Han, S. peng Pei, Mixed

and ground KBr-impregnated calcined snail shell and kaolin as solid base catalysts for biodiesel production, Renew. Energy. (2016). https://doi.org/10.1016/j.renene.2016.03.017.

[70] V. Shankar, R. Jambulingam, Waste crab shell derived CaO impregnated Na-ZSM-5 as a solid base catalyst for the transesterification of neem oil into biodiesel, Sustain. Environ. Res. (2017). https://doi.org/10.1016/j.serj.2017.06.006.

[71] K.N. Krishnamurthy, S.N. Sridhara, C.S. Ananda Kumar, Optimization and kinetic study of biodiesel production from Hydnocarpus wightiana oil and dairy waste scum using snail shell CaO nano catalyst, Renew. Energy. (2020). https://doi.org/10.1016/j.renene.2019.06.161.

[72] H. Mazaheri, H.C. Ong, H.H. Masjuki, Z. Amini, M.D. Harrison, Rice bran oil based biodiesel production using calcium oxide catalyst derived from Chicoreus brunneus shell, Energy. (2017). https://doi.org/10.1016/j.energy.2017.11.073.

[73] M.L. Granados, M.D.Z. Poves, D.M. Alonso, R. Mariscal, F.C. Galisteo, R. Moreno-Tost, J. Santamaría, J.L.G. Fierro, Biodiesel from sunflower oil by using activated calcium oxide, Appl. Catal. B Environ. 73 (2007) 317–326. https://doi.org/10.1016/j.apcatb.2006.12.017.

[74] Y.C. Sharma, B. Singh, J. Korstad, Latest developments on application of heterogenous basic catalysts for an efficient and eco friendly synthesis of biodiesel: A review, Fuel. (2011). https://doi.org/10.1016/j.fuel.2010.10.015.

[75] H. Mahmood Khan, T. Iqbal, C. Haider Ali, A. Javaid, I. Iqbal Cheema, Sustainable biodiesel production from waste cooking oil utilizing waste ostrich (Struthio camelus) bones derived heterogeneous catalyst, Fuel. 277 (2020) 118091. https://doi.org/10.1016/j.fuel.2020.118091.

[76] G. Corro, N. Sánchez, U. Pal, F. Bañuelos, Biodiesel production from waste frying oil using waste animal bone and solar heat, Waste Manag. 47 (2016) 105–113. https://doi.org/10.1016/j.wasman.2015.02.001.

[77] C.H. Ali, A.H. Asif, T. Iqbal, A.S. Qureshi, M.A. Kazmi, S. Yasin, M. Danish, B.Z. Mu,

Improved transesterification of waste cooking oil into biodiesel using calcined goat bone as a catalyst, Energy Sources, Part A Recover. Util. Environ. Eff. 40 (2018) 1076–1083. https://doi.org/10.1080/15567036.2018.1469691.

[78] Y.H. Tan, M.O. Abdullah, J. Kansedo, N.M. Mubarak, Y.S. Chan, C. Nolasco-Hipolito, Biodiesel production from used cooking oil using green solid catalyst derived from calcined fusion waste chicken and fish bones, Renew. Energy. (2019). https://doi.org/10.1016/j.renene.2019.02.110.

[79] J. Nisar, R. Razaq, M. Farooq, M. Iqbal, R.A. Khan, M. Sayed, A. Shah, I. ur Rahman, Enhanced biodiesel production from Jatropha oil using calcined waste animal bones as catalyst, Renew. Energy. 101 (2017) 111–119. https://doi.org/10.1016/j.renene.2016.08.048.

[80] C. Chingakham, C. Tiwary, V. Sajith, Waste Animal Bone as a Novel Layered Heterogeneous Catalyst for the Transesterification of Biodiesel, Catal. Letters. (2019). https://doi.org/10.1007/s10562-019-02696-9.

[81] V. Volli, M.K. Purkait, C.M. Shu, Preparation and characterization of animal bone powder impregnated fly ash catalyst for transesterification, Sci. Total Environ. (2019). https://doi.org/10.1016/j.scitotenv.2019.03.080.

[82] G. Pathak, D. Das, K. Rajkumari, L. Rokhum, Exploiting waste: Towards a sustainable production of biodiesel using: Musa acuminata peel ash as a heterogeneous catalyst, Green Chem. 20 (2018) 2365–2373. https://doi.org/10.1039/c8gc00071a.

[83] B. Changmai, P. Sudarsanam, L. Rokhum, Biodiesel production using a renewable mesoporous solid catalyst, Ind. Crops Prod. 145 (2020) 111911. https://doi.org/10.1016/j.indcrop.2019.111911

[84] B. Nath, B. Das, P. Kalita, S. Basumatary, Waste to value addition: Utilization of waste Brassica nigra plant derived novel green heterogeneous base catalyst for effective synthesis of biodiesel, J. Clean. Prod. 239 (2019) 118112. https://doi.org/10.1016/j.jclepro.2019.118112.

[85] E. Betiku, A.A. Okeleye, N.B. Ishola, A.S. Osunleke, T. V. Ojumu, Development of a

Novel Mesoporous Biocatalyst Derived from Kola Nut Pod Husk for Conversion of Kariya Seed Oil to Methyl Esters: A Case of Synthesis, Modeling and Optimization Studies, Catal. Letters. 149 (2019) 1772–1787. https://doi.org/10.1007/S10562-019-02788-6.

[86] E. Betiku, A.M. Akintunde, T.V. Ojumu, Banana peels as a biobase catalyst for fatty acid methyl esters production using Napoleon's plume (Bauhinia monandra) seed oil: A process parameters optimization study, Energy. 103 (2016) 797–806. https://doi.org/10.1016/j.energy.2016.02.138.

[87] K. Rajkumari, A sustainable protocol for production of biodiesel by transesterification of soybean oil using banana trunk ash as a heterogeneous catalyst, Biomass Conversion and Biorefinery 10 (2020) 839–848. https://doi.org/10.1007/s13399-020-00647-8

[88] S.E. Onoji, S.E. Iyuke, A.I. Igbafe, M.O. Daramola, Transesterification of Rubber Seed Oil to Biodiesel over a Calcined Waste Rubber Seed Shell Catalyst: Modeling and Optimization of Process Variables, Energy and Fuels. 31 (2017) 6109–6119. https://doi.org/10.1021/acs.energyfuels.7b00331.

[89] M. Gohain, A. Devi, D. Deka, Musa balbisiana Colla peel as highly effective renewable heterogeneous base catalyst for biodiesel production, Ind. Crops Prod. 109 (2017) 8–18. https://doi.org/10.1016/j.indcrop.2017.08.006.

[90] M. Sharma, A.A. Khan, S.K. Puri, D.K. Tuli, Wood ash as a potential heterogeneous catalyst for biodiesel synthesis, Biomass and Bioenergy. 41 (2012) 94–106. https://doi.org/10.1016/j.biombioe.2012.02.017.

[91] A.O. Etim, E. Betiku, S.O. Ajala, P.J. Olaniyi, T. V. Ojumu, Potential of ripe plantain fruit peels as an ecofriendly catalyst for biodiesel synthesis: Optimization by artificial neural network integrated with genetic algorithm, Sustain. 10 (2018). https://doi.org/10.3390/su10030707.

[92] M.R. Miladinović, M. V. Zdujić, D.N. Veljović, J.B. Krstić, I.B. Banković-Ilić, V.B. Veljković, O.S. Stamenković, Valorization of walnut shell ash as a catalyst for biodiesel production, Renew. Energy. 147 (2020) 1033–1043.

https://doi.org/10.1016/j.renene.2019.09.056.

[93] B. Oladipo, E. Betiku, Optimization and kinetic studies on conversion of rubber seed (Hevea brasiliensis) oil to methyl esters over a green biowaste catalyst, J. Environ. Manage. (2020). https://doi.org/10.1016/j.jenvman.2020.110705.

[94] M. Kaur, R. Malhotra, A. Ali, Tungsten supported Ti/SiO2 nanoflowers as reusable heterogeneous catalyst for biodiesel production, Renew. Energy. 116 (2018) 109–119. https://doi.org/10.1016/j.renene.2017.09.065.

[95] B. Nath, P. Kalita, B. Das, S. Basumatary, Highly efficient renewable heterogeneous base catalyst derived from waste Sesamum indicum plant for synthesis of biodiesel, Renew. Energy. (2019). https://doi.org/10.1016/j.renene.2019.11.029.

[96] M. Balajii, S. Niju, A novel biobased heterogeneous catalyst derived from Musa acuminata peduncle for biodiesel production – Process optimization using central composite design, Energy Convers. Manag. 189 (2019) 118–131. https://doi.org/10.1016/j.enconman.2019.03.085.

[97] M. Balajii, S. Niju, Banana peduncle – A green and renewable heterogeneous base catalyst for biodiesel production from Ceiba pentandra oil, Renew. Energy. 146 (2020) 2255–2269. https://doi.org/10.1016/j.renene.2019.08.062.

[98] I.M. Mendonça, F.L. Machado, C.C. Silva, S. Duvoisin Junior, M.L. Takeno, P.J. de Sousa Maia, L. Manzato, F.A. de Freitas, Application of calcined waste cupuaçu (Theobroma grandiflorum) seeds as a low-cost solid catalyst in soybean oil ethanolysis: Statistical optimization, Energy Convers. Manag. 200 (2019) 112095. https://doi.org/10.1016/j.enconman.2019.112095.

[99] E. Betiku, † Anietie, O. Etim, O. Pereao, T.V. Ojumu, Two-Step Conversion of Neem (Azadirachta indica) Seed Oil into Fatty Methyl Esters Using a Heterogeneous Biomass-Based Catalyst: An Example of Cocoa Pod Husk, (2017). https://doi.org/10.1021/ACS.ENERGYFUELS.7B00.

[100] O.A. Falowo, M.I. Oloko-Oba, E. Betiku, Biodiesel production intensification via microwave irradiation-assisted transesterification of oil blend using nanoparticles from

elephant-ear tree pod husk as a base heterogeneous catalyst, Chem. Eng. Process. - Process Intensif. 140 (2019) 157–170. https://doi.org/10.1016/j.cep.2019.04.010.

[101] B. Basumatary, S. Basumatary, B. Das, B. Nath, P. Kalita, Waste Musa paradisiaca plant: An efficient heterogeneous base catalyst for fast production of biodiesel, J. Clean. Prod. (2021). https://doi.org/10.1016/j.jclepro.2021.127089.

[102] M. Gohain, K. Laskar, A.K. Paul, N. Daimary, M. Maharana, I.K. Goswami, A. Hazarika, U. Bora, D. Deka, Carica papaya stem: A source of versatile heterogeneous catalyst for biodiesel production and C–C bond formation, Renew. Energy. 147 (2020) 541–555. https://doi.org/10.1016/j.renene.2019.09.016.

[103] H.H. Abdelhady, H.A. Elazab, E.M. Ewais, M. Saber, M.S. El-Deab, Efficient catalytic production of biodiesel using nano-sized sugar beet agro-industrial waste, Fuel. 261 (2020) 116481. https://doi.org/10.1016/j.fuel.2019.116481.

[104] M. Kouzu, J. suke Hidaka, Y. Komichi, H. Nakano, M. Yamamoto, A process to transesterify vegetable oil with methanol in the presence of quick lime bit functioning as solid base catalyst, Fuel. 88 (2009) 1983–1990. https://doi.org/10.1016/j.fuel.2009.03.013.

[105] I.M. Mendonça, O.A.R.L. Paes, P.J.S. Maia, M.P. Souza, R.A. Almeida, C.C. Silva, S. Duvoisin, F.A. de Freitas, New heterogeneous catalyst for biodiesel production from waste tucumã peels (Astrocaryum aculeatum Meyer): Parameters optimization study, Renew. Energy. 130 (2019) 103–110. https://doi.org/10.1016/j.renene.2018.06.059.

[106] M. Gohain, K. Laskar, H. Phukon, U. Bora, D. Kalita, D. Deka, Towards sustainable biodiesel and chemical production: Multifunctional use of heterogeneous catalyst from littered Tectona grandis leaves, Waste Manag. (2020). https://doi.org/10.1016/j.wasman.2019.10.049.

[107] O.A. Falowo, T. V. Ojumu, O. Pereao, E. Betiku, Sustainable biodiesel synthesis from honne-rubber-neem oil blend with a novel mesoporous base catalyst synthesized from a mixture of three agrowastes, Catalysts. 10 (2020) 1–24. https://doi.org/10.3390/catal10020190.

[108] E.A. Olatundun, O.O. Borokini, E. Betiku, Cocoa pod husk-plantain peel blend as a novel

green heterogeneous catalyst for renewable and sustainable honne oil biodiesel synthesis: A case of biowastes-to-wealth, Renew. Energy. (2020). https://doi.org/10.1016/j.renene.2020.11.131.

[109] V.O. Odude, A.J. Adesina, O.O. Oyetunde, O.O. Adeyemi, N.B. Ishola, A.O. Etim, E. Betiku, Application of Agricultural Waste-Based Catalysts to Transesterification of Esterified Palm Kernel Oil into Biodiesel: A Case of Banana Fruit Peel Versus Cocoa Pod Husk, Waste and Biomass Valorization. 10 (2019) 877–888. https://doi.org/10.1007/s12649-017-0152-2.

[110] M.T.H. Siddiqui, S. Nizamuddin, H.A. Baloch, N.M. Mubarak, M. Al-Ali, S.A. Mazari, A.W. Bhutto, R. Abro, M. Srinivasan, G. Griffin, Fabrication of advance magnetic carbon nano-materials and their potential applications: A review, J. Environ. Chem. Eng. 7 (2019). https://doi.org/10.1016/j.jece.2018.102812.

[111] K. Rajkumari, B. Changmai, A.K. Meher, C. Vanlalveni, P. Sudarsanam, A.E.H. Wheatley, S.L. Rokhum, A reusable magnetic nanocatalyst for bio-fuel additives: The ultrasound-assisted synthesis of solketal, Sustain. Energy Fuels. 5 (2021) 2362–2372. https://doi.org/10.1039/d0se01900c.

[112] S.G. Krishnan, F. ling Pua, F. Zhang, A review of magnetic solid catalyst development for sustainable biodiesel production, Biomass and Bioenergy. 149 (2021) 106099. https://doi.org/10.1016/j.biombioe.2021.106099.

[113] S.K. Jena, H. Sahoo, S.S. Rath, D.S. Rao, S.K. Das, B. Das, Characterization and processing of iron ore slimes for recovery of iron values, Miner. Process. Extr. Metall. Rev. (2015). https://doi.org/10.1080/08827508.2014.898300.

[114] F. Zhang, X.H. Wu, M. Yao, Z. Fang, Y.T. Wang, Production of biodiesel and hydrogen from plant oil catalyzed by magnetic carbon-supported nickel and sodium silicate, Green Chem. (2016). https://doi.org/10.1039/c5gc02680f.

[115] F. Zhang, Z. Fang, Y.T. Wang, Biodiesel production directly from oils with high acid value by magnetic Na2SiO3@Fe3O4/C catalyst and ultrasound, Fuel. 150 (2015) 370–377. https://doi.org/10.1016/j.fuel.2015.02.032.

[116] F. Zhang, X.F. Tian, Z. Fang, M. Shah, Y.T. Wang, W. Jiang, M. Yao, Catalytic production of Jatropha biodiesel and hydrogen with magnetic carbonaceous acid and base synthesized from Jatropha hulls, Energy Convers. Manag. 142 (2017) 107–116. https://doi.org/10.1016/j.enconman.2017.03.026.

[117] C.M.H. Goh, Y.H. Tan, N.M. Mubarak, J. Kansedo, U. Rashid, M. Khalid, R. Walvekar, Synthesis of magnetic basic palm kernel shell catalyst for biodiesel production and characterisation and optimisation by Taguchi method, Appl. Nanosci. (2021). https://doi.org/10.1007/s13204-021-01815-6.

[118] B. Changmai, R. Rano, C. Vanlalveni, L. Rokhum, A novel Citrus sinensis peel ash coated magnetic nanoparticles as an easily recoverable solid catalyst for biodiesel production, Fuel. 286 (2021) 119447. https://doi.org/10.1016/j.fuel.2020.119447.

[119] A.M. Dehkhoda, N. Ellis, Biochar-based catalyst for simultaneous reactions of esterification and transesterification, Catal. Today. 207 (2013) 86–92. https://doi.org/10.1016/j.cattod.2012.05.034.

[120] B.K. Ozsel, D. Ozturk, B. Nis, One-pot hydrothermal conversion of different residues to value-added chemicals usıng new acidic carbonaceous catalyst, Bioresour. Technol. (2019). https://doi.org/10.1016/j.biortech.2019.121627.

[121] F.A. Dawodu, O. Ayodele, J. Xin, S. Zhang, D. Yan, Effective conversion of non-edible oil with high free fatty acid into biodiesel by sulphonated carbon catalyst, Appl. Energy. 114 (2014) 819–826. https://doi.org/10.1016/j.apenergy.2013.10.004.

[122] L.J. Konwar, J. Wärnå, P. Mäki-Arvela, N. Kumar, J.P. Mikkola, Reaction kinetics with catalyst deactivation in simultaneous esterification and transesterification of acid oils to biodiesel (FAME) over a mesoporous sulphonated carbon catalyst, Fuel. 166 (2016) 1–11. https://doi.org/10.1016/j.fuel.2015.10.102.

[123] K. Nakajima, M. Hara, Amorphous carbon with SO3H groups as a solid brønsted acid catalyst, ACS Catal. (2012). https://doi.org/10.1021/cs300103k.

[124] M. Toda, A. Takagaki, M. Okamura, J.N. Kondo, S. Hayashi, K. Domen, M. Hara, Biodiesel made with sugar catalyst, Nature. (2005). https://doi.org/10.1038/438178a.

[125] S. Niu, Y. Ning, C. Lu, K. Han, H. Yu, Y. Zhou, Esteri fi cation of oleic acid to produce biodiesel catalyzed by sulfonated activated carbon from bamboo, Energy Convers. Manag. 163 (2018) 59–65. https://doi.org/10.1016/j.enconman.2018.02.055.

[126] F. Shen, T. Guo, C. Bai, M. Qiu, X. Qi, Hydrolysis of cellulose with one-pot synthesized sulfonated carbonaceous solid acid, Fuel Process. Technol. (2018). https://doi.org/10.1016/j.fuproc.2017.10.015.

[127] K.M. Eblagon, M.F.R. Pereira, J.L. Figueiredo, A. Malaika, K. Ptaszy, Solid acid carbon catalysts for sustainable production of biofuel enhancers via transesterification of glycerol with ethyl acetate, 304 (2021). https://doi.org/10.1016/j.fuel.2021.121381.

[128] T.T.V. Tran, S. Kaiprommarat, S. Kongparakul, P. Reubroycharoen, G. Guan, M.H. Nguyen, C. Samart, Green biodiesel production from waste cooking oil using an environmentally benign acid catalyst, Waste Manag. 52 (2016) 367–374. https://doi.org/10.1016/j.wasman.2016.03.053.

[129] M. Mahdavi, Sulfonated Carbon Material as An Efficient Solid Acid Catalyst for Biodiesel Synthesis via Oleic Acid Esterification Under High Voltage Conditions, (2019) 1–9. https://doi.org/10.20944/preprints201909.0110.v1.

[130] A. Iryanti, F. Nata, M.D. Putra, Catalytic performance of sulfonated carbon-based solid acid catalyst on esterification of waste cooking oil for biodiesel production, Biochem. Pharmacol. (2017). https://doi.org/10.1016/j.jece.2017.04.029.

[131] Z. Liu, A. Quek, S. Kent Hoekman, R. Balasubramanian, Production of solid biochar fuel from waste biomass by hydrothermal carbonization, Fuel. 103 (2013) 943–949. https://doi.org/10.1016/j.fuel.2012.07.069.

[132] C. Falco, N. Baccile, M.M. Titirici, Morphological and structural differences between glucose, cellulose and lignocellulosic biomass derived hydrothermal carbons, Green Chem. 13 (2011) 3273–3281. https://doi.org/10.1039/c1gc15742f.

[133] J.M. Fraile, E. García-Bordejé, L. Roldán, Deactivation of sulfonated hydrothermal carbons in the presence of alcohols: Evidences for sulfonic esters formation, J. Catal. 289 (2012) 73–79. https://doi.org/10.1016/j.jcat.2012.01.017.

[134] Y. Zhou, S. Niu, J. Li, Activity of the carbon-based heterogeneous acid catalyst derived from bamboo in esterification of oleic acid with ethanol, Energy Convers. Manag. 114 (2016) 188–196. https://doi.org/10.1016/j.enconman.2016.02.027.

[135] X. Liang, M. Zeng, C. Qi, One-step synthesis of carbon functionalized with sulfonic acid groups using hydrothermal carbonization, Carbon N. Y. 48 (2010) 1844–1848. https://doi.org/10.1016/j.carbon.2010.01.030.

[136] H.H. Mardhiah, H.C. Ong, H.H. Masjuki, S. Lim, Y.L. Pang, Investigation of carbon-based solid acid catalyst from Jatropha curcas biomass in biodiesel production, Energy Convers. Manag. 144 (2017) 10–17. https://doi.org/10.1016/j.enconman.2017.04.038.

[137] B. Behera, M. Selvam S, B. Dey, P. Balasubramanian, Algal biodiesel production with engineered biochar as a heterogeneous solid acid catalyst, Bioresour. Technol. (2020). https://doi.org/10.1016/j.biortech.2020.123392.

[138] A. Endut, S. Hanis, Y. Sayid, N. Hanis, M. Hanapi, S. Hajar, A. Hamid, F. Lananan, M. Khairul, A. Kamarudin, R. Umar, H. Khatoon, International Biodeterioration & Biodegradation Optimization of biodiesel production by solid acid catalyst derived from coconut shell via response surface methodology, (2017). https://doi.org/10.1016/j.ibiod.2017.06.008.

[139] I. Thushari, S. Babel, Sustainable utilization of waste palm oil and sulfonated carbon catalyst derived from coconut meal residue for biodiesel production, Bioresour. Technol. 248 (2018) 199–203. https://doi.org/10.1016/j.biortech.2017.06.106.

[140] K.P. Flores, J.L.O. Omega, L.K. Cabatingan, A.W. Go, R.C. Agapay, Y.H. Ju, Simultaneously carbonized and sulfonated sugarcane bagasse as solid acid catalyst for the esterification of oleic acid with methanol, Renew. Energy. (2019). https://doi.org/10.1016/j.renene.2018.06.093.

[141] S. Dechakhumwat, P. Hongmanorom, C. Thunyaratchatanon, Catalytic activity of heterogeneous acid catalysts derived from corncob in the esterification of oleic acid with methanol, Renew. Energy. 48 (2020) 897–906. https://doi.org/10.1016/j.renene.2019.10.174.

[142] A. Wang, H. Zhang, H. Li, S. Yang, Efficient Production of Methyl Oleate Using a Biomass-Based Solid Polymeric Catalyst with High Acid Density, Adv. Polym. Technol. (2019). https://doi.org/10.1155/2019/4041631.

[143] D.R. Lathiya, D. V. Bhatt, K.C. Maheria, Synthesis of sulfonated carbon catalyst from waste orange peel for cost effective biodiesel production, Bioresour. Technol. Reports. 2 (2018) 69–76. https://doi.org/10.1016/j.biteb.2018.04.007.

[144] C.E. Akhabue, E.O. Osa-Benedict, E.A. Oyedoh, S.K. Otoikhian, Development of a bio-based bifunctional catalyst for simultaneous esterification and transesterification of neem seed oil: Modeling and optimization studies, Renew. Energy. 152 (2020) 724–735. https://doi.org/10.1016/j.renene.2020.01.103.

[145] S.I. Akinfalabi, U. Rashid, R. Yunus, Y.H. Taufiq-Yap, Synthesis of biodiesel from palm fatty acid distillate using sulfonated palm seed cake catalyst, Renew. Energy. (2017). https://doi.org/10.1016/j.renene.2017.04.056.

[146] X. Tang, S. Niu, Preparation of carbon-based solid acid with large surface area to catalyze esterification for biodiesel production, J. Ind. Eng. Chem. (2019). https://doi.org/10.1016/j.jiec.2018.09.016.

[147] M.F. Hussein, A.O. Abo El Naga, M. El Saied, M.M. AbuBaker, S.A. Shaban, F.Y. El Kady, Potato peel waste-derived carbon-based solid acid for the esterification of oleic acid to biodiesel, Environ. Technol. Innov. (2021). https://doi.org/10.1016/j.eti.2021.101355.

[148] A.M. Dehkhoda, A.H. West, N. Ellis, Biochar based solid acid catalyst for biodiesel production, Appl. Catal. A Gen. 382 (2010) 197–204. https://doi.org/10.1016/j.apcata.2010.04.051.

[149] M.K. Kumawat, S.L. Rokhum, Biodiesel Production From Oleic Acid Using Biomass-Derived Sulfonated Orange Peel Catalyst, Front. Catal. 2 (2022) 1–12. https://doi.org/10.3389/fctls.2022.914670.

[150] L.J. Konwar, P. Mäki-Arvela, J.P. Mikkola, SO3H-Containing Functional Carbon Materials: Synthesis, Structure, and Acid Catalysis, Chem. Rev. 119 (2019) 11576–11630. https://doi.org/10.1021/acs.chemrev.9b00199.

[151] A. Wang, H. Li, H. Pan, H. Zhang, F. Xu, Z. Yu, S. Yang, Efficient and green production of biodiesel catalyzed by recyclable biomass-derived magnetic acids, Fuel Process. Technol. 181 (2018) 259–267. https://doi.org/10.1016/j.fuproc.2018.10.003.

[152] Y.Z. Han, L. Hong, X.Q. Wang, J.Z. Liu, J. Jiao, M. Luo, Y.J. Fu, Biodiesel production from Pistacia chinensis seed oil via transesterification using recyclable magnetic cellulose-based catalyst, Ind. Crops Prod. (2016). https://doi.org/10.1016/j.indcrop.2016.05.015.

[153] F. Zhang, X. Tian, M. Shah, W. Yang, Synthesis of magnetic carbonaceous acids derived from hydrolysates of Jatropha hulls for catalytic biodiesel production, RSC Adv. (2017). https://doi.org/10.1039/c6ra28796d.

[154] R.V. Quah, Y.H. Tan, N.M. Mubarak, J. Kansedo, M. Khalid, E.C. Abdullah, M.O. Abdullah, Magnetic biochar derived from waste palm kernel shell for biodiesel production via sulfonation, Waste Manag. 118 (2020) 626–636. https://doi.org/10.1016/j.wasman.2020.09.016.

[155] R.O. Araujo, V.O. Santos, F.C.P. Ribeiro, J. da S. Chaar, A.M. Pereira, N.P.S. Falcão, L.K.C. de Souza, Magnetic acid catalyst produced from acai seeds and red mud for biofuel production, Energy Convers. Manag. (2021). https://doi.org/10.1016/j.enconman.2020.113636.

[156] N.A. Ibrahim, U. Rashid, Y.H. Taufiq-Yap, T.C.S. Yaw, I. Ismail, Synthesis of carbonaceous solid acid magnetic catalyst from empty fruit bunch for esterification of palm fatty acid distillate (PFAD), Energy Convers. Manag. (2019). https://doi.org/10.1016/j.enconman.2019.05.022.

[157] S. Chellappan, K. Aparna, C. Chingakham, V. Sajith, V. Nair, Microwave assisted biodiesel production using a novel BrØnsted acid catalyst based on nanomagnetic biocomposite, Fuel. 246 (2019) 268–276. https://doi.org/10.1016/j.fuel.2019.02.104.

[158] S.N.A. Jenie, A. Kristiani, Sudiyarmanto, D.S. Khaerudini, K. Takeishi, Sulfonated magnetic nanobiochar as heterogeneous acid catalyst for esterification reaction, J. Environ. Chem. Eng. 8 (2020) 103912. https://doi.org/10.1016/j.jece.2020.103912.

[159] S. Chellappan, V. Nair, V. Sajith, K. Aparna, Synthesis, optimization and characterization

of biochar based catalyst from sawdust for simultaneous esterification and transesterification, Chinese J. Chem. Eng. (2018) 2654–2663. https://doi.org/10.1016/j.cjche.2018.02.034.

[160] M.N. Nabi, M.G. Rasul, Influence of second generation biodiesel on engine performance, emissions, energy and exergy parameters, Energy Convers. Manag. (2018). https://doi.org/10.1016/j.enconman.2018.05.066.

[161] L. Du, S. Ding, Z. Li, E. Lv, J. Lu, J. Ding, Transesterification of castor oil to biodiesel using NaY zeolite-supported La2O3 catalysts, Energy Convers. Manag. 173 (2018) 728–734. https://doi.org/10.1016/j.enconman.2018.07.053.

[162] C.W. Mohd Noor, M.M. Noor, R. Mamat, Biodiesel as alternative fuel for marine diesel engine applications: A review, Renew. Sustain. Energy Rev. (2018). https://doi.org/10.1016/j.rser.2018.05.031.

[163] N. Mansir, S.H. Teo, U. Rashid, M.I. Saiman, Y.P. Tan, G.A. Alsultan, Y.H. Taufiq-Yap, Modified waste egg shell derived bifunctional catalyst for biodiesel production from high FFA waste cooking oil. A review, Renew. Sustain. Energy Rev. 82 (2018) 3645–3655. https://doi.org/10.1016/j.rser.2017.10.098.

[164] S.H. Dhawane, T. Kumar, G. Halder, Recent advancement and prospective of heterogeneous carbonaceous catalysts in chemical and enzymatic transformation of biodiesel, Energy Convers. Manag. (2018). https://doi.org/10.1016/j.enconman.2018.04.073.

[165] N. Mansir, S. Hwa Teo, M. Lokman Ibrahim, T.Y. Yun Hin, Synthesis and application of waste egg shell derived CaO supported W-Mo mixed oxide catalysts for FAME production from waste cooking oil: Effect of stoichiometry, Energy Convers. Manag. 151 (2017) 216–226. https://doi.org/10.1016/j.enconman.2017.08.069.

[166] I. Istadi, U. Mabruro, B.A. Kalimantini, L. Buchori, D.D. Anggoro, Reusability and stability tests of calcium oxide based catalyst (K2O/CaO-ZnO) for transesterification of soybean oil to biodiesel, in: Bull. Chem. React. Eng. Catal., 2016. https://doi.org/10.9767/bcrec.11.1.413.34-39.

[167] M.M. Naeem, E.G. Al-Sakkari, D.C. Boffito, M.A. Gadalla, F.H. Ashour, One-pot conversion of highly acidic waste cooking oil into biodiesel over a novel bio-based bi-functional catalyst, Fuel. 283 (2021). https://doi.org/10.1016/j.fuel.2020.118914.

[168] P.K. Brar, B. Örmeci, A. Dhir, Parametric optimization of rice bran-based bi-functional catalyst in the one-pot conversion of indigenous algal biomass into biodiesel using response surface methodology, Biomass Convers. Biorefinery. (2022). https://doi.org/10.1007/s13399-022-02522-0.

[169] J.Z. Yin, M. Xiao, J. Bin Song, Biodiesel from soybean oil in supercritical methanol with co-solvent, Energy Convers. Manag. 49 (2008) 908–912. https://doi.org/10.1016/J.ENCONMAN.2007.10.018.

[170] H.M. Khan, T. Iqbal, S. Yasin, M. Irfan, M.M. Abbas, I. Veza, M.E.M. Soudagar, A. Abdelrahman, M.A. Kalam, Heterogeneous Catalyzed Biodiesel Production Using Cosolvent: A Mini Review, Sustain. 14 (2022) 1–11. https://doi.org/10.3390/su14095062.

[171] O. Nur, U. Rashid, M. Sufri, Esteri fi cation of palm fatty acid distillate (PFAD) to biodiesel using Bi- functional catalyst synthesized from waste angel wing shell (Cyrtopleura costata), 131 (2019). https://doi.org/10.1016/j.renene.2018.07.031.

[172] A.N. Amenaghawon, K. Obahiagbon, V. Isesele, F. Usman, Optimized biodiesel production from waste cooking oil using a functionalized bio-based heterogeneous catalyst, Clean. Eng. Technol. 8 (2022) 100501. https://doi.org/10.1016/j.clet.2022.100501.

[173] R. Naveenkumar, G. Baskar, Biodiesel production from Calophyllum inophyllum oil using zinc doped calcium oxide (Plaster of Paris) nanocatalyst, Bioresource Technology 280 (2019) 493-496. https://doi.org/10.1016/j.biortech.2019.02.078.

[174] N. Mansir, S.H. Teo, U. Rashid, Y.H. Taufiq-Yap, Efficient waste Gallus domesticus shell derived calcium-based catalyst for biodiesel production, Fuel. 211 (2018) 67–75. https://doi.org/10.1016/j.fuel.2017.09.014.

[175] R.F. Abdullah, U. Rashid, Y.H. Taufiq-Yap, M.L. Ibrahim, C. Ngamcharussrivichai, M. Azam, Synthesis of bifunctional nanocatalyst from waste palm kernel shell and its

application for biodiesel production, RSC Adv. 10 (2020) 27183–27193. https://doi.org/10.1039/d0ra04306k.

[176] R.F. Abdullah, U. Rashid, M.L. Ibrahim, B. Hazmi, F.A. Alharthi, I.A. Nehdi, Bifunctional nano-catalyst produced from palm kernel shell via hydrothermal-assisted carbonization for biodiesel production from waste cooking oil, Renew. Sustain. Energy Rev. 137 (2021) 110638. https://doi.org/10.1016/j.rser.2020.110638.

[177] B. Hazmi, U. Rashid, Y.H. Taufiq-Yap, M.L. Ibrahim, I.A. Nehdi, Supermagnetic nano-bifunctional catalyst from rice husk: Synthesis, characterization and application for conversion of used cooking oil to biodiesel, Catalysts. 10 (2020). https://doi.org/10.3390/catal10020225.

[178] B. Hazmi, U. Rashid, M.L. Ibrahim, I.A. Nehdi, M. Azam, S.I. Al-Resayes, Synthesis and characterization of bifunctional magnetic nano-catalyst from rice husk for production of biodiesel, Environ. Technol. Innov. 21 (2021) 101296. https://doi.org/10.1016/j.eti.2020.101296.

[179] K. Liu, R. Wang, M. Yu, An efficient, recoverable solid base catalyst of magnetic bamboo charcoal: Preparation, characterization, and performance in biodiesel production, Renew. Energy. 127 (2018) 531–538. https://doi.org/10.1016/j.renene.2018.04.092.

[180] N.A. Ibrahim, U. Rashid, B. Hazmi, B.R. Moser, F.A. Alharthi, S.L. Rokhum, C. Ngamcharussrivichai, Biodiesel production from waste cooking oil using magnetic bifunctional calcium and iron oxide nanocatalysts derived from empty fruit bunch, Fuel. 317 (2022) 123525. https://doi.org/10.1016/j.fuel.2022.123525.

[181] Y.T. Wang, X.M. Wang, D. Gao, F.P. Wang, Y.N. Zeng, J.G. Li, L.Q. Jiang, Q. Yu, R. Ji, L. Le Kang, Y.J. Wang, Z. Fang, Efficient production of biodiesel at low temperature using highly active bifunctional Na-Fe-Ca nanocatalyst from blast furnace waste, Fuel. 322 (2022) 124168. https://doi.org/10.1016/j.fuel.2022.124168.

[182] X. Mo, D.E. López, K. Suwannakarn, Y. Liu, E. Lotero, J.G. Goodwin, C. Lu, Activation and deactivation characteristics of sulfonated carbon catalysts, Journal of Catalysis 254 (2008) 332–338. https://doi.org/10.1016/j.jcat.2008.01.011.

[183] M. Hara, Biomass conversion by a solid acid catalyst, Energy Environ. Sci., 3 (2010) 601-607. https://doi.org/10.1039/b922917e.

[184] B.F. Lutnaes, G. Luthe, U.A.T. Brinkman, J.E. Johansen, J. Krane, Characterization of monofluorinated polycyclic aromatic compounds by 1H, 13C and 19F NMR spectroscopy, Magn. Reson. Chem. 43 (2005) 588–594. https://doi.org/10.1002/mrc.1584.

[185] A. Bax, J.A. Ferretti, N. Nashed, D.M. Jerina, Complete 1H and 13C NMR Assignment of Complex Polycyclic Aromatic Hydrocarbons, J. Org. Chem. 50 (1985) 3029–3034. https://doi.org/10.1021/jo00217a001.

[186] K. Nakajima, M. Hara, S. Hayashi, Environmentally benign production of chemicals and energy using a carbon-based strong solid acid, J. Am. Ceram. Soc. 90 (2007) 3725–3734. https://doi.org/10.1111/j.1551-2916.2007.02082.x.

[187] L. Roldán, E. Pires, J.M. Fraile, E. García-bordejé, Impact of sulfonated hydrothermal carbon texture and surface chemistry on its catalytic performance in esterification reaction, Catal. Today. 249 (2015) 153–160. https://doi.org/10.1016/j.cattod.2014.10.008.

[188] S. Zhang, L. Wang, J. Wang, J. Yang, L. Fu, Z. Cai, Y. Fu, A novel in situ transesterification of yellow horn seeds to biodiesel using a dual function switchable solvent, Fuel. 312 (2022) 122974. https://doi.org/10.1016/j.fuel.2021.122974.

[189] M. Yusuf, M. Athar, Biodiesel Production Using Hexane as Co-Solvent, J. Biofuels. 6 (2015) 88. https://doi.org/10.5958/0976-4763.2015.00013.6.

[190] N. Hajilary, M. Rezakazemi, Saeed Shirazian, Biofuel types and membrane separation, Environ. Chem. Lett. 17 (2019) 1–18. https://doi.org/10.1007/s10311-018-0777-9.

[191] C. Bartholomew, Catalysts-deactivation-and-regeneration 5 (2001). https://doi.org/10.1002/0471238961.1415021218150209.a01.pub2

[192] M. Malaguti, A.F. Novoa, F. Ricceri, M. Giagnorio, J.S. Vrouwenvelder, A. Tiraferri, L. Fortunato, Control strategies against algal fouling in membrane processes applied for microalgae biomass harvesting, J. Water Process Eng. 47 (2022) 102787. https://doi.org/10.1016/J.JWPE.2022.102787.

[193] J.R. Copeland, I.A. Santillan, S.M.N. Schimming, J.L. Ewbank, C. Sievers, Surface interactions of glycerol with acidic and basic metal oxides, J. Phys. Chem. C. 117 (2013) 21413–21425. https://doi.org/10.1021/JP4078695/SUPPL_FILE/JP4078695_SI_001.PDF.

[194] A. Ochoa, J. Bilbao, A.G. Gayubo, P. Castaño, Coke formation and deactivation during catalytic reforming of biomass and waste pyrolysis products: A review, Renew. Sustain. Energy Rev. 119 (2020) 109600. https://doi.org/10.1016/J.RSER.2019.109600.

[195] C. Zhu, O.Y. Gutiérrez, D.M. Santosa, I. Kutnyakov, R. Weindl, H. Shi, H. Wang, Impact of Coprocessing Biocrude with Petroleum Stream on Hydrotreating Catalyst Stability, Energy and Fuels. 36 (2022) 9133–9146. https://doi.org/10.1021/acs.energyfuels.2c01748.

[196] J. Plácido, S. Capareda, Conversion of residues and by-products from the biodiesel industry into value-added products, Bioresour. Bioprocess. 3 (2016) 1–12. https://doi.org/10.1186/s40643-016-0100-1.

[197] S. Ao, S.L. Rokhum, Recent Advances in the Valorization of Biodiesel By-Product Glycerol to Solketal, Journal of Chemistry 2022 (2022). https://doi.org/10.1155/2022/4938672.

[198] S. Kim, S.N. Nam, A. Jang, M. Jang, C.M. Park, A. Son, N. Her, J. Heo, Y. Yoon, Review of adsorption–membrane hybrid systems for water and wastewater treatment, Chemosphere. 286 (2022) 131916. https://doi.org/10.1016/J.CHEMOSPHERE.2021.131916.

[199] S. Ibragić, N. Smječanin, R. Milušić, M. Nuhanović, S. Ibragi, N. Smje canin, R. Milu si, M. Nuhanovi, Pomelo peel and sugar beet pulp as novel biosorbents in purification of biodiesel, Https://Doi.Org/10.1080/17597269.2021.1920198. 13 (2021) 755–762. https://doi.org/10.1080/17597269.2021.1920198.

[200] N.M. Daud, S.R. Sheikh Abdullah, H. Abu Hasan, Z. Yaakob, Production of biodiesel and its wastewater treatment technologies, Process Saf. Environ. Prot. 94 (2015) 487–508. https://doi.org/10.1016/j.psep.2014.10.009.

[201] H.J. Tanudjaja, C.A. Hejase, V. V. Tarabara, A.G. Fane, J.W. Chew, Membrane-based separation for oily wastewater: A practical perspective, Water Res. 156 (2019) 347–365.

https://doi.org/10.1016/J.WATRES.2019.03.021.

[202] M. Gomes, P. Arroyo, N.P.-J. of M. Science, undefined 2013, Influence of acidified water addition on the biodiesel and glycerol separation through membrane technology, Elsevier. (n.d.). https://www.sciencedirect.com/science/article/pii/S0376738812009556 (accessed October 28, 2022).

[203] R. Ahmed, K. Huddersman, Review of biodiesel production by the esterification of wastewater containing fats oils and grease (FOGs), J. Ind. Eng. Chem. 110 (2022) 1–14. https://doi.org/10.1016/J.JIEC.2022.02.045.

[204] G.F. Ghesti, E.A. Silveira, M.G. Guimarães, R.B.W. Evaristo, M. Costa, Towards a sustainable waste-to-energy pathway to pequi biomass residues: Biochar, syngas, and biodiesel analysis, Waste Manag. 143 (2022) 144–156. https://doi.org/10.1016/J.WASMAN.2022.02.022.

[205] K. Saikia, K. Rajkumari, N.S. Moyon, S. Basumatary, G. Halder, U. Rashid, S.L. Rokhum, Sulphonated biomass-based catalyst for solketal synthesis by acetalization of glycerol – A byproduct of biodiesel production, Fuel Process. Technol. 238 (2022) 107482. https://doi.org/10.1016/J.FUPROC.2022.107482.

[206] A. Das, D. Shi, G. Halder, S. Lalthazuala Rokhum, Microwave-assisted synthesis of glycerol carbonate by transesterification of glycerol using Mangifera indica peel calcined ash as catalyst, Fuel. 330 (2022) 125511. https://doi.org/10.1016/J.FUEL.2022.125511.

[207] Z. Hu, D. Grasso, Water Analysis - Chemical Oxygen Demand, Encycl. Anal. Sci. Second Ed. (2004) 325–330. https://doi.org/10.1016/B0-12-369397-7/00663-4.

[208] O. Chavalparit, M. Ongwandee, Optimizing electrocoagulation process for the treatment of biodiesel wastewater using response surface methodology, J. Environ. Sci. 21 (2009) 1491–1496. https://doi.org/10.1016/S1001-0742(08)62445-6.

[209] J.M. Encinar, A. Pardal, N. Sánchez, An improvement to the transesterification process by the use of co-solvents to produce biodiesel, Fuel. 166 (2016) 51–58. https://doi.org/10.1016/j.fuel.2015.10.110.

[210] A.P. Soares Dias, M. Ramos, M. Catarino, J. Puna, J. Gomes, Solvent Assisted Biodiesel

Production by Co-processing Beef Tallow and Soybean Oil Over Calcium Catalysts, Waste and Biomass Valorization. 11 (2020) 6249–6259. https://doi.org/10.1007/S12649-019-00903-7.

[211] M. Mohadesi, G. Moradi, M. Ghanbari, M.J. Moradi, Investigating the effect of n-hexane as solvent on waste cooking oil conversion to biodiesel using CaO on a new support as catalyst, Meas. J. Int. Meas. Confed. 135 (2019) 606–612. https://doi.org/10.1016/J.MEASUREMENT.2018.12.022.

[212] W.Y. Lou, M.H. Zong, Z.Q. Duan, Efficient production of biodiesel from high free fatty acid-containing waste oils using various carbohydrate-derived solid acid catalysts, Bioresour. Technol. 99 (2008) 8752–8758. https://doi.org/10.1016/j.biortech.2008.04.038.

[213] H. Guo, J. Cheng, Y. Mao, L. Qian, W. Yang, J.Y. Park, Synergistic effect of ultrasound and switchable hydrophilicity solvent promotes microalgal cell disruption and lipid extraction for biodiesel production, Bioresour. Technol. 343 (2022) 126087. https://doi.org/10.1016/J.BIORTECH.2021.126087.

[214] Y. Zhong, P. Zhang, X. Zhu, H. Li, Q. Deng, J. Wang, Z. Zeng, J.J. Zou, S. Deng, Highly Efficient Alkylation Using Hydrophobic Sulfonic Acid-Functionalized Biochar as a Catalyst for Synthesis of High-Density Biofuels, ACS Sustain. Chem. Eng. 7 (2019) 14973–14981. https://doi.org/10.1021/acssuschemeng.9b03190.

[215] Y. Zhong, Q. Deng, P. Zhang, J. Wang, R. Wang, Z. Zeng, S. Deng, Sulfonic acid functionalized hydrophobic mesoporous biochar: Design, preparation and acid-catalytic properties, Fuel. 240 (2019) 270–277. https://doi.org/10.1016/j.fuel.2018.11.152.

[216] A. Mukhtar, S. Saqib, H. Lin, M.U. Hassan Shah, S. Ullah, M. Younas, M. Rezakazemi, M. Ibrahim, A. Mahmood, S. Asif, A. Bokhari, Current status and challenges in the heterogeneous catalysis for biodiesel production, Renew. Sustain. Energy Rev. 157 (2022) 112012. https://doi.org/10.1016/J.RSER.2021.112012.

[217] Z. Jin, L. Wang, Q. Hu, L. Zhang, S. Xu, Hydrophobic Zeolite Containing Titania Particles as Wettability-Selective Catalyst for Formaldehyde Removal Hydrophobic Zeolite Containing Titania Particles as Wettability- Selective Catalyst for Formaldehyde

Removal, (2018). https://doi.org/10.1021/acscatal.8b00732.

[218] R. Kumar, V. Strezov, T. Kan, H. Weldekidan, J. He, S. Jahan, Investigating the Effect of Mono- And Bimetallic/Zeolite Catalysts on Hydrocarbon Production during Bio-oil Upgrading from Ex Situ Pyrolysis of Biomass, Energy and Fuels. 34 (2020) 389–400. https://doi.org/10.1021/acs.energyfuels.9b02724.

[219] Z. Xu, M. He, X. Xu, X. Cao, D.C.W. Tsang, Impacts of different activation processes on the carbon stability of biochar for oxidation resistance, Bioresour. Technol. 338 (2021) 125555. https://doi.org/10.1016/j.biortech.2021.125555.

[220] Z. Zailan, M. Tahir, M. Jusoh, Z.Y. Zakaria, A review of sulfonic group bearing porous carbon catalyst for biodiesel production, Renew. Energy. 175 (2021) 430–452. https://doi.org/10.1016/J.RENENE.2021.05.030.

[221] H. Kefas, R. Yunus, U. Rashid, Y.T.-Y.- Fuel, undefined 2018, Modified sulfonation method for converting carbonized glucose into solid acid catalyst for the esterification of palm fatty acid distillate, Fuel. 229 (2018) 68-78. https://doi.org/10.1016/j.fuel.2018.05.014.

[222] K. Ngaosuwan, J.G. Goodwin Jr, P. Prasertdham, A green sulfonated carbon-based catalyst derived from coffee residue for esterification, Renew. Energy. 86 (2016) 262-269. https://doi.org/10.1016/j.renene.2015.08.010.

[223] R. Guo, H. Takasu, S. Funayama, Y. Shinoda, M. Tajika, T. Harada, Y. Kato, Mechanical stability and heat transfer improvement of CaO-based composite pellets for thermochemical energy storage, Chem. Eng. Sci. 255 (2022) 117674. https://doi.org/10.1016/J.CES.2022.117674.

[224] F. Li, A.R. Zimmerman, X. Hu, Z. Yu, J. Huang, B. Gao, One-pot synthesis and characterization of engineered hydrochar by hydrothermal carbonization of biomass with ZnCl2, Chemosphere. 254 (2020) 126866. https://doi.org/10.1016/J.CHEMOSPHERE.2020.126866.

[225] J. Hou, C. Cao, F. Idrees, X. Ma, Hierarchical porous nitrogen-doped carbon nanosheets derived from silk for ultrahigh-capacity battery anodes and supercapacitors, ACS Nano. 9

(2015) 2556–2564.
https://doi.org/10.1021/NN506394R/SUPPL_FILE/NN506394R_SI_001.PDF.

[226] N. Postaue, J.M. Fonseca, R. Bergamasco, C. da Silva, Impact of biodiesel production on wastewater generation, Eng. Sanit. e Ambient. 27 (2022) 235–244. https://doi.org/10.1590/S1413-415220210086.

[227] I. Chanakaewsomboon, C. Tongurai, S. Photaworn, S. Kungsanant, R. Nikhom, Investigation of saponification mechanisms in biodiesel production: Microscopic visualization of the effects of FFA, water and the amount of alkaline catalyst, J. Environ. Chem. Eng. 8 (2020) 103538. https://doi.org/10.1016/j.jece.2019.103538.

[228] K.T. Lee, T.A. Foglia, K.S. Chang, Production of alkyl ester as biodiesel from fractionated lard and restaurant grease, JAOCS, J. Am. Oil Chem. Soc. 79 (2002) 191–195. https://doi.org/10.1007/s11746-002-0457-y.

[229] A. MacArio, G. Giordano, Catalytic conversion of renewable sources for biodiesel production: A comparison between biocatalysts and inorganic catalysts, Catal. Letters. 143 (2013) 159–168. https://doi.org/10.1007/s10562-012-0949-3.

[230] N. Brun, A. Babeau-Garcia, M. Achard , C. Sanchez , F. Durand , G. Laurent , M. Birot , H. Deleuze, R. Backov, Enzyme-based biohybrid foams designed for continuous flow heterogeneous catalysis and biodiesel production, (Communication) Energy Environ. Sci., 2011, 4, 2840-2844. DOI: 10.1039/C1EE01295A.

[231] O. Muraza, A. Galadima, Isomerization and alkylation of biomass-derived compounds in aqueous media over hydrophobic solid acid catalysts: A mini review, Ind. Eng. Chem. Res. 53 (2014) 17869–17877. https://doi.org/10.1021/ie503310p.

[232] D. Cavuoto, F. Zaccheria, Some Critical Insights into the Synthesis and Applications of Hydrophobic Solid Catalysts, 10 (2020) 1337. https://doi.org/10.3390/catal10111337.

[233] R.M. Batista, A. Converti, J. Pappalardo, M. Benachour, L.A. Sarubbo, Tools for Optimization of Biomass-to-Energy Conversion Processes, Process. 2023, Vol. 11, Page 854. 11 (2023) 854. https://doi.org/10.3390/PR11030854.

[234] S.P. Gouda, A. Dhakshinamoorthy, S.L. Rokhum, Metal-organic framework as a

heterogeneous catalyst for biodiesel production: A review, Chem. Eng. J. Adv. 12 (2022) 100415. https://doi.org/10.1016/J.CEJA.2022.100415.

[235] Y. Subramaniam, T.A. Masron, The impact of economic globalization on biofuel in developing countries, Energy Convers. Manag. X. 10 (2021) 100064. https://doi.org/10.1016/j.ecmx.2020.100064.

[236] J.V. Ruatpuia, B. Changmai, A. Pathak, L.A. Alghamdi, T. Kress, G. Halder, A.E.H. Wheatley, S.L. Rokhum, Green biodiesel production from Jatropha curcas oil using a carbon-based solid acid catalyst: A process optimization study, Renew. Energy. (2023). https://doi.org/10.1016/J.RENENE.2023.02.041.

[237] S.J. Malode, K.K. Prabhu, R.J. Mascarenhas, N.P. Shetti, T.M. Aminabhavi, Recent advances and viability in biofuel production, Energy Convers. Manag. X. 10 (2021) 100070. https://doi.org/10.1016/J.ECMX.2020.100070.